The Plant Vascular System: Structure, Function, and Responses to Environmental Stress

Dissertation Adviser
Noel Michele Holbrook

Author
Brett A. Huggett

The Plant Vascular System: Structure, Function, and Responses to Environmental Stress

ABSTRACT

Environmental stressors such as nutrient deficiency and insect infestation can significantly impact tree health. Despite much research on the ecological effect on forests in the northeastern United States due to calcium depletion and hemlock woolly adelgid infestation, little is known regarding the physiological mechanisms altered by these stress factors. I tested the hypothesis that calcium depletion, associated with sugar maple decline, compromises water transport processes as a result of calcium-related reductions in cell growth and stabilization. A survey of forest-grown sugar maples from a long-term replicated calcium-manipulation study showed no significant impact of calcium deficiency on wood density, stem hydraulic conductivity (K_s), or vulnerability to cavitation (VC). *In vitro* removal of xylem-bound calcium showed no impact on VC or air seeding thresholds (P_t). Results suggest that sugar maple decline is not caused by compromises in xylem function due to calcium deficiency. I also tested the hypothesis that hemlock woolly adelgid (*Adelges tsugae* Annand) (HWA) infestations impact water transport processes and nutrient partitioning in eastern hemlock trees. HWA infestation resulted in higher K_s due to an increase in average tracheid lumen area associated with the proliferation of false rings. HWA-infested trees exhibited higher rates of net photosynthesis and significant changes in foliar nutrient partitioning. These results are the first to demonstrate increases in K_s and alterations in foliar cation levels in response to HWA infestation.

In two additional studies, I investigated methods for evaluating the structure and function of xylem networks. Using sequential sectioning of aerial roots of epiphytic aroids, I directly quantified the topographic relation of vessels in a single organ with measurements of vessel length, diameter, vessel end overlap length, and vessel stelar orientation. In a separate study, I explored the relationship between vessel length and measurements of P_t. In establishing guidelines for estimating whole-stem cavitation with the use of single vessel air injection, I demonstrate that calculations of P_t are influenced by stem length measured and removal of native emboli prior to testing. Improvements in tools to quantify xylem structure and function will enhance our ability to understand the responses of forest trees to environmental stress.

TABLE OF CONTENTS

ACKNOWLEDGEMENTS

I am deeply appreciative of the support I received from my committee members N. Michele Holbrook, Donald H. Pfister, and Elena Kramer. In particular, I would like to thank my adviser N. Michele Holbrook for welcoming me into the lab and providing me with resources and guidance throughout my doctoral journey at Harvard. I owe much gratitude to Donald H. Pfister for launching my science career and for his unending support in every aspect of my education. I thank P.B. Tomlinson for serving as a teacher, mentor, and collaborator; his passion for plant anatomy will serve as a lifelong inspiration. I also thank Jim Wheeler and Juan Pablo Giraldo, classmates whom I have benefited from greatly in terms of knowledge of plant physiology and in enjoying the PhD process. I am grateful to the many Holbrook Lab Affiliates who have assisted me in the lab, field, or office throughout my time at Harvard University. Through the Harvard Forest REU program, I was also fortunate to have collaborators in Harvard Undergraduates: Lee Dietterich, James Onstad, and Alena Tofte.

This research was supported by funds or resources provided by the at Harvard University Department of Organismic and Evolutionary Biology, Harvard Forest REU program, Hubbard Brook Experimental Forest, and the National Science Foundation IGERT Grant.

Lastly, I would like to acknowledge the following contributors:

Chapter 2: A. Tofte, L. Dietterich, J. Onstad, and N. Michele Holbrook.

Chapter 3: J. Savage, G.Y. Hao, E. Preisser, and N. Michele Holbrook.

Chapter 4: P.B. Tomlinson.

Chapter 5: K.H. Jensen, and N. Michele Holbrook.

For my wife Kim, daughters Lucy Ana and Madelyn Reece, parents, siblings and friends, thank you for your love and support.

CHAPTER 1

INTRODUCTION

This thesis focuses on two areas of plant biology: 1) understanding the physiological responses of trees to biotic/abiotic stress, with a particular interest in water-transport processes, and 2) understanding the structure and function of plant vascular networks. Nutrient deficiencies, such as calcium (Ca) depletion, or parasite-host interactions, such as the hemlock woolly adelgid infestation, have the potential to significantly impact the water relations of trees subjected to these stress factors. Evaluating how pressures in the growing environment influence plant structure and function will greatly improve our understanding of tree health and ecosystem dynamics. To arrive at such conclusions, it is crucial to gain an understanding of the complexity in the structure and function of xylem networks.

In Chapter 2, I investigate how calcium (Ca) depletion caused by anthropogenic disturbances might disrupt water relations in sugar maple. There is strong evidence that various anthropogenic factors, including nitrogen saturation, forest harvesting, changing climatic conditions, soil aluminum (Al) mobilization, acid loading, and declines in atmospheric base cation deposition contribute to the well-documented depletion of calcium (Ca) from forest ecosystems in the Northeastern United States and Canada (Mann et al. 1988; Federer et al. 1989; Hedin et al. 1994; Kirchner and Lydersen 1995; Aber et al. 1998; Likens et al. 1998; Bailey et al. 2004). Although decreased availability of this biologically essential element has been considered a causal factor in the decline in health of forested ecosystems, little is known of the underlying mechanisms by which Ca depletion influences the growth and productivity of forests. This research tests the

hypothesis that Ca-related reductions in cell growth and stabilization compromise the properties and function of vascular tissue. The proven correlation between cavitation resistance and wood density and structure provides a potential mechanism linking xylem function with the availability of Ca (Hacke et al. 2001a). Furthermore, perturbations of ion levels in xylem sap may affect ion-mediated regulations of xylem conductivity or resistance to cavitation (Zwieniecki et al. 2001b; Herbette and Cochard 2010). Surveying forest-grown sugar maples (*Acer saccharum* Marsh.*)* from a long-term replicated Ca-manipulation study at the Hubbard Brook Experimental Forest, NH, USA, found no significant impact of Ca-deficiency on wood density, stem hydraulic conductivity, or vulnerability to cavitation. Moreover, no difference in leaf water potential was detected among treatment trees. Laboratory methods evaluating the removal of Ca from stems and the subsequent impact on vulnerability to cavitation and air seeding pressure supported field test results. While documented symptoms of sugar maple decline (i.e. branch dieback and loss of crown vigor) are also associated with impaired water transport, it appears that Ca depletion associated with this decline does not significantly impact xylem function.

Chapter 3 explores the physiological responses in eastern hemlock (*Tsuga canadensis* (L.) Carrière) to infestation by the hemlock woolly adelgid (*Adelges tsugae* Annand). Introduced to the United States from East Asia, hemlock woolly adelgid (HWA) is an invasive insect responsible for the decline and often death of eastern hemlock trees (Souto et al. 1996; Orwig and Foster 1998). First reported in 1951 in the eastern United States, this insect has spread rapidly into the northeastern United States and is currently well established in southern New England (McClure et al. 1999). The HWA feeds on photosynthate storage cells at the base of young needles, ultimately causing loss of vigor and premature needle drop, often to the point of

defoliation (Young et al. 1995). HWA infestations and the subsequent mortality of eastern hemlock trees has been shown to significantly impact ecosystem dynamics (Orwig et al. 2013). At the physiological level, little is known regarding the impact of HWA infestation on water-transport processes and nutrient partitioning in eastern hemlock. Insect infection can directly affect leaf physiology, including photosynthesis, which in turn influences stem traits due to intergradations of plant functions among different parts. Increases in the formation of false rings in response to insect infestations (Gonda-King et al. 2012) could cause changes in xylem properties, such as tracheid size, hydraulic conductivity, and vulnerability to loss of hydraulic function under tension. Furthermore, responses to defoliation events and depletion of photosynthate stores, nutrient partitioning could be significantly altered in response to HWA infestation (Gómez et al. 2012). As part of an established study investigating the impact of HWA infestations in eastern hemlock, I found significantly higher stem conductivity and sapwood:leaf area in HWA-infected trees when compared to HWA-free control trees. Anatomical analyses support these findings, as HWA infestation resulted in an increase in average tracheid lumen area and hydraulic mean diameter. An analysis of leaf water potential and vulnerability to cavitation found no differences between treatments. HWA infested trees exhibited higher rates of net photosynthesis and significant changes in foliar nutrient partitioning. These results are the first to demonstrate an increase in stem hydraulic conductivity and alterations in foliar cation levels in response to HWA infestation. Alterations in tracheid lumen dimensions associated with increased hydraulic conductivity could compromise the biomechanical integrity of stems infested by the HWA.

In Chapter 4, I measure vessel dimensions, most significantly vessel length, in the aerial roots of four epiphytic aroids using a digital camera to photograph sequential sections. Pendulous aerial roots in Araceae can grow from the forest canopy and so reach considerable length (>30 m) before they contact the ground, branch and become anchored. In the free-hanging state the length over which tissue maturation occurs can exceed 1m.I show that the distinctive medullary vessels do not anastomose and each series of vessels, end to end here termed a "pipe," must differentiate without interruption throughout the length of the root but not become fully functional until the ground is reached. Measurements show different vessel parameters including vessel overlap at each vessel end, which is not usually considered in estimates of hydraulic conductivity. This method of measurement is simple and direct and shows the topographic relation of all vessels in a single organ, suggesting that vessels in long plant organs can be measured precisely giving results of value in considering the hydraulic properties of xylem elements.

In Chapter 5, I evaluate the technique of single vessel air injection method as a measurement of vulnerability to cavitation, with sugar maple (*Acer saccharum* Marsh.) as a test species. Cavitation in xylem conduits can lead to the formation of embolism (Zimmermann 1983). The propagation of air bubbles is thought to occur through "air seeding," whereby air is pulled through pores in the inter-conduit pit membranes from embolized conduits into functional conduits (Zimmermann 1983; Sperry and Tyree 1988). Negative pressures in functional conduits required to induce air seeding are equal to and opposite the pressure required to force air across inter-conduit pits (Cochard et al. 1992). Therefore, the method of single vessel air injection is utilized to measure the air seeding threshold pressure of xylem conduits (Zwieniecki et al. 2001a). There is much variation in protocols for the use of this technique in terms of lengths of

stems measured and preparation of material prior to measurement (i.e. flushed to remove reversible embolism or native) (Melcher et al. 2003; Choat et al. 2005; Christman et al. 2009). In my evaluation of this technique, I show a significant relationship between stem length measured and the air seeding pressure of individual vessels. Furthermore, stems flushed with 10 mM KCl prior to measurements significantly increase mean air seeding pressures. Lastly, I incorporate data obtained from vessel length distributions with that of air seeding pressures from single vessel air injections in a comparison of measurements of vulnerability to cavitation generated by the centrifuge technique. Results indicate that the stem segment length measured for air seeding pressure must be similar to the mean vessel length of the species to accurately utilize the method of single vessel air injection to predict whole-stem cavitation in a diffuse-porous species such as *A. saccharum*.

CHAPTER 2

Calcium Deficiency and Whole Plant Water Relations in Sugar Maple (*Acer saccharum* Marsh.)

INTRODUCTION

Long-term research indicates a net loss of calcium (Ca) from forested ecosystems in the northeastern United States (Likens et al. 1998; Bailey et al. 2004). Factors contributing to the removal of Ca from forested ecosystems include: declines in atmospheric deposition of base cations and increases in atmospheric deposition of strong acids (Hedin et al. 1994; Kirchner and Lydersen 1995; Likens et al. 1996; Ouimet et al. 2001); nitrogen (N) saturation, resulting in soil and stream acidification due to an increase in aluminum (Al) mobility (Aber et al. 1998); mass removal of Ca stores through forest harvesting (Mann et al. 1988; Federer et al. 1989); and changing climatic conditions which increase Ca leaching following increased soil acidification due to higher soil temperatures and reduced rainfall (Tomlinson 1993). Lastly, pollution-induced soil Al mobilization can disrupt Ca availability by the ability of Al to: (1) interfere with the uptake of Ca by fine roots, (2) displace plasma membrane- and pectin-bound Ca, and (3) block Ca-specific channels in cells (Shortle and Smith 1988; Marschner 1995; Lawrence et al. 1995; Rengel and Zhang 2003).

Ca depletion, in addition to increased Al mobilization, can impart important limitations on forest structure, growth, and health (Heisey 1995; McLaughlin and Wimmer 1999; Schaberg et al. 2001; Royo and Knight 2012). In particular, Ca depletion is considered responsible for the

documented decline in sugar maple in the northeastern United States and Canada. Decline in the health of sugar maple in the United States and Quebec first occurred in the 1960's, with a steady increase in incidences and severity in recent decades (Mader and Thompson 1969; Allen et al. 1992; Wilmot et al. 1995; Horsley et al. 2002). Conditions symptomatic of sugar maple decline include dieback of fine twigs and branches, a slow loss of crown vigor, and reduced growth frequently ending in tree death. Mineral deficiency (Ca, magnesium, and potassium) in sugar maple results in reduction of growth rates and a compromised stress response to abiotic or biotic factors (Kolb and McCormick 1993; Horsley et al. 2002; Hallett et al. 2006; Long et al. 2009). Decreases in annual basal area growth rates have been attributed to Ca deficiency and increases in Al availability (Heisey 1995; Wilmot et al. 1995; Huggett et al. 2007). Field surveys of sugar maple subjected to Ca deficiency have found increases in branch dieback, decreases in crown health, and reductions in rate of wound closure to abiotic stem wounding (Wilmot et al. 1995; Juice et al. 2006; Schaberg et al. 2006; Huggett et al. 2007). Furthermore, sugar maples with low foliar Ca exhibit lower levels of chlorophyll and a reduction in net photosynthetic rates (Ellsworth and Liu 1994; Liu et al. 1997; Juice et al. 2006). The application of dolomitic lime ($CaMg(CO_3)_2$) to acidic or base-poor soils has been found to reverse the effects of Ca deficiency, resulting in an overall improvement in the sugar maple health and growth rates (Long et al. 1997; Wargo et al. 2002; Moore et al. 2012).

The impact of Ca deficiency on forest and ecosystem health is driven by the fact that Ca is an essential element regulating physiological processes involved in plant growth and response to stress. These processes include: cell wall and membrane synthesis, stabilization, and function; protein synthesis; rates of respiratory metabolism and translocation; stomatal function and

photosynthesis; structural chemistry and function of woody support tissues; and signaling involved in response to abiotic or biotic stimuli (Marschner 1995; McLaughlin and Wimmer 1999; Hepler 2005; Lautner et al. 2007). Recent research highlights the importance of Ca in plant responses to such environmental stresses as low temperature, drought, and fungal and insect infestations (Sheen 1996; DeHayes et al. 1997; McLaughlin and Wimmer 1999; Halman et al. 2008; Schaberg et al. 2011).

In addition to stress response and survival, Ca plays an essential role in the synthesis and stabilization of cell walls and membranes. The Ca-dependent protein calmodulin is responsible for the formation of actin filaments, cytoplasmic streaming, polarized growth, and the cell division cycle (Buchanan et al. 2000). Calcium is also involved in secretory processes and activation of synthesizing enzymes responsible for cell wall formation and strengthening. For example, Ca-dependent transport processes are responsible for the exocytosis of cellulose (Marschner 1995) and lignin precursors, such as peroxidase, which is considered a Ca-dependent enzyme for lignin synthesis. In cell membranes, Ca impacts stability and permeability by bridging proteins and the phosphate and carboxylate groups of the phospholipids (Legge et al. 1982; Davies and Monk-Talbot 1990). Lastly, a large portion of the total calcium in plant tissue is located in the apoplasm where it strengthens cell walls and tissues by cross-linking pectins in the middle lamella (Marschner 1995). These aspects of Ca-dependent cell growth and stabilization strongly influence the formation and function of woody tissue in forest trees (McLaughlin and Wimmer 1999; Lautner and Fromm 2010).

Due to the role that Ca plays in the regulation of cell growth, stabilization, and reinforcement, changes in xylem structure and strength due to Ca deficiency could result in reductions in hydraulic conductivity and resistance to cavitation. In vascular plants, water is transported from the soil to the leaves through xylem under negative pressures. Hydraulic flow through xylem conduits is impeded by viscous losses (essentially friction to flow) and the occurrence to embolisms. Conduit dimensions such as diameter and length have major consequences on hydraulic resistance (Sperry et al. 2006). The presence of embolisms can seriously impair transport and lead to constraints on photosynthesis (Brodribb and Feild 2000) and increases in branch dieback (Rood et al. 2000; Davis et al. 2002). A plant's hydraulic architecture imposes limitations on transpiration rates, growth, photosynthesis and responses to changing environmental conditions such as drought and freezing.

A positive correlation has been demonstrated between resistance to cavitation and increases in xylem density and conduit wall thickness-to-diameter ratio ($(t/b)_h^2$, where (t) is thickness of adjacent vessel walls and (b) is conduit wall span) (Hacke et al. 2001b). A weaker relationship between cavitation resistance and wood density/vessel dimensions among angiosperms, compared to conifers, is due to the indirect reinforcement of conduits by fibers (Jacobsen et al. 2005). In fact, the density of xylem in angiosperms is primarily due to the existence of the fiber matrix between vessels. Jacobsen et al. (2005) also linked increased mechanical strength (greater modulus of elasticity and modulus of rupture) with greater cavitation resistance. The compressive strength and bending stiffness of wood is attributed to production of lignin (Evert and Esau 2007). Lignin also functions to strengthen xylem to resist collapse due to increased negative pressures generated by transpiration and soil drying. Reductions in lignification or cell

growth resulting from Ca deficiency could impair the reinforcement of xylem conduits and the development of thicker xylem wall areas or fibers. In fact, Ca deficiency in trees has been found to significantly inhibit the production of lignin (Eklund and Eliasson 1990), decrease increment growth (Wilmot et al. 1995; Huggett et al. 2007; Fromm 2010), and reduce vessel and fiber length (Lautner et al. 2007; Lautner and Fromm 2010).

Further evidence that Ca may impact cavitation resistance is related to the ability of Ca to form cross-linkages and strengthen pectins in the middle lamella of cells. Sperry and Tyree (1988) found that perfusion solutions containing oxalic-calcium greatly reduce cavitation resistance. It is possible that oxalate in the perfusion solution removed Ca from the pectate fraction of the bordered pit membrane thus increasing the likelihood of air seeding (Sperry and Tyree 1988). Calcium cross-linkages in pectate are thought to prevent pore widening and rupture by reducing the flexibility of the membrane as the pressure difference across the air-water interface increases. Furthermore, Melcher et al. (unpublished results) have shown that increases in Ca concentration of perfusion solutions can reduce cavitation fatigue, which is an increase in the susceptibility of xylem to cavitation after artificial refilling due to weakening of the border pit membrane (Hacke et al. 2001b; Stiller and Sperry 2002). Recently, Herbette and Cochard (2010) found that removal of xylem-bound Ca in stems of *Fagus sylvatica* reduced cavitation resistance. This suggests that alterations in xylem concentration of Ca and Al (which can remove pectin-bound Ca) could influence resistance to cavitation in sugar maple.

Recent insights into xylem hydraulic conductivity have revealed that increased ion concentrations in xylem sap of plants produce rapid and reversible changes in hydraulic

resistance (Zwieniecki et al. 2001b). Pit membrane pectins (hydrogels) shrink or swell in response to changes in pH, ion-concentration, or polarity of perfusion solution. Cross-linking of the pectin matrix by ions compresses hydrogels and increases the size of micro-pores located in the pit membrane (Zwieniecki et al. 2001b). Perfusing stems with KCl or other dissociating solutes (NaCl, KNO_3, and $CaCl_2$) increased flow rates by up to 2.5 times compared to deionized water.

Because of the demonstrated ability of Ca to cross-link and collapse hydrogels (Tibbits et al. 1998), Ca availability in forest trees could influence the extent of ion-mediated enhancement of xylem hydraulic conductivity. Trees with sufficient Ca levels could have ion-saturated pectins, exhibit high rates of hydraulic conductivity, and show little response to ion-mediated regulation of xylem flow. On the other hand, Ca deficiency could result in a reduction of xylem hydraulic conductivity. Decreasing concentrations of Ca or dissociation of Ca cross-linkages can result in marked swelling of pectin gels (Tibbits et al. 1998). Al has the ability to dissociate Ca ions bound to pectate and has been found to reduce the porosity of cell walls by disrupting Ca cross-linkages (Rengel and Zhang 2003). Furthermore, Al binds more strongly with pectins which would further reduce the ability of Ca to bind with hydrogels (Schmohl et al. 2000). Trees subjected to reductions in Ca availability as a result of Al mobilization could exhibit a decrease in xylem hydraulic flow due to increased swelling of hydrogels located in bordered pit membranes.

In this chapter, I examine the following hypotheses: Ca-related reductions in cell growth and stabilization compromise the biomechanical properties and function of water conducting tissues;

Ca depletion weakens the ability of forest trees to resist cavitation by disrupting density, strength, and growth of xylem tissue; changes in ion availability representative of anthropogenic alterations could influence ion-mediated stem hydraulic efficiency; and lastly, removal of xylem-bound Ca could increase stem vulnerability to cavitation and reduce air seeding thresholds of xylem vessels in sugar maple.

Considering the economical and ecological importance of sugar maple, its sensitivity to Ca deficiency, and estimates on the continuation of anthropogenic alteration of Ca availability, further study of the decline of this tree species is warranted. Despite recent efforts to link sugar maple decline specifically to Ca deficiency by evaluating reductions in growth, crown health, and stress responses of sugar maple, a thorough assessment of the impact of Ca deficiency on whole plant water relations is needed. It is possible that common symptoms of sugar maple decline (i.e. branch dieback, reduction in crown vigor, and reduced growth rates) could be attributed to Ca-related compromises in tree water relations, particularly vulnerability to cavitation. Because Ca is essential to the synthesis and strengthening of cell walls (via cross-linking of pectins and lignin formation) Ca deficiency could weaken xylem tissue and increase vulnerability to cavitation in sugar maple. In addition, perturbations in the availability of Ca and Al due to anthropogenic factors could alter ion concentration of xylem sap, which would influence ion-mediated hydraulic properties of xylem.

MATERIALS AND METHODS

Study Sites and Collection

Research was conducted on sugar maple (*Acer saccharum* Marsh.) from two locations: (1) a pre-existing long-term replicated Ca-manipulation study at the Hubbard Brook Experimental Forest, NH, USA (HBEF) and (2) an experimental garden at Harvard University, Cambridge, MA (HU).

The HBEF study area was established in 1995 comprises of twelve forested plots (45 m x 45 m) in a mixed hardwood stand with sugar maple as the dominant canopy species. The twelve plots consist of three treatments equally and randomly divided into: (1) control (no fertilization), (2) soil Ca addition, and (3) soil Al addition (to reduce Ca availability), resulting in four replicates of fertilization. Reference control plots within the adjacent experimental watershed have experienced a long-term reduction in soil Ca (Likens et al. 1998). From 1995 until present, treatment applications have occurred on an annual to semi-annual basis (Table 1.1). In 1998, annual additions of $CaCl_2$ were discontinued and replaced with a single application of wollastonite pellets ($CaSiO_3$, 38 gm^{-2}) to provide a slow release of Ca into the soil (Peters et al. 2004). At the time of this study, a total of 40 g m^{-2} $CaCl_2$ and 9.9 g m^{-2} $AlCl_3$ has been added to the treatment plots. Recent research conducted on these plots show a significant impact of treatments on sugar maple foliar nutrient concentrations and on symptoms characteristic of sugar maple decline (Huggett et al. 2007).

Parameters of water relations and wood growth in this study were conducted at HBEF in 2008 and replicated in 2011. Ten samples in August 2008 (two to three per plot) and eight samples in

Table 1.1. Record of treatment applications at study site (HBEF). In 1998, a one-time application of wollastonite pellets ($CaSiO_3$, $38gm^{-2}$) was added to provide a slow release of Ca into the soil.

	Treatment	
Date	Calcium addition (4 plots)	Aluminum addition (4 plots)
Oct 1995	2 g m^{-2} $CaCl_2$	0.9 g m^{-2} $AlCl_3$
May 1996	3 g m^{-2} $CaCl_2$	0.9 g m^{-2} $AlCl_3$
Nov 1996	2 g m^{-2} $CaCl_2$	0.9 g m^{-2} $AlCl_3$
May 1997	3 g m^{-2} $CaCl_2$	1.8 g m^{-2} $AlCl_3$
Oct 1998	38 g m^{-2} (wollastonite)	0.9 g m^{-2} $AlCl_3$
May 2001		0.9 g m^{-2} $AlCl_3$
Apr 2002		0.9 g m^{-2} $AlCl_3$
May 2004		0.9 g m^{-2} $AlCl_3$
Nov 2005		0.9 g m^{-2} $AlCl_3$
May 2008		0.9 g m^{-2} $AlCl_3$
June 2011		0.9 g m^{-2} $AlCl_3$

June 2011 (two per plot) of intermediate and codominant canopy class sugar maple trees were selected randomly per treatment. Branches approximately 2-4 m in length were cut mid-morning with a pole-pruner from a height of 5.5-7.5 m. In 2008, immediately following collection, each branch was re-cut under water at the base and then placed in large black plastic bags with wet paper towels for transport to the lab. Samples were kept under refrigeration and processed within 48 hours post-collection. In 2011, immediately following collection, the branches were re-cut under water to remove a stem segment 30cm in length, which was placed in a Ziploc bag with water and transported to the lab. For foliar cation analysis in 2011, foliar samples from each branch were collected and placed in a Ziploc. All samples were kept under refrigeration and processed within 24 hrs post-collection.

Tests on ion-mediated stem hydraulic conductivity and studies of the effects of removing Ca on vulnerability to cavitation were conducted on sugar maple trees selected from the experimental garden at HU. All trees were 5-8 m in height; samples were removed with a pole pruner from mid-canopy. Sampling methods were as described above, except individuals were immediately re-cut under water and processed.

Foliar Sampling and Chemistry

Foliar cation analysis was conducted on sample specimens collected in June 2011. From branches removed from mid-canopy tree height, approximately 12 leaves free of damage or fungal infection were collected, stored in Ziploc bags, and kept cooled during transport. Foliar tissue was oven-dried at 55°C prior to shipping to the University of Vermont, Burlington, VT (UVM) for processing. Upon arrival at UVM, samples were once again oven-dried at 55°C prior

to processing. Cation levels (Al, Ca, K, Mn, and Mg) were measured using the method of inductively coupled plasma atomic emission spectrometry (ICPAES, PlasmaSpec 2.5, Perkin-Elmer Optima, Lowell, MA).

Hydraulic Conductivity

Measurements of hydraulic conductivity (K_h) of sugar maple were conducted by measuring flow driven by a gravity head through a stem sample in a pressure-drop flow meter system (2008 measurements) (Tyree et al. 1993; Sack et al. 2011; Melcher et al. 2012) or to an analytical balance (Sartorius CPA225D) (2011 measurements) (Sperry et al. 1988). A perfusion solution of 10 mM KCl in de-ionized ultra-filtered water (DI H_2O) (Millipore MilliQ UV plus) was used. Prior to all measurements, the perfusion solution was re-filtered through a 0.2 μm syringe filter (Pall acrodisc syringe filters). In 2008, hydraulic conductivity was measured on current-year growth, 1.7-3.5 mm diameter and 12.5-17.5 cm in length (2008 measurements). In 2011, hydraulic conductivity measurements were performed on four-six year old stem segments, 5.5-7.5 mm diameter and 14.5 cm in length (2011 measurements). Percentage loss of conductivity (PLC) was calculated as $[100\ (1- K_{initial} / K_{max})]$ where $K_{initial}$ refers to initial conductivity (native) and K_{max} is the maximum conductivity (flushed) measured after removal of embolisms by flushing stems with 10 mM KCl at 0.1 MPa for 20mins. Hydraulic conductivity was referenced to xylem cross-sectional area (xylem-specific conductivity, K_s) or leaf area supported by xylem (leaf-specific conductivity, LSC). Xylem area was measured with digital calipers (Mitutoyo 500-196-20) at the distal end of each stem and calculated by taking the average diameter of perpendicular cross-sectional axes minus pith area. Leaf area was calculated by measuring total

leaf area (LI-3100 Area Meter, Li-Cor, Inc.) distal to the measured stem segment. Huber value was calculated in both 2008 and 2011 as a ratio of sapwood area to leaf area.

Vulnerability to Cavitation

For measurements in 2008, vulnerability of xylem to cavitation was measured using air-injection (Sperry and Saliendra 1994) with a perfusion solution of 10 mM KCl in DI H_2O (Millipore MilliQ UV plus). Prior to all measurements, the perfusion solution was re-filtered through a 0.2 μm syringe filter (Pall acrodisc syringe filters). Four to five year-old stem segments, 9-23 mm in diameter and 10cm in length were used. The technique of air injection (Sperry and Saliendra 1994) was utilized to establish vulnerability curves. Stems were mounted in a double-ended pressure sleeve (5 cm in length) and hydraulic conductivity was measured after each pressure of 0, 0.5, 1, 2, 3, 4, 5 and 6 MPa for the duration of 10mins. Vulnerability to cavitation calculated using PLC [100 (1- K_{result}/ K_{max})] where K_{result} refers to conductivity following each stage of increased pressure and K_{max} is the maximum conductivity (flushed) measured after removal of embolisms by flushing stems (as described above). Stem flow rates were measured utilizing 1.5 mL Eppendorf tubes with paper towels inside to collect, at a total of 15 sec time intervals, perfusion solution forced through each stem driven by gravity head from an elevated reservoir. The difference in weight of Eppendorf tubes pre and post collection was averaged over 10 tubes per measurement to provide calculation of flow rate. All samples were decorticated prior to measurement to prevent leakage of gas of the pressure chamber.

In 2010, the centrifuge technique (Alder et al. 1997) was used with 10 mM KCl perfusion solution in DI H_2O (Millipore MilliQ UV plus). Prior to all measurements, perfusion solution

was re-filtered through a 0.2 μm syringe filter (Pall acrodisc syringe filters). Hydraulic conductivity was calculated by measuring flow driven by a gravity head through each stem sample to an analytical balance (Sartorius CPA225D). Stems ranging 4-6 years old, 5.5-7.5 mm diameter and 14.5 cm in length were used. All stems were decorticated up to 5 mm at each end to allow for proper seal during hydraulic conductivity measurements. Stems were flushed with 10 mM KCl at 0.1 MPa for 20 mins prior to spinning in the centrifuge. Hydraulic conductivity was measured after each pressure of 0, 0.5, 1, 2, 3, 4, 5 and 6 MPa (3 mins of rotation time for each pressure) and vulnerability to cavitation calculated using PLC (as described above).

Leaf Water Relations

In 2008, leaf water potential in relation to treatment was measured using the Scholander pressure-bomb technique (Scholander et al. 1965; Pearcy et al. 1989). Turgor loss point was estimated from pressure-volume curves (Koide et al. 1989) on 7-8 leaves per treatment.

Wood Density

In both 2008 and 2011, wood density of sample trees was measured using the water-displacement method on 4-5 year-old stem segments. Wood samples were oven-dried at 55˚C for >48 hrs. Calculations of density were based on the oven-dried mass/green-wood volume (green wood density).

Ion-Mediated Hydraulic Conductivity

A comparison of perfusion solutions of DI H_2O, 10 mM KCl, 10 mM $CaCl_2$, and 10 mM $AlCl_3$ on K_s was made. All cation perfusion solutions were mixed in DI H_2O (Millipore MilliQ

UV plus) and re-filtered through a 0.2 μm syringe filter (Pall acrodisc syringe filters) prior to measurements. Branches from garden-grown sugar maples at HU were collected as described above. A total of five stem segments three to four years old and 10cm in length were cut from the branch while underwater. During measurements of hydraulic conductivity onto a balance (as described above), each stem was subjected to a series of perfusion solutions for 10-12mins each in the order DI H_2O, KCl, DI H_2O, $CaCl_2$, DI H_2O, and $AlCl_3$. The effect of each cation solution on K_s was calculated by taking the percent increase K_s of each cation perfusion solution over the baseline K_s perfused with DI H_2O.

Impact of Xylem-Bound Ca on Vulnerability to Cavitation and Air Seeding Thresholds

Utilizing $NaPO_4$ as a Ca chelating agent, the removal of xylem-bound Ca and the subsequent impacts on vulnerability to cavitation and air seeding threshold of individual vessels was tested. $NaPO_4$ at pH10 was found to increase vulnerability to cavitation in certain tree species, suggesting that it was an effective Ca chelating agent of xylem-bound Ca (Herbette and Cochard 2010). In this study, $NaPO_4$ pH4 had no impact on PLC compared to the standard perfusion solution of KCl. In this study, branches from garden-grown sugar maples were collected as described above. To check for a seasonal effect, measurements were conducted in December of 2011 and June of 2012. Stem segments three to four years old and 15 cm in length were removed from the 2-4 m branch (collection methods as described above) by cutting under water and then flushed at 0.1 MPa with 10ml perfusion solutions of 10 mM $NaPO_4$ pH10 or 10 mM $NaPO_4$ pH4. All cation perfusion solutions were mixed in DI H_2O (Millipore MilliQ UV plus) and re-filtered through a 0.2 μm syringe filter (Pall acrodisc syringe filters) prior to measurements. Stems were

then trimmed to 14.5 cm with a fresh razor blade and processed utilizing the centrifuge technique for generating vulnerability to cavitation curves (see above).

To assess the impact of removing xylem-bound Ca on the air seeding threshold of single vessels, the technique of single vessel air injection developed by Melcher et al (2003) was utilized. Branches from garden-grown sugar maples were collected as described above. Stem segments three to four years and 15cm in length were removed from the 2-4 m branch (collection methods as described above) by cutting under water. Following removal, stems were flushed at 0.1 MPa with 10 ml of one of the following perfusion solutions: 10 mM $NaPO_4$ pH10; 10 mM $NaPO_4$ pH4; 10 mM KCl pH10; 10 mM KCl pH4; or 10 mM EGTA pH4. The use of KCl at pH10 and pH4 was introduced to account for any differences due to pH in perfusion with $NaPO_4$ pH10 compared to $NaPO_4$ pH4. EGTA was introduced due to its well-known effectiveness as a Ca chelating agent. All cation perfusion solutions were mixed in DI H_2O (Millipore MilliQ UV plus) and re-filtered through a 0.2 μm syringe filter (Pall acrodisc syringe filters) prior to measurements. After perfusion, stems were trimmed underwater to a length of 5 cm and the distal end (youngest end) stained for better visualization of conduits with Toluidine Blue filtered through a 0.2 μm syringe filter (Pall acrodisc syringe filters). In each stem segment, measurements were conducted on second or third year growth rings as Melcher et al. (2003) showed no change in vulnerability to cavitation between such growth rings. A horizontal micropipette puller (PUL-1, World Precision Instruments, Hertfordshire, UK) was utilized to reduce the diameter of the glass pipettes to a size suitable for fitting within the lumen of individual vessels. Stems were then attached to a micromanipulator and a glass microcapillary tube was inserted into the lumen of an individual vessel in the distal end of the stem. The

insertion of the microcapillary tube was then fixed to the stem with fast-setting glue (ZAP A Gap CA+ Glue). The microcapillary was attached to a regulated source of nitrogen gas, which allowed for a slow increase in the amount of air pressure forced into the individual vessel. The proximal end of the stem segment was submerged in water for visualization of air bubbles resulting from gas being pressurized through individual vessels. Initially, 0.10 MPa was applied to the conduit; if no air bubbles appeared out the proximal end, the conduit was considered closed (i.e. with vessel ends). Gas was then applied at a rate of 0.1 MPa min^{-1} until bubbles emerged from the proximal end. This pressure was considered the air seeding threshold for the individual vessel. Pressures exceeding 6 MPa were avoided due to the possibility of blowing the microcapillary out of the apparatus; vessels exhibiting this level of resistance to pressure were considered obstructed. After each measurement, the microcapillary was careful removed from the vessel lumen and inserted into another vessel within the same stem; 3-6 measurements per stem were possible.

Statistical Analyses

For continuous data collected at HBEF, differences between treatments were determined by analysis of variance (ANOVA). A nested design was utilized for significance tests, which tested treatment differences with plot within treatment, and plot differences with tree within treatment (Montgomery 2001). Differences among means were further tested utilizing two mutually exclusive orthogonal contrasts: 1) Ca vs. Al and Control and 2) Al vs. Control. These contrasts provided a better evaluation of two important aspects of the study: 1) the influence of elevated Ca availability above ambient and reduced levels, and 2) the influence of reduced Ca levels below ambient (Huggett et al. 2007). For all tests of vulnerability to cavitation, the standard of

50% loss of conductivity (P50) and mean cavitation pressure (MCP) was used for comparisons between treatment trees; each parameter was calculated from fitting data by least square regression using the Weibull function. An ANOVA with the Tukey-Kramer HSD test was used to evaluate differences between treatments of cation perfusion solutions on K_s. Similar statistical analyses were used to evaluate treatment differences in air seeding threshold measurements. A one-sided Student's t-test was used to evaluate comparisons of P50 and MCP between treatments in the removal of xylem-bound Ca and the impact on vulnerability to cavitation.

RESULTS

Evaluation of Treatment Regimes

Evaluation of foliar nutrient concentrations in 2011 showed a significant difference in foliar Ca concentrations among treatment plots (Table 1.2). Trees growing on plots amended with Ca exhibited greater foliar Ca than trees on control plots or Al-addition plots ($P = 0.0364$, Ca $N = 8$, Control $N = 8$, Al $N = 7$). There was no difference in foliar Ca in trees growing on control plots compared to the Al-addition plots. There was no difference between treatments in levels of foliar Al, Mg, Mn, or KCl ($P > 0.1$).

Hydraulic Conductivity

In 2008, an analysis of native K_s exhibited no differences in comparisons between treatments (Figure 1.1; $P = 0.203$, $N = 10$). After native embolisms were removed by flushing, results of maximum K_s (flushed) showed no significant difference in trees grown on Ca plots compared to control and Al-addition plots ($P = 0.058$, $N = 10$), but did show a significant difference in trees grown on Al-addition plots compared to control plots ($P = 0.047$, $N = 10$) with higher rates of K_s

Table 1.2. Foliar cation concentrations for *A. saccharum* trees in 2011 from Ca-addition, Control, and Al-addition study plots. A reference to published range of foliar cations for healthy sugar maples is provided (Kolb and McCormick 1993). Results are means ± SE (Ca N = 8, Control N = 8, Al N = 7).

	Treatment means (mg · kg^{-1})			Significance of contrasts (*P* value)	
Element	Ca	Control	Al	Ca vs. Control and Al	Control vs. Al
Ca	6935 ± 444	4927 ± 682	5123 ± 543	0.036	0.824
Al	35.9 ± 3.4	38.5 ± 2.5	37.9 ± 4.6	0.613	0.925
Mg	1533 ± 83.7	1237 ± 182	1113 ± 135	0.105	0.593
Mn	970 ± 73	821 ± 80	1133 ± 186	0.981	0.229
K	9342 ± 533	9301 ± 372	8517 ± 373	0.562	0.382

Element	Range for healthy sugar maple (mg · kg^{-1}) (Kolb and McCormick, 1993)
Ca	5000–21900
Al	32–60
Mg	1100–4000
Mn	632–1630
K	5500–10400

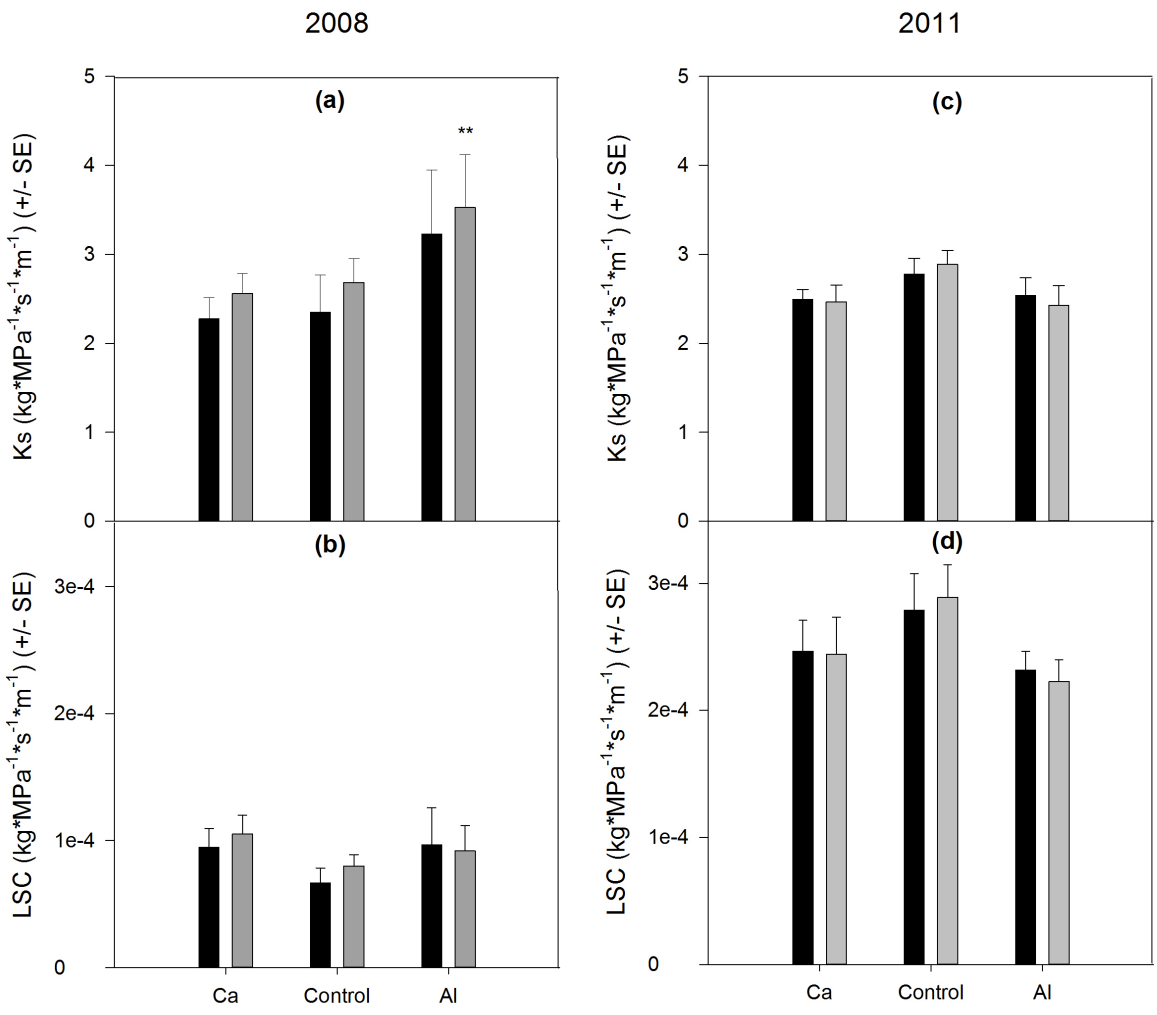

Figure 1.1. Comparison of hydraulic conductivity in *A. saccharum* across treatments for 2008 (left column) and 2011 (right column). Measurements were made for both native (initial conductivity: black bars) and flushed (native embolisms removed: grey bars). Values were adjusted for xylem-specific conductivity (Ks) (a,c) and for leaf-specific conductivity (LSC) (b,d). Values are means ± SE (2008 N = 10; 2011 N = 8).

in trees amended with Al. An analysis of LSC for both native and flushed stems showed no significant differences in comparisons between treatments. There were no significant treatment differences in the existence of native embolisms (native K_s vs. flushed K_s) for either K_s or LSC ($P = 0.946$, $n = 10$; $P = 0.685$, $n = 10$; respectively). In 2011, there were no differences in comparisons between treatments for either K_s (Figure 1.1; $P = 0.229$, $N = 8$) or LSC (Figure 1.1; $P = 0.068$, $N = 8$). Furthermore, in 2011 there were no differences in treatment comparisons for the existence of native embolisms (native K_s vs. flushed K_s) in either K_s or LSC ($P = 0.518$, $n = 8$; $P = 0.581$, $n = 8$; respectively). An analysis of Huber Value showed no differences between treatment comparisons in 2008 (Figure 1.2; $P = 0.206$, $N = 10$) or 2011 (Figure 1.2; $P = 0.612$, $N = 8$).

Vulnerability to Cavitation

In both 2008 and 2011, there were no significant differences in comparisons of treatments in vulnerability to cavitation (Figure 1.3). In 2008, there was no significant difference between treatments in P50 ($P = 0.136$, $N = 5$) or in MCP ($P = 0.356$, $N = 5$). Similarly, in 2011 there was no significant difference between treatments in P50 ($P = 0.689$, $N = 8$) or in MCP ($P = 0.853$, $N = 8$).

Wood Density

A comparison of wood density (dry weight per fresh volume) was made for both the 2008 and 2011 collection (Figure 1.4). In 2008, there was no treatment difference in wood density ($P = 0.215$, $N = 10$). Similarly, in 2011 there was no treatment difference in wood density ($P = 0.258$, $N = 8$).

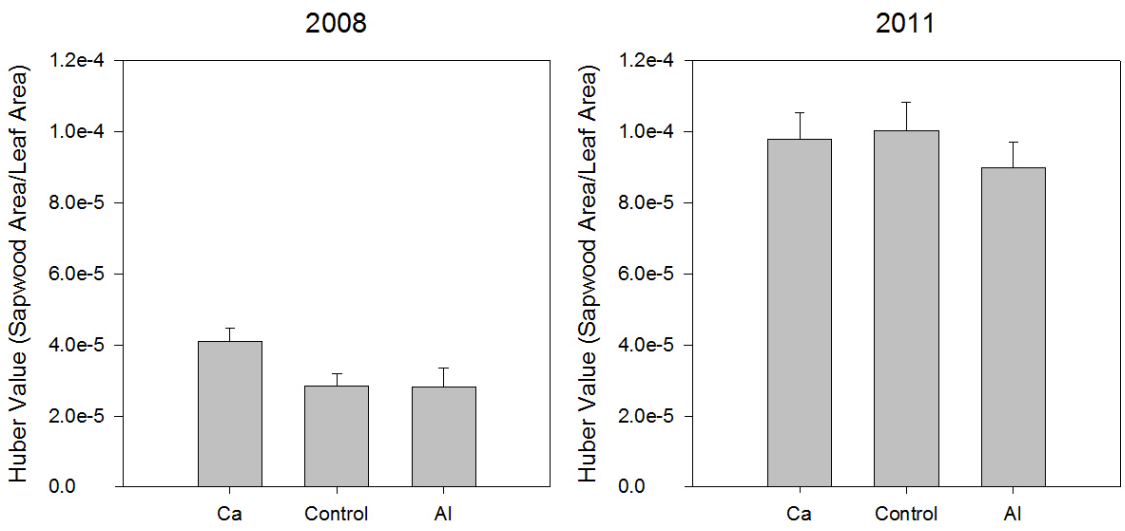

Figure 1.2. Treatment differences in Huber Value of *A. saccharum* for both the 2008 (left panel) and 2011 (right panel) collection. Values are averages of the sapwood area/leaf area ± SE (2008 N = 10; 2011 N = 8).

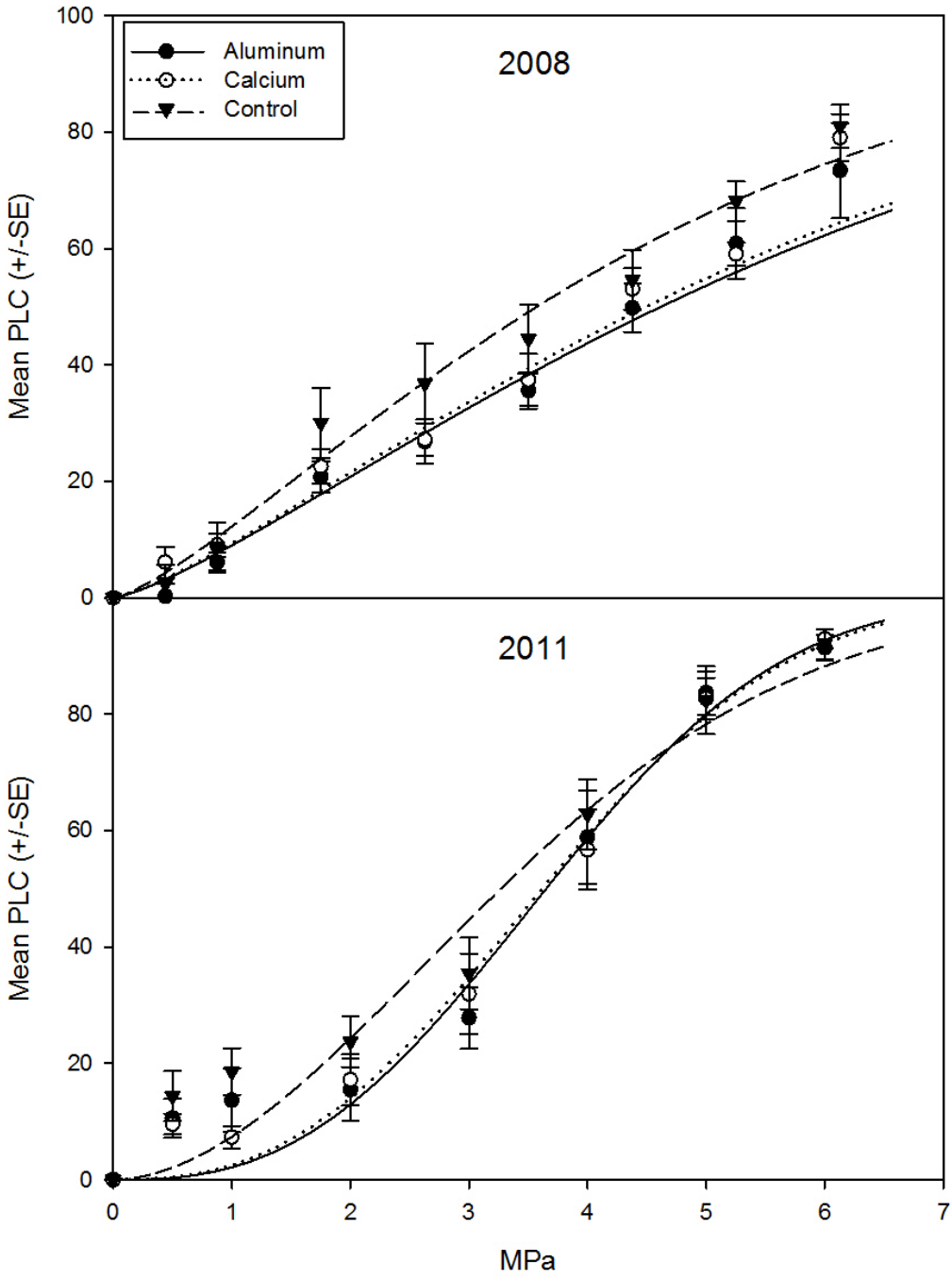

Figure 1.3. Treatment differences in *A. saccharum* PLC for both the 2008 (top panel) and 2011 collections (bottom panel). The data are fitted by least squares regression with a Weibull function. In 2008, there were no treatment differences in P50 (P = 0.146, N =5) or MCP (P = 0.219, N = 5). In 2011, there no treatment differences in P50 (P = 0.689, N = 8) or in MCP (P = 0.853, N = 8). Values are the average PLC ± SE (2008 N = 5; 2011 N = 8).

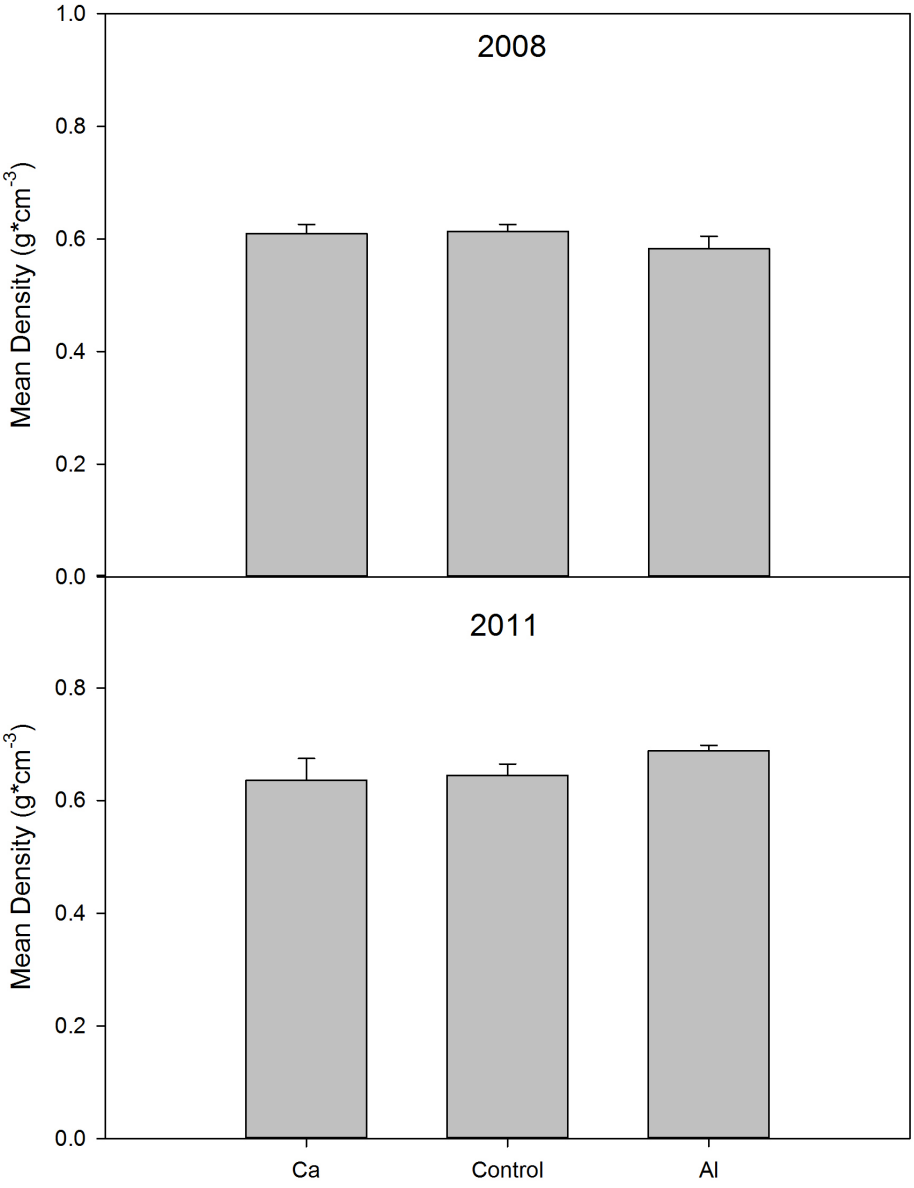

Figure 1.4. Treatment differences in wood density (dry weight per fresh volume) in *A. saccharum* for both 2008 (top panel) and 2011 (bottom panel). Values are means ± SE (2008 N = 10; 2011 N = 8).

Leaf Water Relations

In 2008, an analysis of leaf water relations showed no significant differences in the turgor loss point in trees growing on Ca-amended, control, or Al-amended plots (Figure 1.5). There was no clear separation in the turgor loss point in regards to treatment (Ca N = 7, Control N = 8, Al N = 8).

Ion-Mediated Stem Flow

There was a significant difference in the percent increase in K_s as a result of changing ionic composition of perfusion solution (i.e. 10 mM KCl, 10 mM $CaCl_2$, or 10 mM $AlCl_3$) over perfusion with DI H_2O (Figure 1.6) ($P < 0.001$, N = 5). Perfusion solution with $AlCl_3$ resulted in a significantly higher increase in flow rate over DI H_2O (55%) compared to perfusion solution of KCl or $CaCl_2$. There was no difference in the percent increase in K_s between KCl or $CaCl_2$.

Xylem-Bound Ca on Vulnerability to Cavitation and Air Seeding Thresholds

Analyses of the impact on vulnerability to cavitation resulting from the removal of xylem-bound Ca in sugar maple were conducted in both mid-winter 2011 and mid-summer 2012 (Figure 1.7). In December 2011, there was no significant difference between treatments of $NaPO_4$ pH10 compared to $NaPO_4$ pH4 in P50 ($P = 0.146$, N =5) or MCP ($P = 0.219$, N = 5). In June 2012, there was no significant difference between treatments of $NaPO_4$ pH10 compared to $NaPO_4$ pH4 in P50 ($P = 0.096$, N = 5) or in MCP ($P = 0.111$, N = 5).

A comparison of perfusion solutions of 10 mM $NaPO_4$ pH10, 10 mM $NaPO_4$ pH4, 10 mM KCl pH10, 10 mM KCl pH4, or 10 mM EGTA pH4 on the air seeding threshold pressure of

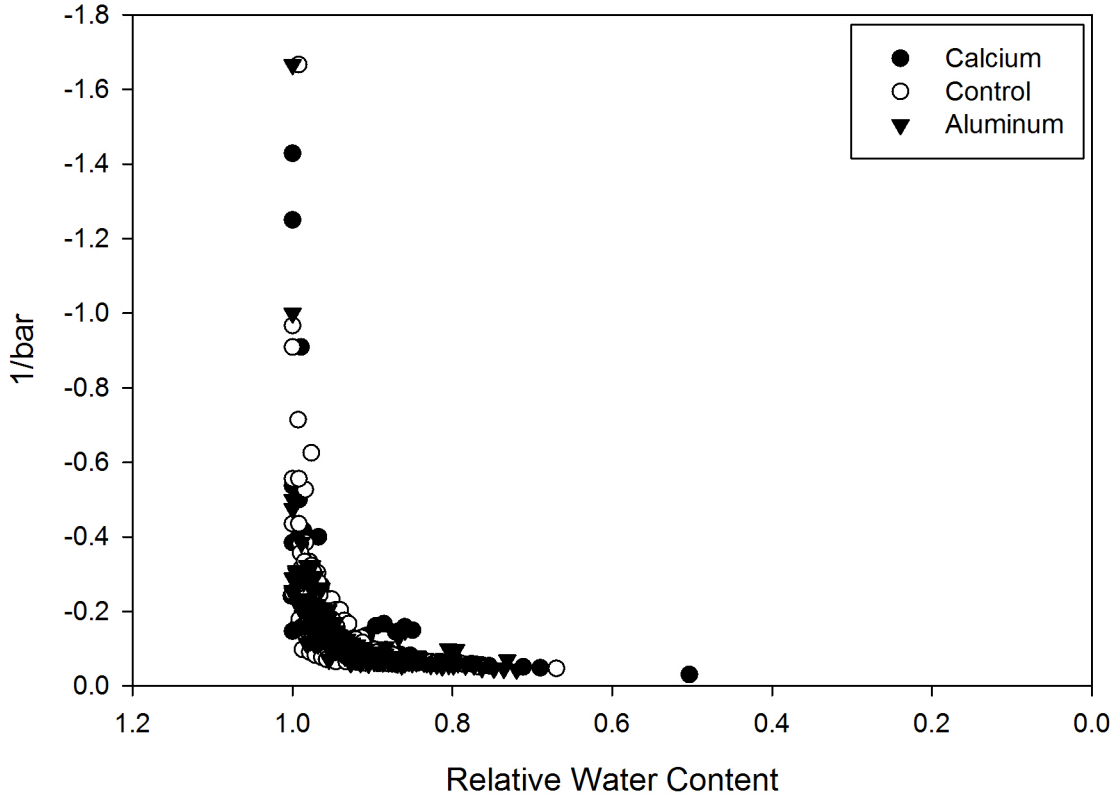

Figure 1.5. Pressure-volume curve for *A. saccharum* leaves collected from each treatment. Relative water content is mass of the final water content (g) per initial water content (g) (Ca N = 7, Control N = 8, Al N = 8)

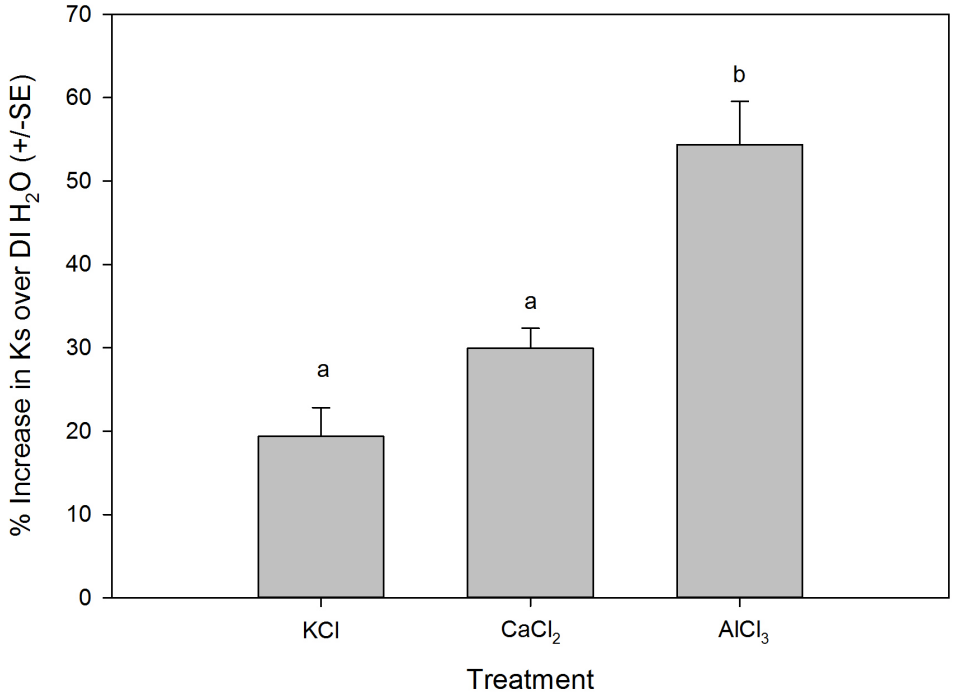

Figure 1.6. Effect of ionic solution on xylem-specific hydraulic conductivity in *A. saccharum*. Values are calculated as the mean percent increase in K_s compared to DI H_2O (± SE). Different letters are significantly different according to a Tukey-Kramer HSD test ($P < 0.001$, $N = 5$).

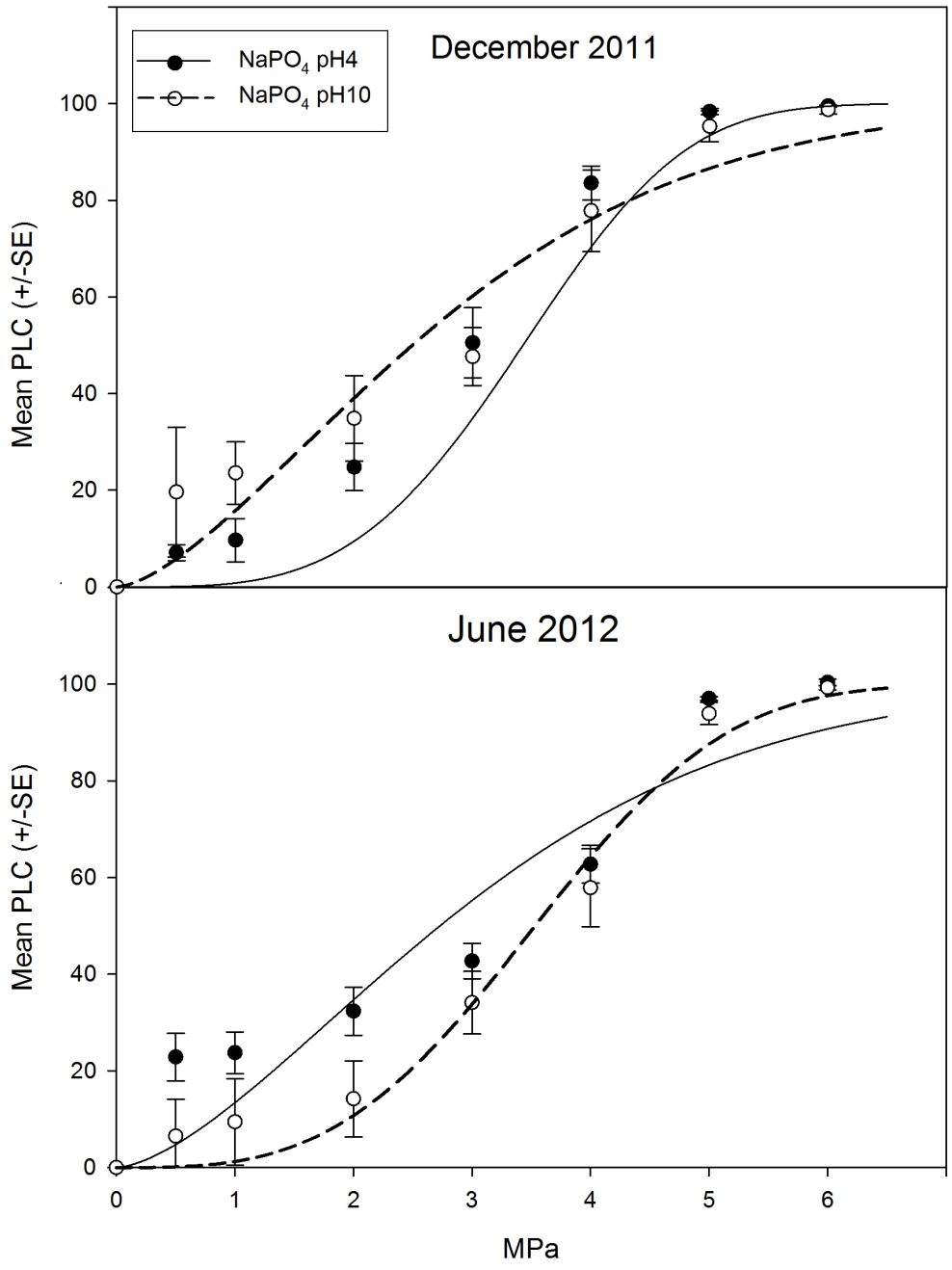

Figure 1.7. Vulnerability to cavitation in stems of *A. saccharum* following perfusion with 10mM $NaPO_4$ pH4 or 10mM $NaPO_4$ pH10. Tests were conducted in both mid-winter (upper panel) and mid-summer (lower panel). In December 2011, there were no treatment differences in P50 (P = 0.146, N =5) or MCP (P = 0.219, N = 5). Similarly, in June 2012, there were no treatment differences in P50 (P = 0.096, N = 5) or in MCP (P = 0.111, N = 5). The data are fitted by least squares regression with a Weibull function. Values are the average PLC ± SE.

individual vessels in sugar maple found no difference between treatments (Figure 1.8) ($P = 0.094$; $NaPO_4$ pH10 N = 28, $NaPO_4$ pH4 N = 27, KCl pH10 N = 8, KCl pH4 N = 9, or EGTA N = 7). Specifically, perfusion solutions of 10 mM $NaPO_4$ pH10 and 10 mM EGTA, which were previously shown to increase vulnerability to cavitation in both conifers and angiosperms as a result of removal of xylem-bound Ca (Herbette and Cochard 2010), showed no significant impact on the pressure required to force gas across bordered pit membranes of individual vessels in sugar maple.

DISCUSSION

The hypothesis that Ca-related reductions in cell growth and stabilization compromise the function of conductive tissue was tested. The proven correlation between cavitation resistance and wood density and structure provided a potential mechanism linking xylem function with the availability of Ca. Surveying forest-grown sugar maples (*Acer saccharum* Marsh.*)* from a long-term replicated Ca-manipulation study at HBEF, there was no significant impact of Ca-deficiency on wood density, stem hydraulic conductivity, or vulnerability to cavitation. Furthermore, no difference in leaf water potential was detected between treatment trees. Experiments investigating the removal of xylem-bound Ca on stem hydraulic properties revealed no treatment impact on vulnerability to cavitation or on single vessel air seeding thresholds.

Analyses of foliar cation content in trees used for the HBEF study confirm the effectiveness of the established treatment regime (Table 1.2). But, since the last assessment of foliar cation levels (Huggett et al. 2007), there appears to be a decline in the impact of treatments. In comparing foliar cation levels collected in 2011 to that of 2004 (Table 1.3), there appears to be less of a

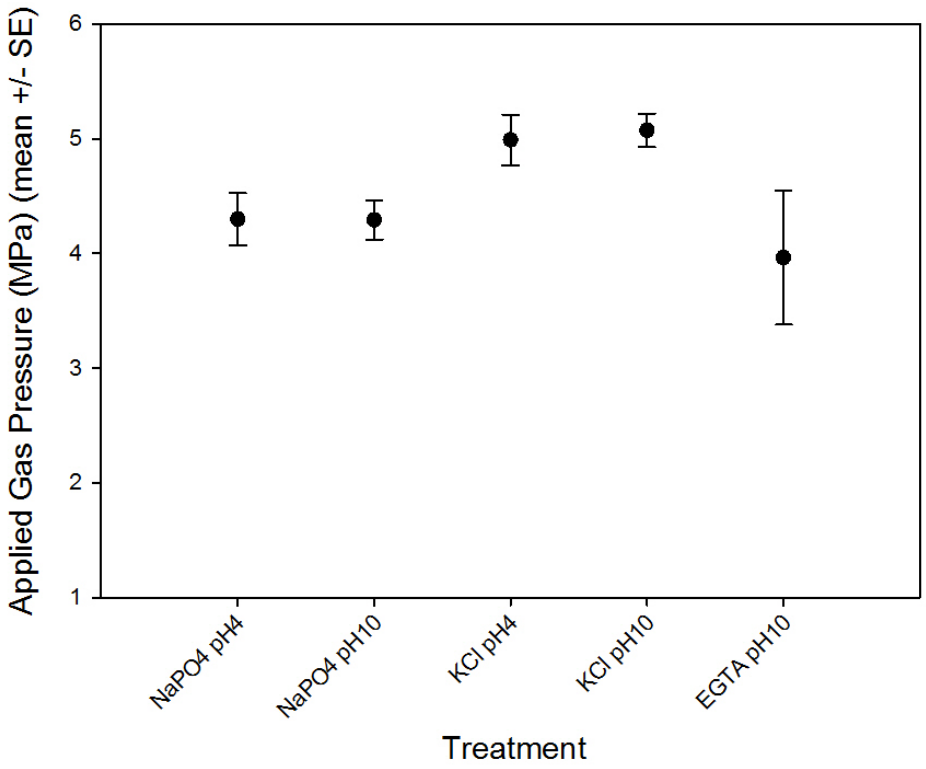

Figure 1.8. Air seeding thresholds of individual vessels in *A. saccharum* following various perfusion solutions (10mM $NaPO_4$ pH10, 10mM $NaPO_4$ pH4, 10mM KCl pH10, 10mM KCl pH4, or 10mM EGTA pH4). Analysis using the Tukey-Kramer HSD test showed no significant difference between treatments (P = 0.092). Values are means ± SE for $NaPO_4$ pH10 N = 28, $NaPO_4$ pH4 N = 27, KCl pH10 N = 8, KCl pH4 N = 9, or EGTA N = 7.

Table 1.3. Comparison of foliar cation concentrations for *A. saccharum* trees in 2011 and in 2004 from Ca-addition, Control, and Al-addition study plots. A reference to published range of foliar cations for healthy sugar maples is provided (Kolb and McCormick 1993). Results are means ± SE for 2011 (Ca N = 8, Control N = 8, Al N = 7) and for 2004 (N = 20 for each treatment). NOTE: Data for the 2004 collection were originally published in Huggett et al. (2007), and are being reprinted here for comparison.

		Treatment means (mg · kg^{-1})			Significance of contrasts (P value)	
	Element	Ca	Control	Al	Ca vs. Control and Al	Control vs. Al
2011	Ca	6935 ± 444	4927 ± 682	5123 ± 543	0.036	0.824
	Al	35.9 ± 3.4	38.5 ± 2.5	37.9 ± 4.6	0.613	0.925
	Mg	1533 ± 83.7	1237 ± 182	1113 ± 135	0.105	0.593
	Mn	970 ± 73	821 ± 80	1133 ± 186	0.981	0.229
	K	9342 ± 533	9301 ± 372	8517 ± 373	0.562	0.382
2004	Ca	7960 ± 478	5505 ± 440	4507 ± 392	0.004	0.283
	Al	30.5 ± 1.4	37 ± 1.7	40 ± 2.4	0.029	0.410
	Mg	1128 ± 71	1006 ± 74	882 ± 82	0.304	0.538
	Mn	1107 ± 79	1113 ± 107	1097 ± 108	0.984	0.999
	Fe	44.8 ± 2.0	45.3 ± 1.2	48.0 ± 2.1	0.443	0.356
	K	6941 ± 227	7596 ± 191	7493 ± 279	0.058	0.769

Element	Range for healthy sugar maple (mg · kg^{-1}) (Kolb and McCormick 1993)
Ca	5000–21900
Al	32–60
Mg	1100–4000
Mn	632–1630
Fe	59–130
K	5500–10400

significant treatment impact on total foliar Ca levels in trees growing on the Ca-amended plots compared to both the control and Al-amended plots. Differences in foliar Ca levels on control plots compared to Al-amended plots in both years remain insignificant, but levels consistently border the minimum threshold associated with healthy sugar maple published by Kolb and McCormick (1993). Unlike 2004, total foliar Al levels in 2011 were not significantly lower in trees grown on the Ca-amended plots compared to the control of Al-amended plots. These results indicate an overall decline in treatment effectiveness at the study plots. Possible explanations for declines in foliar Ca levels could be related to the gradual degradation in the release of Ca from the single Wollastonite pellet application in 1998 (Table 1.1). Furthermore, the lack of significant difference in total foliar Al levels in 2011 could result from the frequency of Al addition to the plots, which has declined from annual applications from Oct. 1995 until Oct. 1998, to sporadic applications eventually occurring every three years from Nov. 2005 until June 2011. A final explanation for the lower levels of foliar Ca collected in 2011 compared to 2004 could be a result of collection methods. In 2004, leaves were collected from the sun exposed upper canopy with the use of a shotgun, compared to 2011 in which leaves were collected mid-canopy shade leaves with the use of pole pruners. The difference in sun (2004) vs. shade (2011) leaves could account for the observed reduction in total foliar Ca levels and treatment effectiveness due to the fact that transport of Ca into foliar tissue via the xylem is strongly related to levels of transpiration (Marschner 1995).

In both the 2008 and 2011 study of hydraulic conductivity, specifically K_s and LSC, in trees from HBEF showed no effect of treatment (Figure 1.1). In 2008, measurements were made utilizing the pressure drop flow meter. Due to lengthy transport times post-collection, the

processing time of 3.5 days, and the intricacy of the flow meter technique, there was justification to repeat such measurements in 2011. Despite shortening the transport and processing times, and transitioning to measuring hydraulic conductivity using a balance, the collection in 2011 produced similar results in terms of the treatment impacts on K_s or LSC. Although in 2008 there was significantly higher rates of flushed K_s in trees growing on Al-amended plots compared to Ca-amended or control plots, these findings were not replicated in 2011. Furthermore, in both 2008 and 2011, there were no treatment differences in the existence of native embolisms (native K_s vs. flushed K_s) in either K_s or LSC. Differences in LSC are often driven by the Huber Value, calculated as the transverse xylem area per gram dry weight of leaves distal to measurement. In 2008 and 2011 analyses, there were no treatment differences in Huber Value of sampled trees.

The initial study in 2008 investigating the treatments impacts at HBEF on vulnerability to cavitation in sugar maple showed no significant differences between treatments in either P50 or MCP (Figure 1.3). Concerns over transport and processing times, in addition to problems inherent with the air injection method, led to a replication of measurements in 2011. With the use of the centrifuge technique in producing vulnerability curves, processing time could be reduced and some of the problems with the air injection method could be avoided, such as the tendency for stems to release gas for considerable amounts of time post-air injection and prior to measurements of hydraulic conductivity. Despite improved methods in 2011, there existed no treatment differences in vulnerability to cavitation, either for P50 or MCP (Figure 1.3). For both 2008 and 2011, there were no treatment differences in wood density (Figure 1.4). As a baseline measurement, differences in wood density resulting from Ca deficiency were expected to reflect

in vulnerability to cavitation due to the positive correlation demonstrated between resistance to cavitation and increased xylem density (Hacke et al. 2001b).

Studies on ion-mediated stem hydraulic conductivity revealed that sugar maple stems perfused with high amounts of $AlCl_3$ resulted in a significant increase in flow rate (55%) compared to stems perfused with DI H_2O (Fig 1.6). The expectation was that increased amounts of Al would decrease flow rates because of the ability of Al dissociate Ca ions bound to pectate and to reduce the porosity of cell walls by disrupting Ca cross-linkages (Rengel and Zhang 2003). Zwieniecki et al. (2001b) hypothesized that cross-linking of the pectin matrix by ions compresses hydrogels and increases the size of micro-pores located in the pit membrane, resulting in higher rates of hydraulic conductivity. It is possible that despite the abilities of Al to dissociate Ca from pectate, Al itself acts as a strong ion cross-linking the pectin matrix and thus increases the hydraulic conductivity of xylem in sugar maple. These results imply that forest-grown sugar maples subjected to Al toxicity may have higher rates of stem hydraulic conductivity.

To investigate the impact of Ca removal on vulnerability to cavitation and single vessel air seeding thresholds, sugar maple stems were perfused with various Ca chelators to remove xylem-bound Ca. Herbette and Cochard (2010) recently found that stems perfused with $NaPO_4$, EGTA and oxalic acid successfully removed xylem-bound Ca and increased vulnerability to cavitation, particularly in *Fagus sylvatica*. Testing these perfusion solutions on other species, they found that the greatest increases in vulnerability to cavitation due to removal of xylem-bound Ca was found in tree species with higher resistance to cavitation. Considering that sugar maple is similar *Fagus sylvatica* in that P50 is generally around -4 MPa, these methods were adopted in an effort

to better understand the role of Ca in sugar maple vulnerability to cavitation and strength of border pit membranes. Perfusion solutions of 10 mM $NaPO_4$ pH10 and 10 mM EGTA, which were previously shown to increase vulnerability to cavitation as a result of removal of xylem-bound Ca (Herbette and Cochard 2010), showed no significant impact on sugar maple vulnerability to cavitation or the pressure required to force gas across border pit membranes of individual vessels (Figs. 1.7 and 1.8). Herbette and Cochard (2010) hypothesize that variation in the shift of vulnerability to cavitation in response to removal of Ca is due to the presence of specific pectin domains (i.e. homogalacturonan) and the activity of pectin methyl esterase (PME), which removes methyl ester groups allowing for Ca cross-linking of pectin chains. Based on this hypothesis, sugar maples may exhibit a minimal level of PME activity, which would reduce the amount of Ca cross-linking of pectin chains (Pelloux et al. 2007); hence the inability to significantly increase vulnerability to cavitation or to reduce the air seed threshold of individual vessels in this tree species by the removal of xylem-bound Ca.

The impact of Ca depletion on the water relations of sugar maple remains inconclusive. There are factors contributing to these negative results, first of which being the effectiveness of treatments at the HBEF. Considering the declines in treatment-related differences in total foliar cation levels (particularly Ca and Al) (Table 1.3), it is possible that levels of Ca have not reached a deficiency threshold that would impact the stem water relations of sugar maple. Secondly, considering the documented treatment-related incidences in severity of both branch dieback and reduction in crown vigor of sugar maple on these plots (Huggett et al. 2007), methods included the collection of uniformly healthy branches to avoid confounding results. The decision to select only healthy branches was reflected in findings of no treatment differences in turgor loss point of

leaves. It is possible, that the impacts of Ca deficiency on stem structure and function are not yet prevalent in healthy branches across treatments. Lastly, based on tests investigating the impact of removing xylem-bound Ca on vulnerability to cavitation and air seeding thresholds of single vessels, it is possible that Ca does not play as crucial a role in sugar maple xylem structure and function due to the lack of cross-linking of pectin chains in bordered pit membranes compared to other species.

CHAPTER 3

The Impact of Hemlock Woolly Adelgid (*Adelges tsugae* Annand) Infestation of the Water Relations of Eastern Hemlock (*Tsuga canadensis* (L.) Carrière).

INTRODUCTION

Hemlock woolly adelgid (HWA) (*Adelges tsugae* Annand) is an invasive insect introduced to the United States from East Asia. First reported in 1951 in the eastern United States (Souto et al. 1996), this insect has spread rapidly into the northeastern United States and has been responsible for the decline and often death of many eastern hemlock trees (Orwig et al. 2002). HWA feed on xylem ray parenchyma cells at the base of young needles, ultimately causing loss of vigor and premature needle drop to the point of defoliation (Young et al. 1995; Stadler et al. 2005). Feeding cycles of the HWA on eastern hemlock occur in the spring to early summer and again in the fall with a period of aestivation during the warmer summer months (Stadler et al. 2005). Mature stands of eastern hemlock can succumb to death within 4 years of HWA infection (McClure 1991).

Although infestations and subsequent impacts on forest health are well documented (Orwig et al. 2013), little is known regarding the exact physiological processes in eastern hemlock altered by this invasive pathogen. One hypothesis is that the HWA depletes photosynthate stores in the parenchyma cells of eastern hemlock resulting in needle loss and an overall reduction in growth and crown vigor (i.e. branch dieback, bud mortality) (McClure 1991; Young et al. 1995). Based on the major role of foliar nitrogen in photosynthetic enzymes, Domec et al. (2013) hypothesized that increased foliar nitrogen in response to HWA infestation was an indication that trees

compensate for the loss of photosynthate by increasing rates of photosynthesis. Increases in photosynthetic rates in response to insect infestation and subsequent defoliation has been documented in *Larix leptolepis*, *Pinus resinosa*, *Pinus radiate*, and *Aesculus hippocastanum* (Hoogesteger and Karlsoon 1992; Vanderklein and Reich 1999; Eyles et al. 2011)

Recent studies have further hypothesized that eastern hemlock mortality resulting from HWA infestation is due to a decline in hydraulic conductivity resulting from the HWA-induced formation of abnormal wood, primarily false rings (Gonda-King et al. 2012; Domec et al. 2013). False rings are the formation of dark colored latewood bands of thick-walled tracheids that are not continuous in circumference in the stem and exhibit a gradual transition to earlywood on either side of the band (Stokes and Smiley 1996). The formation of false rings (termed "rotholz") in Fraser fir (*Abies faseri*) in response to balsam woolly adelgid (*Adelgis piceae* (Ratzeburg) (BWA) was documented by Hollingsworth and Hain (1992). Based on experiments conducted on BWA infested *Abies sp.* utilizing acid fuchsin dye infusion (Mitchell 1967) and water-permeability of stems under suction (Puritch 1971), Hollingsworth and Hain (1992) concluded that BWA infestation caused a reduction in effective sapwood area and subsequently an increase in flow resistance. Domec et al. (2013) have recently drawn a correlation between the formation of abnormal xylem cells (i.e. false rings and increased parenchymal cells) in mature eastern hemlock trees infested by HWA and a decline in the stem hydraulic conductivity measured with a hydraulic conductance flow meter . Gonda-King et al. (2012) and Domec et al. (2013) concluded that a greater proliferation of latewood type cells in response to HWA infestation would reduce hydraulic conductivity (Gonda-King et al. 2012; Domec et al. 2013). Contrary to this hypothesis, if growing conditions are favorable following formation of false rings, tracheids

could be larger and thinner than the previous latewood-like cells (Wimmer et al. 2000). Supporting this claim, recent studies on the impact of artificial or insect-induced defoliation events have found no effect on tracheid lumen area and in some cases, an overall increase in xylem production per year with wider conduits as a result of an increased presence of false rings (Salleo et al. 2003; Thomas et al. 2006; Rossi et al. 2009). An increase in stem hydraulic conductivity will be associated with this increase in conduit area, which could be a mechanism for the tree to compensate for the limitation in nutrient and water supply as a result of insect-induced defoliations (Salleo et al. 2003).

Considering that HWA feed on photosynthate stores in the tree and as a result, induce changes in photosynthetic rates, alter xylem structure and function, and cause defoliation, such infestations could alter plant nutrient partitioning. During the first year of HWA infestation of eastern hemlocks, levels of %N were found to be lower in infested compared to uninfested trees and equal after a second year post-infection (Miller-Pierce et al. 2010). Analysis of %N levels in trees several years post-infection by HWA show a strong increase in foliar N levels compared to uninfected trees (Stadler et al. 2005; Gómez et al. 2012; Domec et al. 2013). In particular, HWA infestation caused changes in foliar amino acid composition such as increased levels of proline, a common response in plants to water stress, and glutamine, which functions as an assimilatory enzyme for ammonia (Rhodes et al. 1999; Miflin and Habash 2002; Gómez et al. 2012). Changes in total foliar cation concentrations in response to HWA have not been investigated, but pre-existing differences in the foliar cation composition of eastern hemlock trees has been hypothesized to increase susceptibility to the HWA (Pontius et al. 2006).

Previous research indicates that HWA insect infection at the leaf level affects photosynthesis, wood formation, and nutrient partitioning. Uncertainty remains as to what extent such changes in stem anatomy affect hydraulic conductivity and function. An increase in false rings in response to HWA infestation could lead to larger tracheid lumen area and thus, higher hydraulic conductivity, but such changes may increase vulnerable to cavitation. Furthermore, alterations in stem hydraulic conductivity, photosynthesis, and increased defoliations, might impact nutrient partitioning in response to HWA infestation. The goal of this study is to investigate the impact that HWA infestation have on the water relations, stem structure and function, and nutrient partitioning in eastern hemlock.

MATERIALS AND METHODS

Study Site

Experiments were conducted at a pre-existing experimental manipulation site established by Miller-Pierce et al. (2010) to investigate the impact of infestation of hemlock woolly adelgid (*A. tsugae*) (HWA) and elongate hemlock scale (*Fiorinia externa*) on the growth and foliar chemistry of Eastern hemlock (*Tsuga canadensis*). Details of this experimental site are outlined in Miller-Pierce et al. (2010) and Gonda-King et al. (2012) and are as follows. In 2007, 0.7-1 m hemlock saplings were collected from Pelham, MA; this site is on the northern boundary distribution limit for both *A. tsugae* and *F. externa*. Observations of both saplings and surrounding trees confirmed the absence of either insect infestation. The saplings were transplanted in a rectangular grid in an open field located at East Farm, University of Rhode Island, (Kingston, RI). Utilizing a randomized complete block design, trees within each row were randomly assigned a treatment of *A. tsuga*, *F. externa*, or control. Inoculations occurred in

spring 2007-2011. To prevent cross contamination, each tree was covered by an 1 x 1 x 2 m (length x width x height) enclosure consisting of PVC piping and mosquito netting. Analysis of insect densities conducted in fall and spring from 2007-2010 (Gómez et al. 2012) and again in summer of 2011 and spring 2012 (Soltis and Orians, unpublished data) confirm effectiveness of treatments.

Only HWA infested hemlock trees and control hemlock trees were used for comparisons in this study. Collection of plant material occurred on June 9th 2011 and June 16th 2011. For measurements of stem hydraulics, entire branches were removed from each tree with hand pruners in the early morning. Prior to excision, the branch was wrapped in plastic and filled with water to ensure that the initial cut was made while underwater (Wheeler et al. 2013, *in revision*). After excision, the branch was immediately recut under water to remove a 30 cm stem segment. Stem samples were kept submerged in water and cooled for transport to the laboratory and until processing. Branches and needles distal to the cut stem segment were collected, stored in large Ziploc bags, and kept cool for transport and until processing.

Hydraulic Conductivity

Measurements of hydraulic conductivity (K_h) of hemlock were conducted by measuring flow driven by a gravity head through a stem sample to an analytical balance (Sartorius CPA225D) (Sperry et al. 1988). A perfusion solution of 10 mM KCl in de-ionized ultra-filtered water (DI H_2O) (Millipore MilliQ UV plus) was used. Prior to all measurements, the perfusion solution was re-filtered through a 0.2 μm syringe filter (Pall acrodisc syringe filters). From the 30 cm stem segments collected in the field, a section three to seven years old, 3.25-8.7 mm diameter

and 14.5 cm in length, was re-cut underwater. Prior to measurements, both ends of the stem were shaved with a sharp razor blade. Percentage loss of conductivity (PLC) was calculated as [100 (1- $K_{initial}$ / K_{max})] where $K_{initial}$ refers to initial conductivity (native) and K_{max} is the maximum conductivity (flushed) measured after removal of embolisms by flushing stems with 10 mM KCl at 0.1 MPa for 20min. Hydraulic conductivity was referenced to xylem cross-sectional area (xylem-specific conductivity, K_s) or leaf area supported by xylem (leaf-specific conductivity, LSC). Xylem area was measured with image analysis (ImageJ Software, National Institutes of Health) of xylem cross sections from the distal end of each stem and calculated by taking the average diameter of two perpendicular cross-sectional axes. Leaf area distal to the measured stem segment was calculated with the LI-3100 Area Meter (Li-Cor, Inc.). Using three foliar subsamples form each branch, a ratio of average needle area to mass was calculated. This ratio was then multiplied by the total needle mass per branch to provide the total needle area per branch. Huber value was calculated as a ratio of sapwood area to needle area.

Vulnerability to Cavitation

Vulnerability of xylem to cavitation was measured the centrifuge technique (Alder et al. 1997) with a perfusion solution of 10 mM KCl in DI H_2O (Millipore MilliQ UV plus). Prior to all measurements, the perfusion solution was re-filtered through a 0.2 μm syringe filter (Pall acrodisc syringe filters). Hydraulic conductivity was calculated by flow driven from a gravity head through each stem sample to an analytical balance. Stem segments were prepared as stated above. All stems were decorticated up to 5 mm at each end to allow for proper seal during hydraulic conductivity measurements and flushed with 10 mM KCl at 0.1 MPa for 20mins prior to spinning in the centrifuge. Hydraulic conductivity was measured after each pressure of 0, 0.5,

1, 3, 5, 7, and 9 MPa (3mins of rotation time for each pressure) and vulnerability to cavitation calculated using PLC [100 (1- K_{result}/ K_{max})] where K_{result} refers to conductivity following each stage of increased pressure and K_{max} is the maximum conductivity (flushed) measured after removal of embolisms by flushing stems. Mean cavitation pressure (MCP) was calculated by plotting vulnerability curves as the loss of hydraulic conductivity per unit xylem pressure change (compared to PLC which is plotted as the cumulative loss of conductance). Then the mean of this distribution is calculated based on the mid-point of each pressure change (Sperry and Ikeda 1997).

Photosynthesis and Stomatal Conductance

On June 9th 2011, six HWA infected trees and eight control trees were measured for net photosynthetic rate and stomatal conductance. Measurements were made on adelgid-free current year needles from randomly chosen, sun-exposed, upper canopy branches using a portable photosynthesis system (LI-6400, LiCor, Lincoln, Nebraska, USA). Use of a LiCor Needle Chamber (LiCor 6400-07) with a clear Propafilm window chamber top allowed for measurements under natural light. An average of three measurements per shoot were taken. A photograph through the clear chamber top was taken of each set of needles measured and used to calculate needle density using image analysis (ImageJ Software, National Institutes of Health). A dot matrix image scaled to the chamber size and consisting of 294 evenly spaced dots was layered on top of each image. The number of dots overlaying needle tissue was counted and calculated as a fraction of the total number of dots. This percentage was used to represent the density of needles in the chamber exposed to light. Needles shaded by the stem or other needles

were not included in the calculation of needle density. The net rate of photosynthesis was adjusted using this parameter of needle density.

Leaf Water Potential

Leaf water potential in relation to treatment was measured using the Scholander pressure-bomb technique (Scholander et al. 1965). At pre-dawn and at mid-day, two shoots per tree, of current year growth and 10cm in length, were collected, sealed in individual Ziploc bags with a wet paper towel, and covered in a dark container. Samples were immediately transported back to the laboratory for processing. For each sample, the entire 10cm shoot was placed inside the pressure-bomb chamber for measurement and an average water potential of 2-3 shoots per tree was taken.

Wood Anatomy and Growth Rate

From 30cm stem segments collected in the field, a distal portion of the stems used for hydraulic measurements was collected and fixed in formalin : acetic acid : ethyl alcohol (FAA; 1 : 1 : 9) for anatomical measurements. The base of each stem was mounted on a sliding microtome and two 40 μm sections per branch were taken. Sections were placed in 0.1% safranin O stain solution (filtered through a 0.2 μm syringe filter) for 2 min and rinsed in DI H_2O for 2 min. Sections were then mounted on glass slides with 50% glycerol to prevent dehydration. Analysis of cross-sections was conducted using fluorescent microscopy at 20x magnification. Samples were photographed in a series of four radial files extending from the bark to the pith. In each sample, one radial file free of compression wood was analyzed for tracheid dimensions with the use of ImageJ Software; an average of 958 tracheids per stem was measured. Average

tracheid lumen area (A_t) was calculated as the total lumen area in each image divided by the total number of tracheids in each image. Tracheid diameter was calculated to determine the hydraulically weighted mean diameter (D_h) based on the calculation $D_h=\sum d^5/\sum d^4$, where d is the diameter of a conduit (Sperry et al. 1994). Based on the Hagen-Poiseuille law, the D_h weights tracheid diameter with the estimated hydraulic conductance of the conduits. Growth rate was calculated by dividing the age of each stem by the total area of each stem.

Foliar Chemical Analysis

Foliar cation analysis was conducted on sample specimens collected on June 9th 2011 and June 16th 2011. From branches removed for measurements of hydraulic conductivity and vulnerability to cavitation, needles of mixed age classes were collected and oven-dried at 55°C. Levels of %N in addition to P, K, Ca, Mg, Na, Zn, Cu, Mn, Fe, and B were measured using the method of inductively coupled plasma atomic emission spectrometry performed by the University of Massachusetts Soil and Plant Tissue Testing Laboratory (Amherst, MA, USA).

Statistical Analysis

Prior to all analyses, a Levene's Test for equality of variances was run. Independent two-sample t-tests were used to compare differences in means between HWA infested trees and control (HWA free) trees. All analyses were performed using SPSS statistical software.

RESULTS

Hydraulic Conductivity and Cavitation Resistance

Analyses of K_s and LSC showed significant differences between HWA infested tree (N = 13) and control trees (N = 16) (Figure 2.1). There were significantly higher rates of flow for HWA trees compared to control trees for both native K_s and flushed K_s ($P = 0.046$, $P = 0.05$; respectively). Similarly, HWA infested trees had higher rates of conductivity for both native LSC and flushed LSC ($P < 0.001$). All comparisons between native and flushed K_s and for native and flushed LSC within treatments were insignificant ($P > 0.1$). Differences in LSC between treatments are largely driven by the higher Huber Value in HWA trees compared to control trees (Figure 2.2; $P < 0.001$, HWA N = 13, control N = 16). There were no significant treatment differences in vulnerability to cavitation (Figure 2.3, HWA N = 13, control N = 15). Specifically, there was no significant difference between treatments in P50 ($P = 0.136$) or in MCP ($P = 0.356$).

Photosynthesis and Stomatal Conductance

A comparison of net photosynthetic rate (μmol CO_2 m^{-2} s^{-2}) showed a significant difference between treatments (Figure 2.4; $P = 0.038$). There were significantly higher rates of photosynthesis on HWA trees compared to controls trees. Although there was a trend for higher rates of stomatal conductance (mmol m^{-2} s^{-2}) in HWA trees compared to control trees, there was no significant difference between treatments (Figure 2.4; $P = 0.155$).

Leaf Water Potential

Measurements of leaf water potential at pre-dawn and mid-day showed no significant treatment differences (Figure 2.5; $P = 0.219$, $P = 0.181$, respectively).

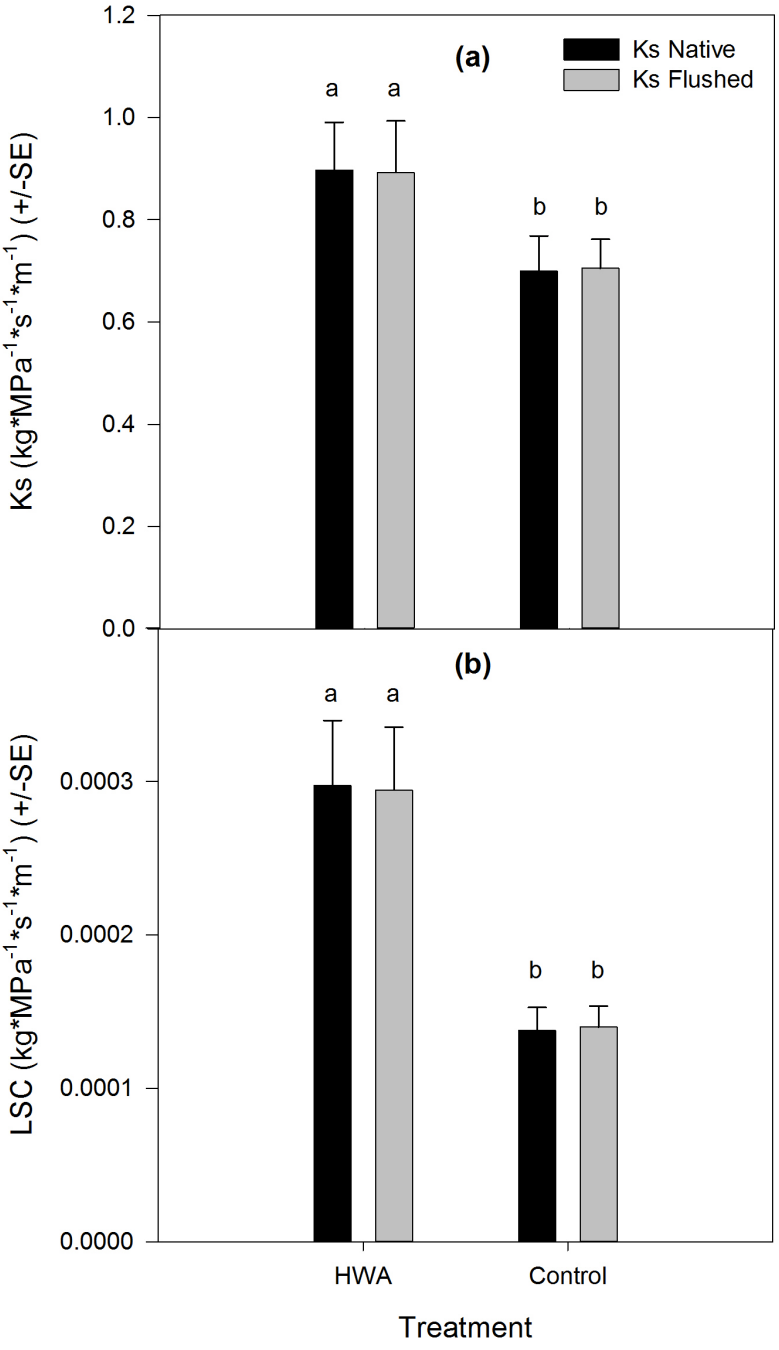

Figure. 2.1. Comparison of hydraulic conductivity in *T. canadensis* across treatments of Hemlock Woolly Adelgid (HWA) and control. Measurements are of native (initial conductivity: black bars) and flushed (native embolisms removed: grey bars) hydraulic conductivity. Values were adjusted for xylem-specific conductivity (K_s) (a) and for leaf-specific conductivity (LSC) (b). Values are means ± SE (HWA N = 13; Control N = 16). Different letters are significantly different according to an independent two-sample t-test at the $P < 0.05$ level.

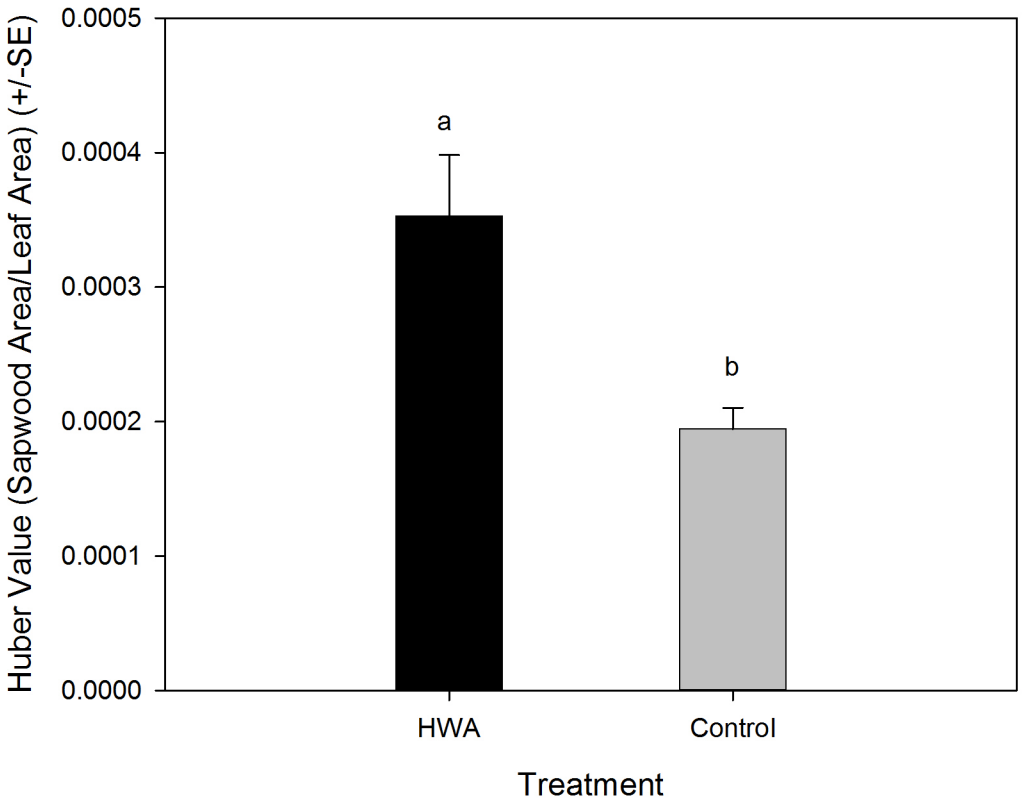

Figure. 2.2. Treatment differences in Huber Value in *T. canadensis*. Values are averages of the sapwood area/leaf area ± SE (HWA N = 13; Control N = 15). Different letters are significantly different according to and independent two-sample t-test at the $P < 0.05$ level.

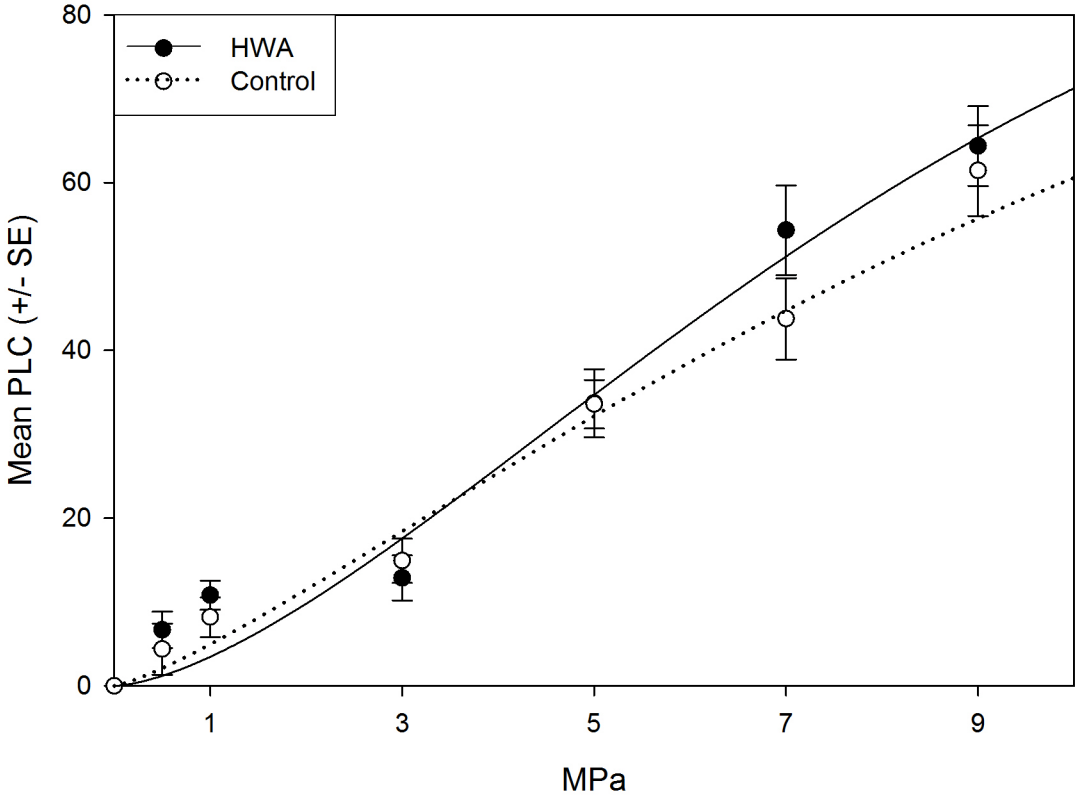

Figure. 2.3. Treatment differences in *T. canadensis* percent loss of conductivity (PLC). The data are fitted by least squares regression with a Weibull function. There are no treatment differences in P50 (P = 0.136) or MCP (P = 0.356). Values are the average PLC ± SE (HWA N = 13; Control N = 15).

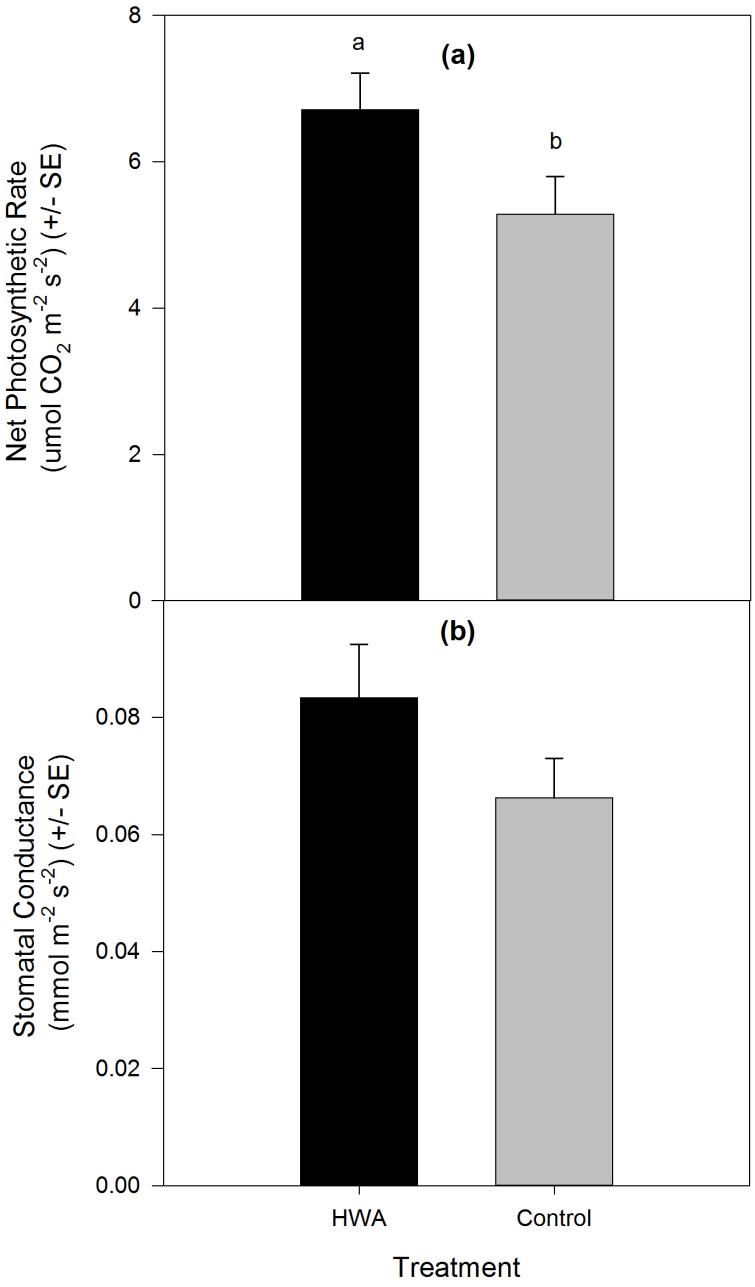

Figure. 2.4. Treatment differences in *T. canadensis* net photosynthetic rate (a) and stomatal conductance (b) (HWA N = 6; Control N = 8). Different letters are significantly different according to an independent two-sample t-test at the $P < 0.05$ level.

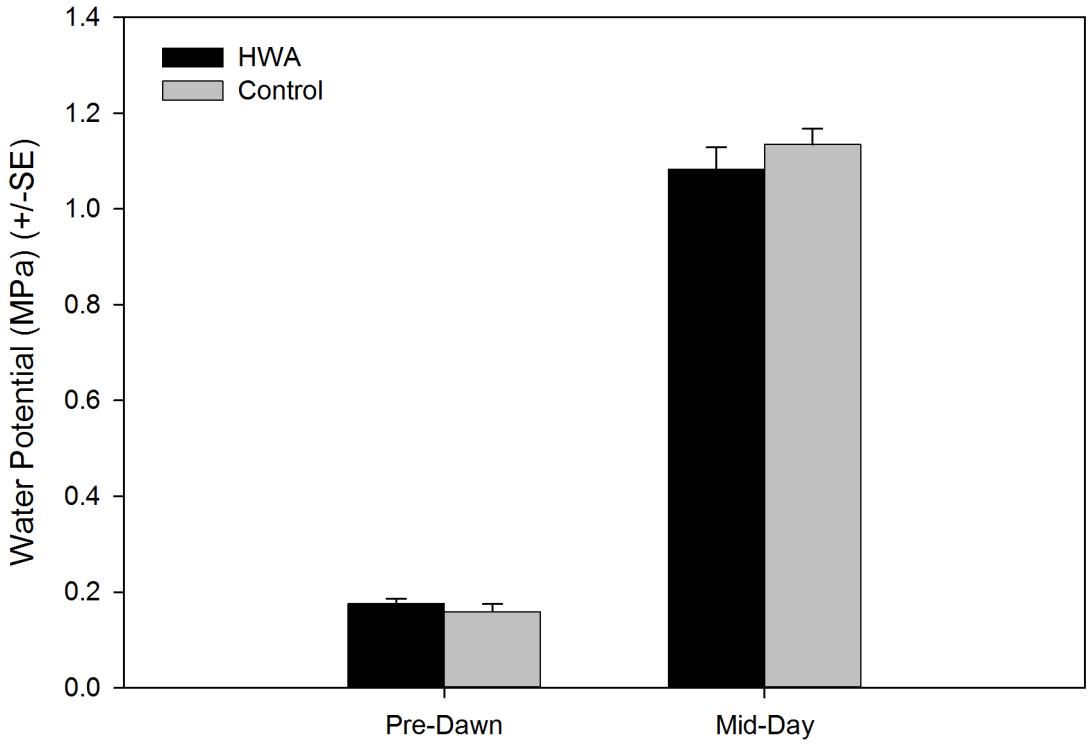

Figure. 2.5. Treatment differences in leaf water potential in *T. canadensis* at pre-dawn and mid-day (HWA N = 6; Control N = 8).

Wood Anatomy and Growth Rates

Trees infected with HWA exhibited larger A_t compared to control trees (Table 2.1, $P < 0.01$). Similarly, HWA trees had a higher D_h compared to control trees (Table 2.1, $P < 0.01$). There was no difference between treatments in the growth rate of stems (Table 2.1, $P = 0.331$).

Foliar Chemistry

An analysis of total foliar chemistry of hemlock needles found significant differences between treatments (Table 2.2). Compared to control trees, HWA trees exhibited higher levels of %N in addition to higher levels of P, K, Mg, B, Fe, Na and Mn. There were no treatment differences in the foliar levels of Ca, Mg, Zn, Mn, or Cu.

DISCUSSION

The results from this study are the first to demonstrate that HWA infestations result in an increase in stem hydraulic conductivity. Furthermore, this study demonstrates that HWA infestation can significantly alter the partitioning of foliar nutrients in eastern hemlock trees. Similar to previous studies, HWA infestation can result in an increase in net photosynthetic rates, an increase in %N, and significant changes to the structure and function of wood anatomy. In these sample trees, alterations in xylem structure, particularly the growth of earlywood-type tracheids associated with false rings, results in higher stem hydraulic conductivity and larger tracheid lumen area in trees infested with HWA. The observed treatment differences in foliar nutrient partitioning in HWA infested trees could be in response to higher levels of net photosynthetic rates and frequent defoliation events.

Table 2.1. Treatment differences in wood anatomy and growth rates of *T. canadensis*. Results are means ± SE (HWA N = 13; Control N = 15). Means in the same row with different letters are significantly different ($P \leq 0.05$). A_t, average tracheid lumen area; D_h, hydraulically weighted mean diameter.

	HWA	Control
	Mean ±SE	Mean ±SE
A_t (μm^2)	$128.37 \pm 10.04_a$	$89.80 \pm 8.92_b$
D_h	$16.24 \pm 0.56_a$	$13.65 \pm 0.60_b$
Growth Rate	$46.05 \pm 5.38_a$	$42.22 \pm 5.39_a$

Table 2.2. Analysis of treatment differences in foliar chemistry of *T. canadensis*. Results are means ± SE (HWA N = 13; Control N = 15). Means in the same row with different letters are significantly different ($P \leq 0.05$).

	HWA	Control
Element	Mean ± SE	Mean ± SE
%N	$2.23 \pm 0.08_a$	$1.96 \pm 0.06_b$
P (ppm)	$2623 \pm 96_a$	$2238 \pm 106_b$
K (ppm)	$5189 \pm 254_a$	$4441 \pm 267_b$
B (ppm)	$28.4 \pm 1.7_a$	$21.0 \pm 0.9_b$
Fe (ppm)	$47.8 \pm 2.1_a$	$42.6 \pm 0.9_b$
Na (ppm)	$93.6 \pm 4.8_a$	$75.1 \pm 3.5_b$
Ca (ppm)	$3453 \pm 274_a$	$3477 \pm 293_a$
Mg (ppm)	$1249 \pm 98_a$	$1372 \pm 105_a$
Zn (ppm)	$19.5 \pm 1.9_a$	$17.2 \pm 1.3_a$
Mn (ppm)	$26.2 \pm 3.2_a$	$26.6 \pm 5.5_a$
Cu (ppm)	$3.73 \pm 0.31_a$	$3.55 \pm 0.34_a$

Gonda-King et al. (2012) have calculated that trees from this study show a 50% increase in false rings in branches of HWA infested trees compared to control trees. Unlike recent studies (i.e. Domec et al. 2013), an increase in the amount of false rings is not negatively associated with K_s. It should be noted that tests conducted by Domec et al. (2013) were on mature 40 year-old trees; although infection history was similar, an age-affect cannot be ruled out. These results from 3–7 year-old branches show increases in K_s and LSC in branches of trees infested with HWA compared to control trees (Figure 2.1). Measurements of LSC are strongly inflated by insect-induced defoliations of infected trees, as reflected by an increase in Huber Value (Figure 2.2). But increases in K_s in this study can only be attributed to alterations in xylem anatomy in response to HWA infestation. In support of this finding, anatomical measurements of tracheid dimensions of these trees showed an increase in A_t and H_d in trees infected with HWA compared to control trees. As suggested by Wimmer et al. (2000), in the case of treatment trees in this study, favorable growing conditions such as adequate light and nutrient availability could have resulted in the observed increases in A_t and H_d as growth resumes following periods of stress and false ring formation. Although there was no treatment-induced difference in growth rates (Table 2.1), these findings were quite similar to Salleo et al. (2003) who showed that insect-induced defoliation events resulted in an increase in the occurrence of false rings which in turn were associated with the production of more wood per year with wider conduits and higher conductive area. In response to HWA infestation and loss of photosynthetic tissue due to defoliation, higher K_s could be a response by the tree to transport more water and nutrients to remaining needles in an effort to meet the demands of increased photosynthetic rates (Figure 2.4).

Branches sampled from HWA infested trees were not water-stressed compared to branches collected from control trees. In measurements of native vs. flushed K_s and LSC, there were no significant differences between treatments, suggesting that HWA infested trees were not subject to a greater degree of impaired hydraulic transport due to higher rates of embolisms (2.1). Further tests showed that despite an overall increase in K_s due to associated increases in A_t and H_d, HWA infested trees did not exhibit an increased vulnerability to cavitation compared to control trees (Figure 2.3). This result is counter to the expectation of a trade-off of higher vulnerability to cavitation associated with increased tracheid conductive area (Sperry et al. 1994; Lens et al. 2010). Lastly, there was no treatment-induced difference in leaf water potential, implying that HWA trees were not under increased water stress compared to control trees.

Analysis of foliar %N levels and total foliar cations showed significant differences between treatments. Similar to previous studies (Stadler et al. 2005; Gómez et al. 2012; Domec et al. 2013), there was an increase in foliar %N in response to HWA infestation. Coupled with this result was that HWA trees exhibited a significant increase in net photosynthesis, and a trend although not significant, towards higher stomatal conductance (Figure 2.4). Increases in both foliar %N and photosynthetic rates could be a stress response of the tree in an effort to compensate for depleted photosynthate stores (Domec et al. 2013) and loss of foliage (Eyles et al. 2011) due to HWA infestation. In addition, increases in foliar nutrient levels could be a product of reduced leaf mass due to repeated HWA-induced defoliations. In trees subjected to HWA infestation, there were significantly higher levels of foliar P, K, B, Fe, and Na (Table 2.2). HWA-induced increases in photosynthesis could drive the demand for ions such as P, (involved in protein synthesis), K, (a key component of stomatal regulation and ATP synthesis via

photophosphorylation), Fe (an essential element for chlorophyll development and function) and B (involved in membrane integrity and function, particularly facilitating transport of K for guard cell regulation) (Marschner 1995). Due to the various roles of Ca in regulating many of the physiological processes involved in plant growth and responsiveness to environmental stress (e.g. direct or signaling roles in systems involved in plant defense and repair of damaged tissue) (McLaughlin and Wimmer 1999), foliar Ca levels were expected to be higher in plants subjected to HWA infestation. An explanation for the lack of treatment difference in foliar Ca levels could be that Ca transported through the xylem is bound to cell walls in cation exchange complexes (CEC) (Kirkby and Pilbeam 1984). The observed increase in the tracheid lumen area of HWA infested trees might have resulted in greater cell wall area and a higher number of CEC's serving as binding sites, or sinks, for Ca in the xylem (Clarkson 1984). However, the similar levels of foliar Ca in the two treatments does serve as confirmation that sampling across treatments was of equal aged needles, as levels of total foliar Ca have been shown to double with an increase of 1 year in needle age due to the relative inability of plants to translocate Ca out of leaves via phloem (DeHayes et al. 1997).

The results from this study suggest possible mechanisms for the decline in health and frequent death of eastern hemlock in response to HWA infestation. The correlation between increased hydraulic conductivity and tracheid lumen area could come at a biomechanical cost, as increases in tracheid lumen area following false ring formation could result in compromises in the biomechanical integrity of the woody tissue. Such results would support the findings that HWA infestation decreases the strength and flexibility of branches below the infection site (Soltis et al. 2012). In regards to impact on foliar nutrient partitioning, an explanation put forth by Gómez et

al. (2012) is applicable in that due to the seasonal feeding habits of HWA, intermittent stress events resulting in elevated foliar nutrient levels could in turn make individual eastern hemlocks more palatable to the HWA. This theory is supported by research showing that foliar chemistry (particularly increased N and K) can greatly increase eastern hemlock susceptibility to HWA (Pontius et al. 2006). It is clear that HWA-induced defoliation is a vital segment of this disease cycle, which ultimately leads to death of eastern hemlock trees. This research demonstrates that alterations in wood anatomy in response to HWA infestations do not result in an inadequate supply of water that would precipitate such defoliation events. For this reason, more work is needed to understand how HWA feeding habits, and subsequent stress responses in the tree, might impact transport processes at the leaf level, which could lead to defoliation and mortality in these trees.

CHAPTER 4

Aspects Of Vessel Dimensions in the Aerial Roots of Epiphytic Araceae

This chapter has been reformatted from the published version:

Huggett, B.A., and Tomlinson, P.B. 2010. Aspect of Vessel Dimensions in the Aerial Roots of Epiphytic Araceae. International Journal of Plant Sciences 171: 362-369.

INTRODUCTION

We describe a simple method of determining vessel dimensions in aerial roots of epiphytic Araceae. We chose this material because of their accessibility, extreme length and distinctive stelar organization. The method requires little more than a digital camera, optical microscope, and a computer. Vessel dimensions can be measured accurately and objectively *in situ*.

Vessels in angiosperms are composed of linear series of cells (vessel elements) that lose their contents at maturity so that they function as hollow conduits in water transport. Although vessels are routinely described and some dimensions often given, these dimensions are never complete in the absence of a statement about vessel length, which is rarely provided. Nevertheless, vessel length is an important component of the conductive properties of plant organs, as is knowledge of any interconnection among vessels (Zimmermann 1983; Sperry et al. 2007).

The parameters of vessel networks can only be obtained by three-dimensional analysis and this has been done using serial sections of wood samples of limited size, thereby demonstrating the vessel network in secondary xylem (Zimmermann and Jeje 1981). A diversity of methods, some extremely innovative, has been developed especially to deal with particularly intractable plants, like palms and lianes mainly in order to measure very long vessels. Cinematographic methods, whereby serial or sequential sections are photographed frame-by-frame with a ciné camera, have been employed extensively (Zimmermann 1976) and used to measure metaxylem vessel length in the palm *Rhapis excelsa* in relation to its vascular configuration (Zimmermann et al. 1982). For lianes the air-method and "paint method" were devised, but these require the vessels to be cut off at one or both ends, so that an estimate, rather than a measure, of vessel length is obtained. The vessel casting method of André (2005) is an alternative approach, but is based on a measure of a model, rather than the organ itself. A common obstacle is the notion that these methods are intrinsically tedious (Kitin et al. 2004) and can be supplanted by more sophisticated equipment, but tedium is an essential element of the scientific process. Here we employ a simple, cost-effective method of analysis that provides in situ measurements of vessel length, vessel end overlap length, vessel diameter, and vessel stelar orientation. Our method is applied to a particularly distinctive plant organ, but its inherent simplicity suggests it could have wide application.

Aerial roots in many epiphytic or hemi-epiphytic members of the Araceae can be conspicuous components of the tropical forest and have unusual developmental and structural properties. They arise adventitiously from the rhizomes (but not underground) of plants growing along the branches of high canopy trees, the roots growing downwards as free-hanging structures until they

reach the ground, whereupon they branch and become anchored in the soil, providing a direct hydraulic pathway to the parent axis. Unimpeded these roots remain unbranched in air, but may branch if they are damaged. Eschrich (1983) measured rates of growth in greenhouse conditions of up to 2.5 cm per day. Physiologically they are distinctive because they only assume a major water transport function after they reach the soil, even though their vascular tissues are completely mature, as described later. Simple experiments (P. B. Tomlinson and C. J. Quinn, unpublished) show that the xylem does transport water upwards in the free-hanging state, possibly as back-flow from phloem sap moving acropetally. There is only limited comparative study of aroid aerial roots (Keating 2003) and we restrict ourselves to stelar anatomy although cortical tissues can be quite diverse, (e.g., the familiar H-shaped trichosclereids of *Monstera* (Bloch 1946)).

MATERIALS AND METHODS

Fresh material was obtained from the Kampong Garden of the National Tropical Botanic Garden and Fairchild Tropical Garden, 10901 Old Cutler Road Coral Gables, FL 33156 USA, either from a tall tree with the help of a mechanical hoist (Figure 3.1 A), or as reachable directly from the ground (Figure 3.1 B). J.B. Fisher and Gustavo Romero supplied additional dried material. Four taxa were investigated, each with a distinctive stelar anatomy. *Heteropsis spruceana* Schott, *Monstera deliciosa* Liebm., and *Philodendron* sp. (a hybrid cultivar of horticultural origin) and *Philodendron undulatum* Eng.. Roots up to 7 m long were coiled and either fixed in F.A.A. (85 parts 70% ethanol, 10 parts glacial acetic acid, 5 parts 40% formaldehyde) or examined fresh. Fixation was used to minimize the possibility of tylose formation, although this seems to occur rarely in these roots. After fixation roots were washed

Figure 3.1. Morphology and development of roots of epiphytic aroids. A, Pendulous aerial roots being collected from *Philodendron* sp., a high-climbing aroid growing in a specimen of *Quercus virginiana* at Fairchild Tropical Botanic Garden. B, Distal and proximal portions of the aerial root system of *Monstera deliciosa* (~1.0 cm to 1.5 cm diameter) growing on a specimen of *Pimenta officinalis* at the Kampong, Coconut Grove, including apex of an unattached aerial root (foreground) and older-attached roots (background) some of them branched after damage. C, Transverse sections (freehand) cut in sequence at 10 cm intervals from developing root, as in B; stained for lignin with phloroglucinol and concentrated HCl to show that maturation of stelar tissues continues beyond 1 m; at 200 cm the tissues are mature (scale bar at 10 cm = 2 mm; scale bar at 200 cm = 4 cm).

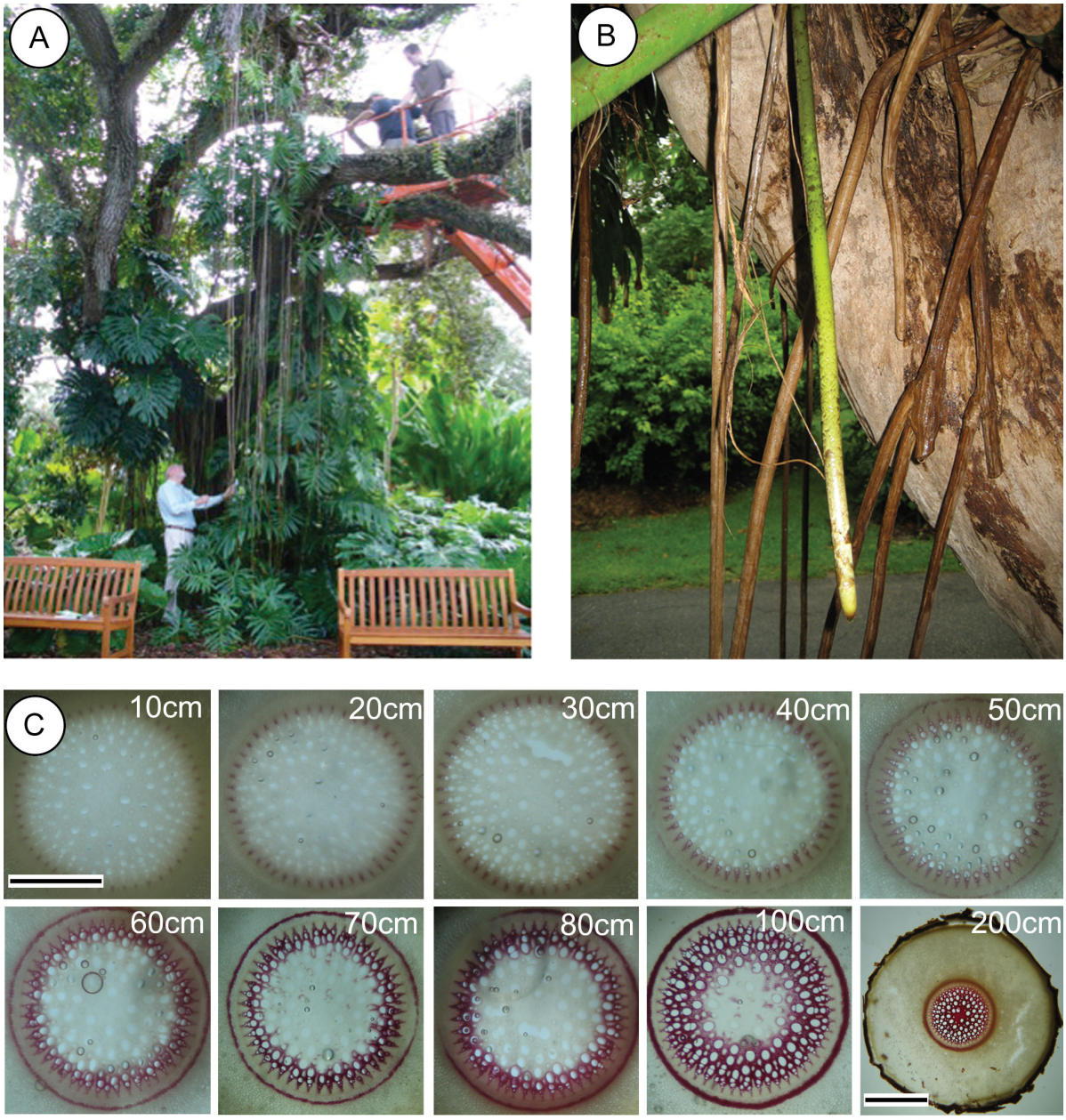

Figure 3.1 (Continued)

well in water and air-dried.

In a preliminary investigation of *Monstera deliciousa* (Figure 3.1 B), complete thick freehand sections (~ 150 μm) of fresh roots were cut sequentially at 1 cm intervals with a single-edge razor blade and mounted individually on slides in dilute glycerine-water (1:1 by volume) ready for photography (Figure 3.2 A). To estimate the longitudinal extent over which stelar tissue was being differentiated, a series from a root tip was cut at 10 cm intervals (Figure 3.1 C) and stained for lignin in phloroglucinol (a saturated solution in 95% ethanol) and concentrated HCl. A longitudinal groove cut along the axis of the root, which appeared in the section as a notch was used for preliminary orientation during photography.

In later work on subsequent other species the roots were decorticated and the stele cut at 1 cm intervals, the sample numbered using an oil-based marking pencil with a constant orientation (e.g., the distal surface to the left of the number), the numbered pieces then stored in sequence. A cut with a sharp edge was necessary to produce a clean surface (Figure 3.2 B-D). For decorticated samples a line was drawn along the surface of the stele to provide preliminary orientation comparable to the notch in sections. The 1 cm lengths of dried root samples were stored in order and could be kept indefinitely.

To examine in detail the type of perforation plate in vessel elements, thin slivers of root stele were macerated, first by boiling for 5 min in 10% aqueous KOH, followed after washing well in water by 20% chromic acid (aqueous CrO_2) for ~ 20 min. The softened material was washed well and teased apart in dilute glycerine on a microscope slide. Such material, after being well

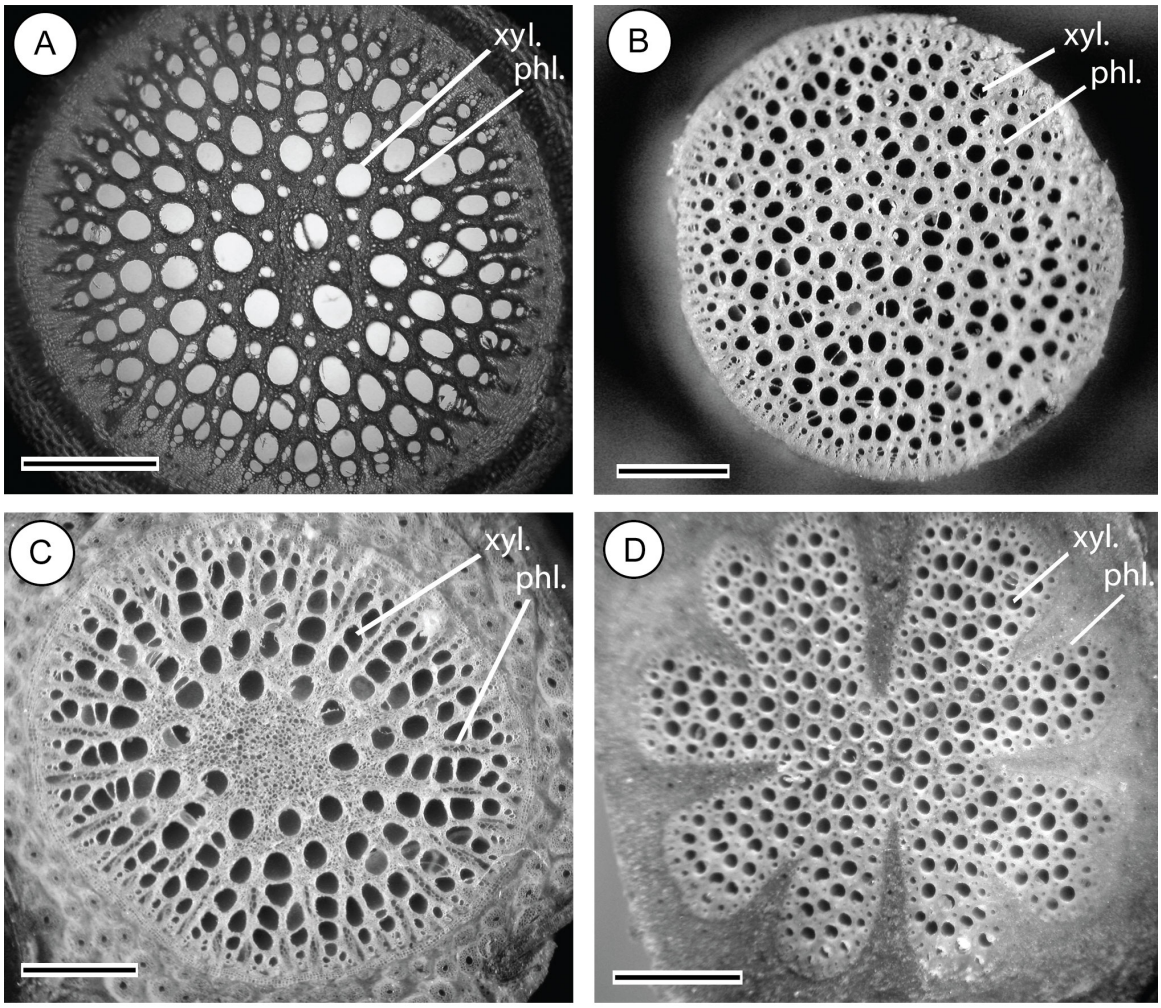

Figure 3.2. Stelar type in aerial roots of representative aroids with xylem (xyl.) and phloem (phl.) labeled. *A*, *Monstera deliciosa*, thick transverse section in transmitted light (scale bar = 1mm). B-D, Planed transverse surface of stele from dried root material. B, *Heteropsis spruceana* (scale bar = 1mm). C, *Philodendron* sp. (scale bar = 1mm). D, *Philodendron undulatum* with stellate stele (scale bar = 3 mm).

washed could be stained in 0.1% toluidine blue and individual elements selected for measurement (Figure 3.3 A). For microscopic details of histology and the distribution of vascular tissue sections 20-30 μm thick were cut on a sliding microtome, stained in 0.1% toluidine blue and mounted in dilute glycerine.

Specimens were photographed in numerical sequence with a digital camera (Coolpix 4500, Nikon Instruments, Tokyo, Japan) either through 2x objective on a Wild M20 compound microscope (Wild, Heerberg, Switzerland) for thin sections, or for the surface of the 1 cm segments by reflected light using an Olympus BH2 dissecting microscope (Olympus, Tokyo, Japan). Photography was done at low resolution and produced a sequence of images with approximately constant orientation.

Images were precisely stacked into superposed layers in sequential order using Photoshop C3 (Version 10.0, Adobe Systems, Inc., USA). Layers were then imported into an animation set at 0.5 or 1.0 second per frame. The resulting animation could be analyzed to determine the length and configuration of every vessel observed throughout the full sequence. For presentations, animations can be exported and projected in movie format. Parameters measured included vessel length, vessel diameter, the length of vessel-vessel end overlap, and vessel position in the stele (radial distance form the center). Statistical analyses comparing vessel dimensions were achieved using simple linear regression. For all tests, analyses were considered statistically significant if $P \leq 0.05$.

Figure 3.3. Details of vessel features in aerial roots of aroids. A, *Monstera deliciosa*, scalariform perforation plate from a vessel element isolated by maceration. B-D, *Monstera deliciosa*, three successive images each 1 cm apart from a movie sequence to show that vessel overlap (v.o.) is longer than 1 cm, but perforation plates (p.p.) are shorter than 1 cm because they only appear in one image. E, *Philodendron undulatum,* one lobe of the stele from a thin (30 μm) transverse section photographed in transmitted light. Three vessel overlaps (v.o.) are included. F, *Philodendron undulatum*, cut surface of the dried stele photographed in reflected light and including four vessels with evident scalariform perforation plates (p.p). Scale bars; A = 400 μm, B-D = 400 μm, E = 400 μm and F = 400 μm.

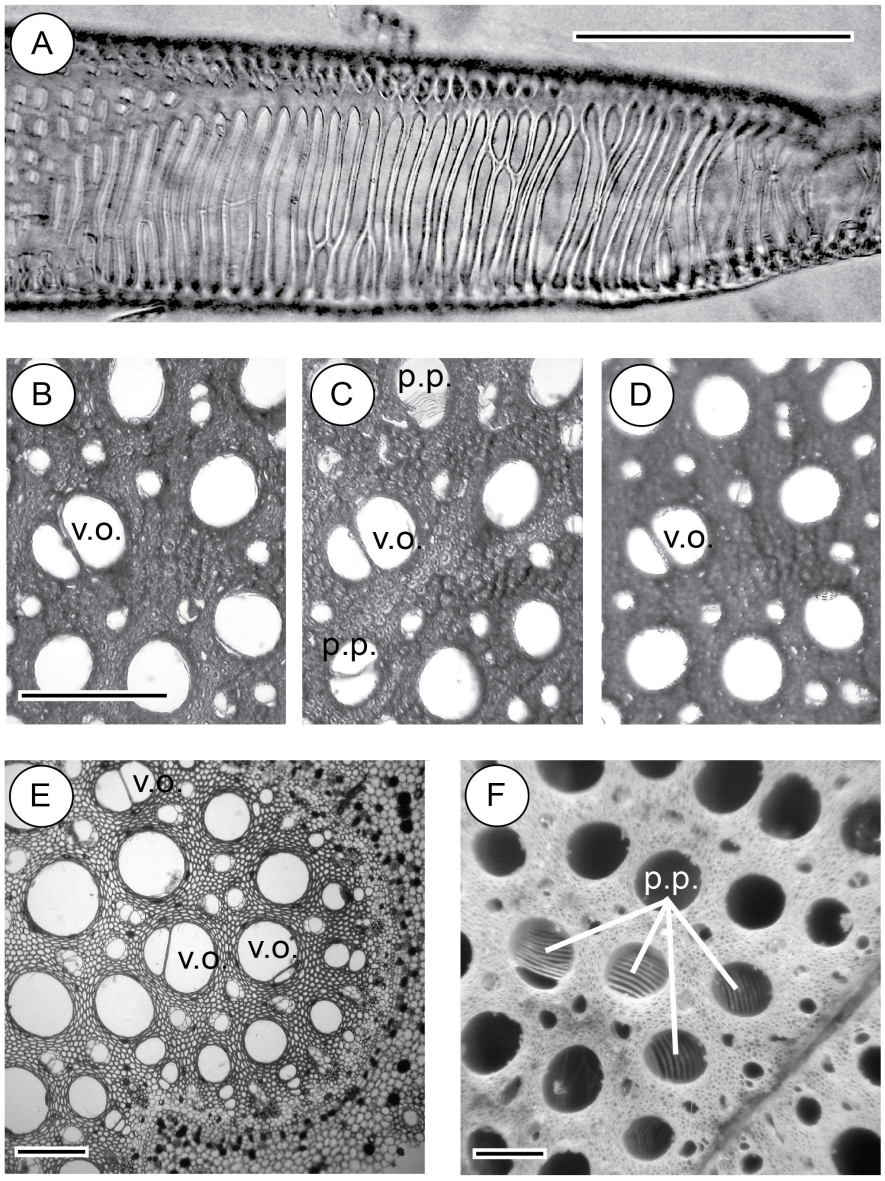

Figure. 3.3. (Continued)

RESULTS

Root morphology and development

Aerial roots of the kind we studied can grow unimpeded as pendulous free-hanging structures until they reach the ground (Figure 3.1 A). If damaged they can regenerate a new root apex in a process that may be characteristic of all roots but remains unstudied. We examined only unbranched roots. The distal end of the root (Figure 3.1 B) is flexible and proximally changes from white to yellow to green (chlorophyllous) to brown as the surface layers mature and ultimately develops a thin periderm. Examination of the maturation of the stelar tissues in *Monstera deliciosa* as indicated by progressive lignification (Figure 3.1 C) in successive sections at 10 cm intervals shows that xylem tissue differentiation continues over a distance of at least 1 m, accounting for the flexibility of the distal end of the root. This long distance and flexibility is a character scarcely possible for roots in soil, but is common in aerial roots that are unimpeded by a solid substrate (e.g., *Rhizophora*). One notes the progressive centripetal maturation of the medullary vessels, with the normal polyarch system maturing first.

Root anatomy

The stele in *Monstera deliciousa*, *Heteropsis spruceana*, and *Phiolodendron* sp. are cylindrical (Figure 3.2 A-C) but a fluted configuration in Philodendron undulatum produces a stellate pattern in transverse section in the wider roots (Figure 3.2 D). The most unusual feature of all plants studied is the presence of xylem (xyl. in Figure 3.2 A-D) and phloem (phl. in Figure 3.2 A-D) interspersed within the medulla which becomes occupied by vessels and sieve tubes; in our material each taxon showing individualistic distribution patterns, either phloem strands

scattered among the metaxylem vessels (Figure 3.2 A, B, and 3.3 E) or radially extended strands (Figure 3.2 C).

Vessel Dimensions

Maceration demonstrates that in all taxa the vessel elements have long oblique scalariform perforation plates with many thickening bars (e.g., p.p. in Figure 3.3 A). In *Philodendron* sp., there are also frequent elements with reticulate perforation plates. In our method of analysis, vessel ends are seen as a gradual tapered overlap between one vessel and the next, separated by a thick common wall (Figure 3.3 B-D). The ending vessel gradually tapers until it disappears; the beginning vessel has a narrow start, which gradually increases in diameter to a maximum. Both vessel overlap (i.e. vessel ends) and perforation plates (i.e. vessel element ends) can be seen in sections (Figure 3.3 C) or surface images (Figure 3.3 E, F) but are easily distinguished; vessel ends each occupy a sequence of images (v.o. in Figure 3.3 B-D), but vessel element ends are never longer than 1 cm (as confirmed by maceration) and so appear in only one image of a series (p.p. in Figure 3.3 C). The number of images in which a vessel end appears is a measure of vessel overlap length to the nearest 1 cm.

In one sample of *Monstera deliciosa*, vessel overlap length ranged from 1 cm to 14 cm with an average vessel overlap of 6 cm (n = 100). In a second sample of *Monstera*, vessel overlap length ranged from 1 cm to 23 cm with an average vessel overlap length of 6 cm (N =109). In our sample of *Heteropsis spruceana*, vessel overlap length ranged from 1 cm to 13 cm with an average vessel overlap length of 5 cm (N =51). Similarly, in *Philodendron* sp., we found vessel overlap lengths from 1cm to 13cm with an average of 5cm (N =55). Vessel overlap length was

not strongly related to stelar position (i.e. distance from center of root) in both samples of *Monstera* ($R^2 = 0.162$, $P < 0.001$; $R^2 = 0.047$, $P = 0.026$; Figure 3.4 A) and in *Philodendron* sp., ($R^2 = 0.0236$, $P = 0.0035$). In *Heteropsis*, analysis of vessel overlap length in relation to stelar position was insignificant ($P = 0.7$).

The frequency of vessel ends in any one section is a qualitative indication of overall vessel length, i.e., few vessel ends implies long vessels. The length of any single vessel can be seen where one pipe includes axially two well-separated overlapping end walls. There is no vessel network in these aerial roots of *Araceae* as in dicotyledonous woods because vessels in all species do not anastomose in a conventional sense since each vessel is continuous axially with another vessel forming an open series of continuous cell lumina, interrupted at wide intervals by vessel ends. We propose the term "pipe" to describe this continuous and un-branched series of vessels.

In our first sample of *Monstera,* vessel length ranged from 9 cm to 163 cm with an average vessel length of 83 cm (N =60). A total of 5 vessels located in the center of the stele lacked overlapping vessel ends indicating that such vessels were much longer than the length of root sectioned (i.e. 181 cm). In our second sample of *Monstera*, vessel lengths ranged from 9 cm to 217 cm, with an average vessel length of 90 cm (N =59). *Heteropsis* exhibited vessel lengths ranging from 10 cm to 51 cm with an average vessel length of 27 cm (N =12). Finally, *Philodendron* sp. contained vessel lengths on the order of 14 cm to 122 cm with an average vessel length of 55 cm (N =27). In an analysis of 60 vessels in a 48 cm long root of *Philodendron undulatum*, there were only two complete vessels measuring 39 cm and 44 cm – a

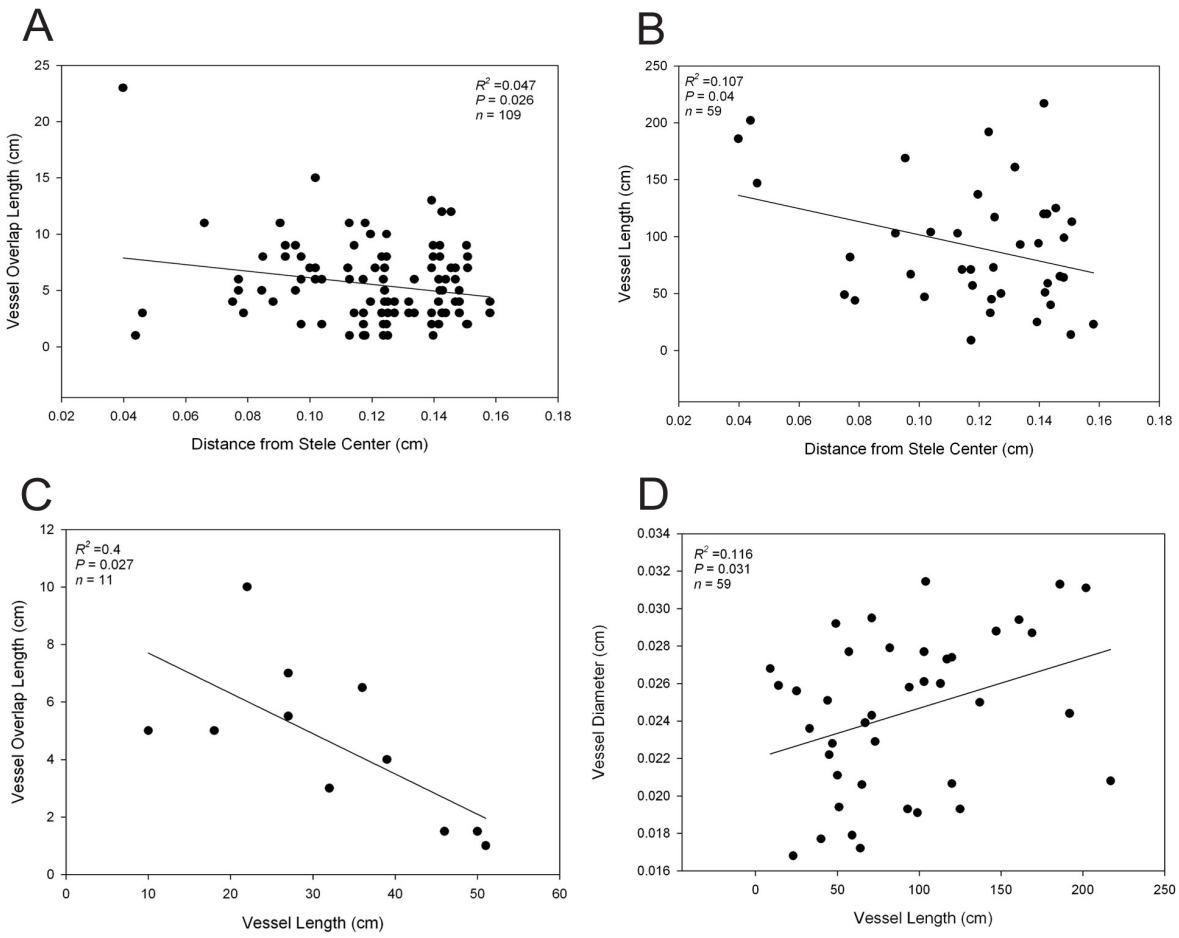

Figure 3.4. Examples of the comparisons of vessel dimensions. *A, Monstera deliciosa*, analysis of vessel overlap length in relation to stelar position; *B*, *Monstera deliciosa*, vessel length in relation to stelar position; *C*, *Heteropsis spruceana*, average vessel overlap length in relation to corresponding vessel length; *D*, *Monstera deliciosa*, vessel diameter in relation to vessel length.

lack of vessel overlap in 55 of the 60 vessels analyzed indicates that vessels in this species are longer than the length of root sectioned (i.e. 48 cm).

Vessel length in relation to stelar position was not strongly related for both samples of *Monstera* ($R^2 = 0.122$, $P = 0.018$; $R^2 = 0.107$, $P = 0.04$; Fig 3.4 B); analyses for *Heteropsis* and *Philodendron* sp. were insignificant ($P = 0.7$ and $P = 0.5$, respectively). A comparison of vessel overlap length in relation to corresponding vessel length showed an inverse relationship in *Heteropsis* ($R^2 = 0.467$, $P = 0.027$; Fig 3.4 C), but was weakly related in both samples of *Monstera* ($R^2 = 0.135$, $P = 0.004$; $R^2 = 0.065$, $P = 0.05$) and insignificant in *Philodendron* sp. ($P = 0.6$).

Vessel diameter in *Monstera, Heteropsis,* and *Philodendron* sp. is not constant along a given radius; peripheral metaxylem elements, as with the outermost elements of the normal polyarch protoxylem poles, are narrow, inner elements are progressively wider. There was a weak relationship between vessel diameter and the corresponding vessel length in *Monstera,* ($R^2 = 0.116$, $P = 0.031$; Fig 3.4 D). Analyses of vessel diameter in relation to vessel length were insignificant in *Heteropsis* ($P = 0.44$) and *Philodendron* sp., ($P = 0.392$).

DISCUSSION

The primary objective of this paper is to demonstrate a simple method for measuring vessel length directly, using a subject easily studied by this approach. The method is objective since vessel ends are easily recognized and provide, via stored images, a complete documentation of the structures observed. The equipment is simple and readily available; single-edged razor blades

or at most a sliding microtome, a digital camera than can be attached to a dissecting or compound microscope, and a computer with appropriate software. Images can thus be captured over a wide range of magnifications. Frame number provides axial dimensions and radial dimensions need only measurement using a stage micrometer. The only limiting factor might be the patience of an observer prepared to cut and align many sections.

In a sense, this method is an extension of the ciné method developed at Harvard Forest in the 1960s (Zimmermann 1976), but now substituting digital for conventional photographic images. Zimmermann's method had been used to measure vessel lengths of up to 40 cm in the small palm *Rhapis excelsa* (Zimmermann et al. 1982). The approach was very easily modified according to the subject under investigation, from herbaceous stems and roots to wood samples sawn into narrow "sticks," as in the demonstration movie of Zimmermann (1971). These earlier methods also included direct photography of planed surfaces ("surface method") viewed under low magnification. Similar image capture using our digital method is clearly another option. Although our objective here is to measure vessel length precisely, additional calculations can be made by this three-dimensional method for understanding plant structures. The ability to measure vessel overlap as well as vessel length could facilitate the understanding of total vessel hydraulic resistance (Sperry et al. 2007). Another advantage of this method is that measurements of vessel length according to position (as we have done with peripheral versus central medullary vessels) or in relation to diameter can be made. Furthermore, the resulting movies are easily projected as a PowerPoint presentation and could provide useful teaching tools. In the much neglected discipline of plant anatomy (Tomescu 2007), a dynamic illustration of the three-dimensional histology of plant organs could be a re-vitalizing force attractive to students. At the

same time we recognize that there is considerable recent interest in three-dimensional reconstruction of histological features of plants using elegant methods to capture serial images. By means of the epifluorescence and confocal laser scanning microscope, Kitin et al. (2004) reconstructed the vessel network in wood segments up to 21.2 mm long thus enabling them to plot every vessel in the sample. Another study (Kitin et al. 2003) investigated aspects of secondary xylem differentiation using similar methods on similar size samples. At the cellular level and in the biomedical field there is extensive serial section microscopy done at the ultrastructural level with great precision using specially designed software (Fiala 2005). Our method was designed to answer a specific problem on samples that are several orders of magnitude larger than those used in existing studies, which require very limited technology. We acknowledge that our method does not eliminate the tedium that these authors comment upon in this kind of approach, but point out that within a few days one can make an analysis of a long sample of root in a way that is not possible using more sophisticated approaches.

CHAPTER 5

An Evaluation of the Method of Single Vessel Air Injection in Calculating Vulnerability to Cavitation in Sugar Maple (*Acer saccharum* Marsh.)

INTRODUCTION

Plants rely on negative hydrostatic pressure (i.e. tension) to transport water through the xylem, a theory first proposed by Dixon and Joly (1894). This pressure gradient is transferred through the water column and is created by transpiration at the leaf surface. Under conditions of water stress, tension on the xylem sap can exceed the vapor pressure of water leading to the rapid phase change from liquid water to vapor (Zimmermann 1983). Xylem conduits that become embolized as the result of cavitation exhibit a reduction in hydraulic conductivity, which can impart limitations on photosynthesis and growth (Hubbard et al. 2001; Brodribb and Cochard 2009). The propagation of emboli is thought to occur through "air seeding" where air is aspirated from embolized conduits into functional conduits through pores in the inter-conduit pit membranes (Zimmermann 1983; Sperry and Tyree 1988). Vulnerability to air seeding can vary greatly depending upon inter-conduit pit size and quantity, as well as pit membrane thickness and porosity (Choat et al. 2008; Christman et al. 2009; Lens et al. 2010).

Based on evidence that negative pressures required to induce air seeding are equal to and opposite the pressure required to force air across inter-conduit pits (Cochard et al. 1992), the method of single vessel air injection is utilized to measure the air seeding threshold pressure of individual vessels (Zwieniecki et al. 2001a). Air seeding threshold (P_t) represents the pressure

required to force air across pit membranes. A lower P_t corresponds with a greater vulnerability to cavitation, as less tension is required to induce air seeding (Choat et al. 2005). This technique is used to understand differences in vulnerability to cavitation of vessels in relation to location within the plant (Choat et al. 2005) and age of conductive tissue (Melcher et al. 2003), in addition to the porosity of pit membranes (Choat et al. 2004). Furthermore, air seeding threshold measurements illustrate the correlation between the frequency of leaky pit membranes and a species' vulnerability to cavitation (Christman et al. 2009).

Variations in protocol for the use of single vessel air injections to measure air seeding threshold pressures raises many questions regarding the use of this technique. In some studies, plant material is either flushed with perfusion solution to remove reversible emboli or tested under native conditions (Melcher et al. 2003; Choat et al. 2005; Christman et al. 2009). It has been demonstrated with use of the centrifuge technique, that stems flushed with perfusion solution exhibit increased vulnerability to cavitation compared to stems with native embolism (Choat et al. 2010). The induction of microbubbles in the perfusion solution is considered the cause in decreased vulnerability to cavitation. This artifact induced by flushing has not been tested in the method of single vessel air injection.

Calculations of P_t with the single vessel air injection technique could be impacted by the length of stem segment measured in relation to the mean vessel length for a given species. Utilizing a similar technique of whole stem air injection, Christman et al. (2009) showed a positive correlation between P_t and the length of stem measured. While this study demonstrated theoretically that P_t is driven by the number of end-walls by which air must pass and the extent

of inter-vessel pitting, the range of stem length classes measured exceeded the mean vessel length for each species. In a more recent study, Christman et al.(2012) analyzed single vessel air injection of *Quercus gambelii* at one stem length bordering the mean vessel length for this species. These measurements are compared to a probability model for calculating the change in P_t with increasing length, number of end-walls, and pits per end-wall. An evaluation of P_t across a range of stem length classes below and above the associated mean vessel length of a species has yet to be conducted.

A comparison of single vessel measurements of P_t to whole-stem vulnerability to cavitation as measured by the centrifuge or bench-top drying method, provides insights into the accuracy of these two techniques (Christman et al. 2009; Christman et al. 2012). The use of a centrifuge to analyze vulnerability to cavitation, with inherent technical limitations on length of stem measured (i.e. 14.5 cm), is under scrutiny due to possible artifacts related to the measuring large-vessel species (Choat et al. 2010; Cochard et al. 2010; Sperry et al. 2012). Measurement of species with long vessels in relation to the stem segment being centrifuged will result in a high proportion of open vessels leading to increased vulnerability to cavitation due to the introduction of microbubbles during processing (Choat et al. 2010; Cochard et al. 2010). If cavitation is occurring by air seeding, this underestimation of vulnerability to cavitation by centrifuge of long vessel species could be linked to the correlation between P_t and the ratio of vessel length to stem length measured (i.e. number of end-walls) by single vessel air injections.

In this study, an evaluation is conducted of the technique of single vessel air injection method as a measurement of vulnerability to cavitation, with sugar maple (*Acer saccharum* Marsh.) as a test

species. Incorporating measurements of vessel distribution, the impact on P_t in regards to stem length measured (i.e. number of end-walls) is assessed. Furthermore, P_t across a range of varying stem lengths is compared to vulnerability to cavitation measurements produced by the centrifuge technique. Lastly, variations in protocol regarding flushing of stems prior to measurements of P_t are evaluated.

MATERIALS AND METHODS

Experimental Site and Collection

All tests were conducted in early December 2012 on sugar maple (*Acer saccharum* Marsh.) trees selected from an experimental garden at Harvard University, Cambridge, MA (HU). Trees were 5-8 m in height. Branches approximately 2-4 m in length were cut mid-morning with a pole-pruner from a height of 5.5-7.5 m. Individual samples were immediately transported back to the lab, re-cut under water, and processed.

Air Seeding Threshold of Individual Vessels

To assess the air seeding threshold of single vessels, we employed the technique of single vessel air injection developed by Melcher et al. (2003). Branches from garden-grown *A. saccharum* were collected as described above. Stem segments three to four years and 15 cm in length were removed from the branch by cutting under water. Following removal from the branch, stem segments were processed either as native or flushed (to remove embolisms). For removal of embolisms prior to measurements, stems were flushed at 0.1 MPa with 10ml 10 mM KCl. Perfusion solutions were mixed in DI H2O (Millipore MilliQ UV plus) and re-filtered through a 0.2 μm syringe filter (Pall acrodisc syringe filters) prior to measurements. Stems were

trimmed underwater to a length of 0.5, 2, 5, 14.5 cm and the distal end (youngest end) stained for better visualization of conduits with Toluidine Blue filtered through a 0.2μm syringe filter (Pall acrodisc syringe filters). The length of 14.5 cm was chosen for comparison to the conventional length measured by the centrifuge method for determination of vulnerability to cavitation. In each stem segment, measurements were conducted on current year growth rings. A horizontal micropipette puller (PUL-1, World Precision Instruments, Hertfordshire, UK) was utilized to reduce the diameter of the glass microcapillaries to a size suitable for fitting within the lumen of individual vessels. Stems were then attached to a micromanipulator and a glass microcapillary tube was inserted into the lumen of an individual vessel in the distal end of the stem. Closely spaced vessels were avoided. The insertion of the microcapillary tube was then fixed to the stem with fast-setting glue (ZAP A Gap CA+ Glue). The microcapillary was attached to a regulated source of nitrogen gas, which allowed for a slow increase in the amount of air pressure forced into the individual vessel. The proximal end of the stem segment was submerged in water for visualization of air bubbles resulting from gas being pressurized through individual vessels. Initially, 0.1 MPa was applied to the conduit; if no air bubbles appeared out the proximal end, the conduit was considered closed (i.e. with vessel ends). Gas was then applied at a rate of 0.1 MPa min^{-1} until bubbles emerged from the proximal end. This pressure was considered the air seeding threshold for the individual vessel. Pressures exceeding 6 MPa were avoided due to the possibility of blowing the microcapillary out of the apparatus; vessels exhibiting this level of resistance to pressure were considered obstructed. After each measurement, the microcapillary was carefully removed from the vessel lumen and inserted into another vessel within the same stem; 3-6 measurements per stem were possible.

Vulnerability to Cavitation

Vulnerability to cavitation was assessed utilizing the centrifuge technique (Alder et al. 1997). A perfusion solution of 10 mM KCl in DI H_2O (Millipore MilliQ UV plus) re-filtered through a 0.2 μm syringe filter (Pall acrodisc syringe filters) was used for all measurements. Hydraulic conductivity was calculated by flow driven from a gravity head through each stem sample to an analytical balance (Sartorius CPA225D). Stem segments of current year growth, 5.5-7.5 mm diameter and 14.5 cm in length were used. All stems were decorticated up to 5 mm at each end to allow for proper seal during hydraulic conductivity measurements. Stems were flushed with 20 mM KCl at 0.1 MPa for 20 mins prior to spinning in the centrifuge. Hydraulic conductivity was measured after each pressure of 0, 0.5, 1, 2, 3, 4, 5 and 6 MPa and vulnerability to cavitation calculated using PLC [100 (1- K_{result}/ K_{max})] where K_{result} refers to conductivity following each stage of increased pressure and K_{max} is the maximum conductivity (flushed) measured after removal of embolisms by flushing stems.

Vessel Length Distribution

Vessel length distributions of *A. saccharum* were obtained using the method of silicon injection (Hacke et al. 2007; Christman et al. 2009). Silicone used was a mixture of 10 : 1 silicone : hardener mix (RTV-141; Bluestar Silicones, York, SC, USA). To aid in detection of vessels perfused with silicone, a fluorescent optical brightener (2,5-Bis (5-*tert*-butyl-benzoxazol-2-yl) thiophene; Sigma-Aldrich, Allentown, PA, USA) was mixed with chloroform (1% w/w) and added to the silicone (one drop g^{-1}). Prior to injection, the silicone mixture was subjected to vacuum pressure to remove air bubbles. Five stems 30 cm in length were flushed with 20 mM KCl at 0.1 MPa for 20mins then injected with silicone at 0.05-0.075 MPa pressure overnight.

After silicone was hardened in an oven (55˚C), stems were sectioned at six positions proximal from the injection end starting at 4mm and ending at 12 cm. Utilizing fluorescent microscopy, the fraction of vessels filled with silicone at each length of sectioning was counted and analyzed based on calculations of vessel length distributions detailed in Sperry et al. (2005), Christman et al. (2009), and K. Jenson (unpublished, 2013).

Statistics

Comparison of mean P_t in relation to stem segment was conducted using ANOVA with Tukey HSD comparison. Comparison of mean P_t in relation to flushing at each stem length class was done utilizing the independent two-sample t-tests. Means are reported as ±SE. For tests of vulnerability to cavitation, the standard of 50% loss of conductivity (P50) and mean cavitation pressure (MCP) were used for reference; each parameter was calculated from fitting data by a least square regression using the Weibull function.

RESULTS

Air Seeding Threshold of Individual Vessels

A total of 10 stems were sampled and 799 individual vessels measured for air seeding threshold pressure (Table 4.1). For each length class of stem section, the percent of open vessels (without end-walls) was: 0.5 cm = 91.9%, 2 cm = 51.9%, 5 cm = 10.9%, and 14.5 cm = 0%. In each length class of stem section (0.5, 2, 5, and 14.5 cm) the percent of all vessels measured exceeding 6 MPa was 0.17, 3.8, 18.2, and 33.3% (respectively). Measurement of open vessels and those exceeding 6 MPa are not included in analyses of air seeding thresholds between length classes or treatments, but provide an indication as to the likelihood of crossing at least one or

Table 4.1. Statistics of air seeding threshold measurements for 4 stem length classes in *A. saccharum*. The percent of total vessel open and percent of measured vessels over 6Mpa not utilized in comparisons of air seeding pressures, but used to estimate the number of end-walls in relation to stem segment length.

Length of Stems Measured (cm)	Total Vessels Measured	Count of Closed Vessels	Count of Open Vessels	Percent of Total Vessels Open	Percent of Measured Vessels Over 6MPa
0.5	594	49	545	92%	2%
2	129	62	67	52%	8%
5	55	49	6	11%	20%
14.5	21	21	0	0%	33%

more end-walls during air seeding tests. The distribution of percent of vessels air seeding across a range of increasing pressure (0 – 6 MPa) shifts from a right-skewed distribution to a left-skewed distribution with increasing length of stem samples measured (Figure 4.1).

For stems flushed with 10 mM KCl prior to measurements, the mean air seeding threshold pressure (±SE) for each length class of stem section was: 0.5 cm = 1.81±0.29 MPa (N = 21), 2 cm = 2.81±0.32 MPa (N = 28), 5 cm = 3.99±0.31 MPa (N = 17), and 14.5 cm = 4.98±0.32 MPa (N = 12). There was a significant difference in mean P_t between length classes based on ANOVA ($P < 0.001$) (Figure 4.2). A failure probability plot was constructed for each length class across the range of increased pressure of air seeding based on calculations by K. Jenson (unpublished, 2013) (Figure 4.3).

A comparison between treatments of flushing with 10 mM KCl and native stems at each length class showed no significant difference at stem length of 0.5 cm ($P = 0.143$) but a significant difference at length class of 2 cm ($P = 0.031$) and 5 cm ($P = 0.007$) (Figure 4.4). For native stems at each stem length class, the mean air seeding threshold pressures (±SE) are: 0.5 cm = 1.39±0.25 MPa (N = 23), 2 cm = 2.03±0.26 MPa (N = 29), and 5 cm = 2.86±0.31 MPa (N = 21).

Vessel Length Distribution

The method of silicone injection and distribution analysis of vessel lengths resulted in a mean vessel length of 3.1±1.5 cm (±SD).

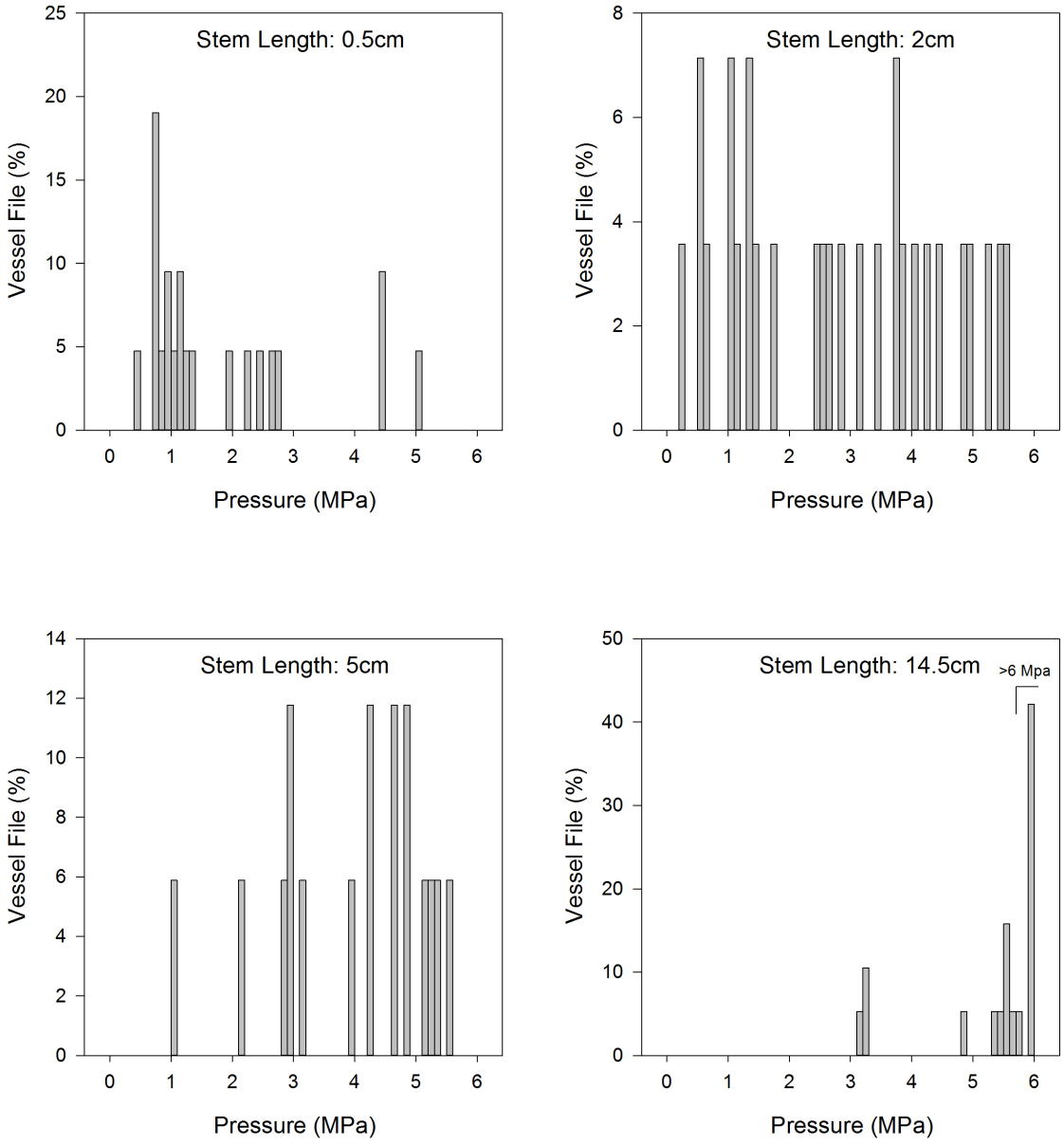

Figure 4.1. Percentage of vessels air seeding at increasing pressures of 0.1MPa increments for each stem length class measured (0.5, 2, 5, and 14.5cm) for *A. saccharum*.

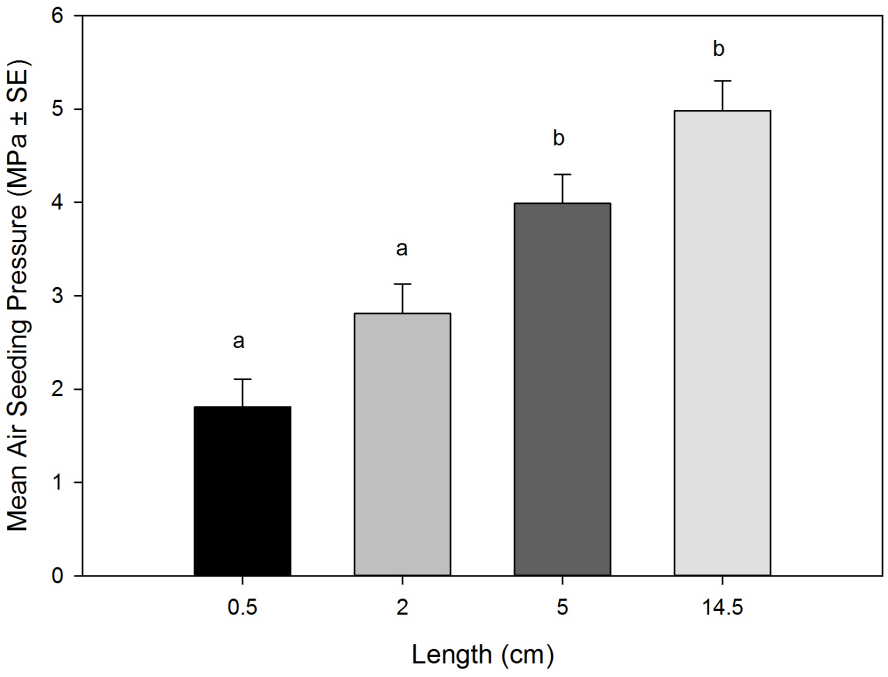

Figure 4.2. A comparison of mean air seeding pressure in relation to stem length class measured for *A. saccharum*. Different letters are significantly different according to a Tukey-Kramer HSD test ($P < 0.001$; 0.5cm N = 21, 2cm N = 28, 5cm N = 17, 14.5cm N = 12).

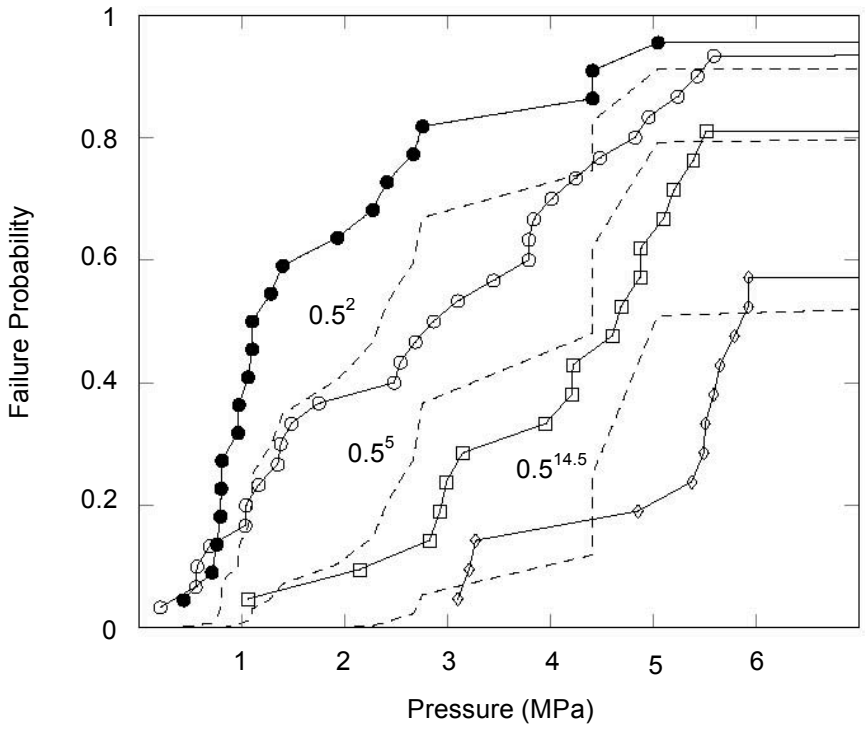

Figure 4.3. Experimental data and model predictions for the probability of vessel end-wall failure in *A. saccharum*. Solid lines represent the stem length class measured: 0.5cm (closed circles), 2cm (open circles), 5cm (open squares), and 14.5cm (open diamonds). Each dashed line represents the model prediction of increasing the number of end-walls per stem segment by raising 0.5cm to the 2, 5, and 14.5 power: 0.5^2 (2 end-walls), 0.5^5 (5 end-walls), and $0.5^{14.5}$ (14.5 end-walls) K. Jenson (2013, unpublished).

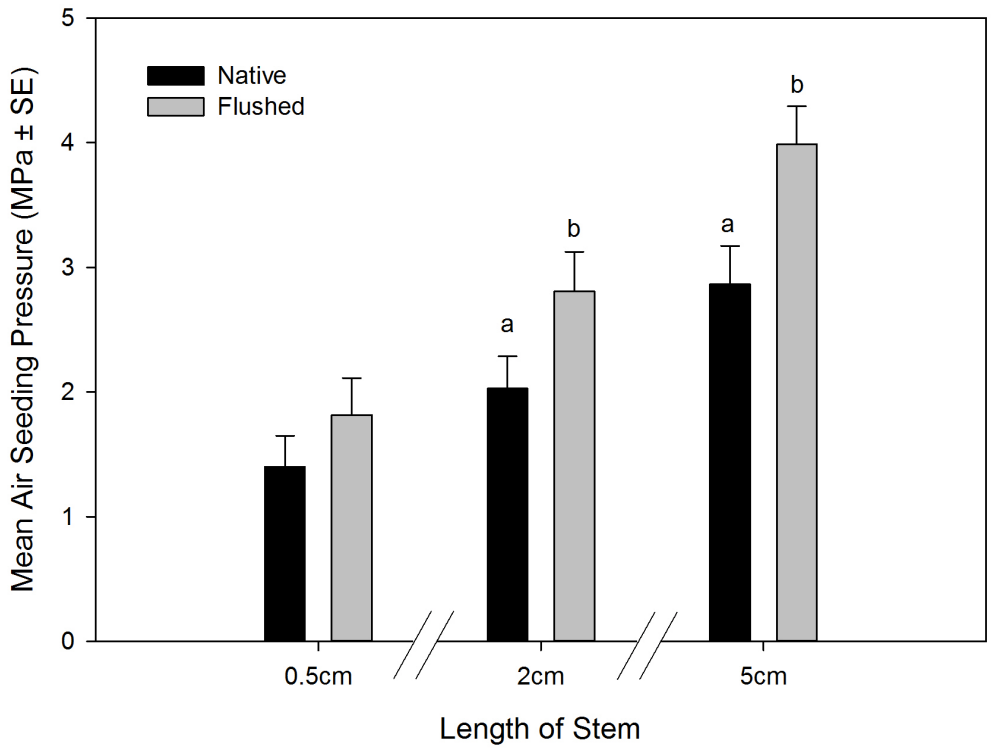

Figure 4.4. The effect of flushing on air seeding threshold pressures in *A. saccharum*. A comparison of flushed vs. native was conducted for each stem length class. Different letters are significantly different according to independent two-sample t-tests at significance level of $P < 0.05$.

Vulnerability to Cavitation

An analysis of eight stems resulted in a vulnerability curve with a mean P50 (±SE) = 4.01±0.17 and MCP (±SE) = 4.05±0.16 (Figure 4.5).

DISCUSSION

The results of this study indicate that length of stem segment measured during tests of single vessel air injection has a significant impact on the air seeding threshold pressure required to force air axially along a conduit fraction (Figs. 4.1 and 4.2). The increase in air seeding pressure with an increase in stem length corresponds with the likelihood of forcing gas across an increasing number of end-walls. The mean vessel length of 3.1±1.5 cm (±SD) in *A. saccharum* acquired from vessel length distribution analysis, compared with the percent of total open vessels (Table 4.1), can provide an estimate of the amount of end-walls in each stem segment. For example, in the 0.5 cm stem segment, 92% of all vessels measured are open, indicating a high probability that air is being forced across only one vessel end-wall. As expected, a stem length of 14.5 cm, which extends past the mean vessel length of this species, results in an observed 0% of total vessels open. Of the stem length classes measured, the 2 cm stem segment corresponds closest to the mean vessel length of 3.1 cm and results in 52% open vessels (Table 4.1).

An analysis of the probability of failure in relation to increased pressure (Figure 4.3) shows a distinct shift from lower P_t in short stem segments (i.e. 0.5cm) to higher P_t in longer segments (i.e. 14.5 cm). If we assume the existence of one vessel end-wall in the 0.5cm segment, the probability of failure in relation to number of end-walls can be predicted by raising 0.5 to the power of 2, 5, and 14.5 (dashed lines). The dashed lines indicate the probability failure when

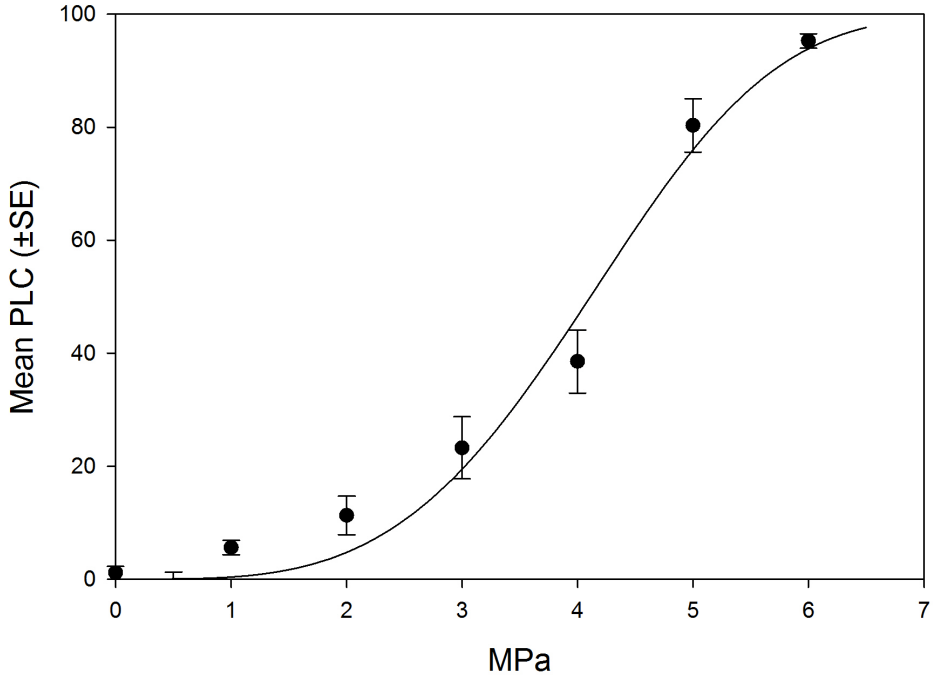

Figure 4.5. Vulnerability curve of *A. saccharum* generated by the centrifuge technique. The data are fitted by least squares regression with a Weibull function. P50 (±SE) = 4.01±0.17 and MCP (±SE) = 4.05±0.16.

having 2, 5, or 14.5 end-walls. This prediction demonstrates that the air seeding threshold of a stem segment with the high probability of having only one end-wall can be scaled up to closely match the failure probability of a stem segment length of 14.5 cm.

In comparing the failure probability of P_t to the vulnerability curve produced by the centrifuge technique, a measured stem segment length closest to the mean vessel length of 3.1 cm (i.e. between the observed 2 cm and 5 cm stem lengths, with roughly 50% of vessels closed), would most closely match the P50 (50% loss of conductivity) of 4.01 MPa. Recent studies have demonstrated the method of bench-top drying as a more reliable method for analyzing vulnerability to cavitation compared to the centrifuge technique (Choat et al. 2010; Cochard et al. 2010). An analysis of vulnerability to cavitation in *A. saccharum* with use of the bench-top drying method produces a P50 of 3.49 MPa (Wheeler et al. 2013). Based on the decrease in P_t as stem length is shortened (i.e. lower number of end-walls), it is likely that the use of long vessel species in relation to the stem length measured in estimating vulnerability to cavitation with the centrifuge technique could underestimate the value of P50.

The use of P_t in *A. saccharum* in relation to stem length and vessel length as a predictor of whole stem vulnerability to cavitation is not entirely consistent with Christman et al. (2012). In their study, a stem segment of *Quercus gambelii* roughly equal in length to the mean vessel length resulted in 44% of open vessels; quite similar to the 55% of open vessels in the 2 cm stem segment in this study. Using model predictions, Christman et al. (2012) similarly predicted whole-stem vulnerability based on a measured stem length roughly equal to the mean vessel length, their distribution of air seeding pressures was markedly different. In a 75 cm stem

segment of *Q. gambelii*, 40% of closed vessels exhibited air seeding pressures below 1 MPa, resulting in a right-skewed distribution similar to measurements of 0.5 cm stem length of *A. saccharum* (Figure 4.1). Christman et al. (2012) compared the right-skewed distribution of air seeding threshold pressure to the r-shaped vulnerability curve of *Q. gambelii* with a steep drop in stem conductivity at low sap tensions; with mean air seeding cavitation pressures of 1.02 MPa and a mean cavitation tension of 1.22 MPa. In comparison to *Q. gambelii*, vulnerability curves for *A. saccharum* exhibit an s-shaped curve (Figure 4.5). Data here demonstrates that vulnerability curves (and predicted P50) for *A. saccharum* are more closely related to stem lengths with an even distribution of air seeding pressures (i.e. 2 cm; Figure 4.1). The difference in these two studies in the relationship between air seeding pressure distributions and vulnerability curves could result from comparing a ring-porous species (*Q. gambelii*) with that of a diffuse-porous species (*A. saccharum*).

Considering evidence showing that flushing of stems with 10 mM KCl to remove native embolisms prior to measurement increases vulnerability to cavitation (Choat et al. 2010), it is expected that flushing would reduce the air seeding threshold pressure of individual vessel in *A. saccharum*. Results from this study contradict this expectation in that in stems 2 cm and 5 cm in length exhibited significantly higher air seeding threshold pressures in stems flushed with 10 mM KCl compared to native stems (Figure 4.4). One explanation for this effect is the impact of ion concentration on hydraulic conductivity and vulnerability to cavitation. Increases in the concentration of K and Ca in xylem sap can reduce hydraulic resistance due to alterations of microchannels in pit membranes as ions bind with, and contract pectin layers (Zwieniecki et al. 2001a). In the case of air seeding, Ca reduces vulnerability to cavitation by crosslinking with,

and strengthening pit membranes, which are forced to undergo substantial stretching and deformations due to the pressure difference between embolized and functional conduits (Herbette and Cochard 2010). Due to the similarity of K to Ca in influencing pit membrane porosity due to binding of pectins, it seems possible that perfusion with 10 mM KCl in this study results in a increase in the stem concentration of ionic K and a subsequent strengthening of the pit membranes similar to the effect of Ca. In support of this hypothesis, P_t of 5 cm stems flushed with DI H_2O compared to native stems showed no significant difference in treatment ($P = 0.727$; flushed $N = 5$, native $N = 7$). Previous tests do raise doubt regarding this ion-effect, as no impact was found on vulnerability to cavitation by the removal of xylem-bound Ca in *A. saccharum* (B.A. Huggett, Chapter 1, unpublished data). Future studies utilizing the single vessel air injection technique should account for possible artifacts due to the flushing process.

The results of this study illustrate important aspects of the method of single vessel air injection in determining air seeding pressure. The length of stem measured in relation to the mean vessel length of the species tested has a significant impact on P_t. As length of stem segment increases, so does the P_t as greater pressure is required to force air across an increasing number of vessel end-walls. In studies investigating the P_t of individual vessels, measurements should be conducted on a stem segment length significantly shorter than the mean vessel length to increase the probability of forcing air across only one vessel end-wall (e.g. 0.5cm in the case of *A. saccharum*). To accurately predict whole-stem cavitation in the diffuse-porous species *A. saccharum* utilizing the single vessel air seeding method, the measured stem segment length must be similar to the mean vessel length. Lastly, flushing of stem segments prior to measurements of single vessel air injection can significantly inflate air seeding pressures.

REFERENCES

Aber, J., McDowell, W., Nadelhoffer, K., Magill, A., Bernston, G., Kamakea, M., McNulty, S., Currie, W., Rustad, L., and Fernandez, I. 1998. Nitrogen saturation in temperate forest ecosystems. BioScience 48: 921-934.

Alder, N.N., Pockman, W.T., Sperry, J.S., and Nuismer, S. 1997. Use of centrifugal force in the study of xylem cavitation. Journal of Experimental Botany 48: 665.

Allen, D.C., Barnett, C.J., Millers, I., and Lachance, D. 1992. Temporal change (1988-1990) in sugar maple health, and factors associated with crown condition. Canadian Journal of Forest Research 22: 1776-1784.

André, J.P. 2005. Vascular organization of angiosperms: A new vision. Science Publishers, Enfield, NH.

Bailey, S.W., Horsley, S.B., Long, R.P., and Hallett, R.A. 2004. Influence of edaphic factors on sugar maple nutrition and health on the Allegheny plateau. Soil Science Society of America Journal 68: 243-252.

Bloch, R. 1946. Differentiation and pattern in *Monstera deliciosa*. The idioblastic development of the trichosclereids in the air root. American Journal of Botany: 544-551.

Brodribb, T.J., and Cochard, H. 2009. Hydraulic failure defines the recovery and point of death in water-stressed conifers. Plant Physiology 149: 575-584.

Brodribb, T.J., and Feild, T.S. 2000. Stem hydraulic supply is linked to leaf photosynthetic capacity: evidence from New Caledonian and Tasmanian rainforests. Plant, Cell & Environment 23: 1381-1388.

Buchanan, B.B., Gruissem, W., and Jones, R.L. 2000. Biochemistry & molecular biology of plants. American Society of Plant Physiologists, Rockville, Md.

Choat, B., Cobb, A., and Jansen, S. 2008. Structure and function of bordered pits: new discoveries and impacts on whole-plant hydraulic function. New Phytologist 177: 608-626.

Choat, B., Drayton, W.M., Brodersen, C., Matthews, M.A., Shackel, K.A., Wada, H., and McElrone, A.J. 2010. Measurement of vulnerability to water stress-induced cavitation in grapevine: a comparison of four techniques applied to a long-vesseled species. Plant, Cell & Environment 33: 1502-1512.

Choat, B., Jansen, S., Zwieniecki, M., Smets, E., and Holbrook, N. 2004. Changes in pit membrane porosity due to deflection and stretching: the role of vestured pits. Journal of Experimental Botany 55: 1569-1575.

Choat, B., Lahr, E., Melcher, P., Zwieniecki, M., and Holbrook, N. 2005. The spatial pattern of air seeding thresholds in mature sugar maple trees. Plant, Cell & Environment 28: 1082-1089.

Christman, M.A., Sperry, J.S., and Adler, F.R. 2009. Testing the 'rare pit' hypothesis for xylem cavitation resistance in three species of Acer. New Phytologist 182: 664-674.

Christman, M.A., Sperry, J.S., and Smith, D.D. 2012. Rare pits, large vessels and extreme vulnerability to cavitation in a ring-porous tree species. New Phytologist 193: 713-720.

Clarkson, D. 1984. Calcium transport between tissues and its distribution in the plant. Plant, Cell & Environment 7: 449-456.

Cochard, H., Cruiziat, P., and Tyree, M.T. 1992. Use of positive pressures to establish vulnerability curves: further support for the air-seeding hypothesis and implications for pressure-volume analysis. Plant Physiology 100: 205-209.

Cochard, H., Herbette, S., Barigah, T., Badel, E., Ennajeh, M., and Vilagrosa, A. 2010. Does sample length influence the shape of xylem embolism vulnerability curves? A test with the Cavitron spinning technique. Plant, Cell & Environment 33: 1543-1552.

Davies, H.V., and Monk-Talbot, L.S. 1990. Permeability characteristics and membrane lipid composition of potato tuber cultivars in relation to Ca^{2+} deficiency. Phytochemistry 29: 2833-2835.

Davis, S.D., Ewers, F.W., Sperry, J.S., Portwood, K.A., Crocker, M.C., and Adams, G.C. 2002. Shoot dieback during prolonged drought in Ceanothus (Rhamnaceae) chaparral of california: A possible case of hydraulic failure. American Journal of Botany 89: 820-828.

DeHayes, D.H., Schaberg, P.G., Hawley, G.J., Borer, C.H., Cumming, J.R., and Strimbeck, G.R. 1997. Physiological implications of seasonal variation in membrane-associated calcium in red spruce mesophyll cells. Tree Physiology 17: 687-695.

Dixon, H.H., and Joly, J. 1894. On the ascent of sap. Proceedings of the Royal Society of London 57: 3-5.

Domec, J.C., Rivera, L.N., King, J.S., Peszlen, I., Hain, F., Smith, B., and Frampton, J. 2013. Hemlock woolly adelgid (*Adelges tsugae*) infestation affects water and carbon relations of eastern hemlock (*Tsuga canadensis*) and Carolina hemlock (*Tsuga caroliniana*). New Phytologist.

Eklund, L., and Eliasson, L. 1990. Effects of calcium ion concentration on cell wall synthesis. Journal of Experimental Botany 41: 863-867.

Ellsworth, D.S., and Liu, X. 1994. Photosynthesis and canopy nutrition of four sugar maple forests on acid soils in northern Vermont. Canadian Journal of Forest Research 24: 2118-2127.

Eschrich, W. 1983. Phloem unloading in aerial roots of *Monstera deliciosa*. Planta 157: 540-547.

Evert, R.F., and Esau, K. 2007. Esau's plant anatomy. 3rd ed. J. Wiley, Hoboken, N.J.

Eyles, A., Smith, D., Pinkard, E.a., Smith, I., Corkrey, R., Elms, S., Beadle, C., and Mohammed, C. 2011. Photosynthetic responses of field-grown *Pinus radiata* trees to artificial and aphid-induced defoliation. Tree Physiology 31: 592-603.

Federer, C., Hornbeck, J., Tritton, L., Martin, C., Pierce, R., and Smith, C. 1989. Long-term depletion of calcium and other nutrients in eastern US forests. Environmental Management 13: 593-601.

Fiala, J. 2005. Reconstruct: a free editor for serial section microscopy. Journal of Microscopy 218: 52-61.

Fromm, J. 2010. Wood formation of trees in relation to potassium and calcium nutrition. Tree Physiology 30: 1140-1147.

Gómez, S., Orians, C.M., and Preisser, E.L. 2012. Exotic herbivores on a shared native host: tissue quality after individual, simultaneous, and sequential attack. Oecologia 169: 1015-1024.

Gonda-King, L., Radville, L., and Preisser, E.L. 2012. False ring formation in eastern hemlock branches: impacts of hemlock woolly adelgid and elongate hemlock scale. Environmental Entomology 41: 523-531.

Hacke, U.G., Sperry, J.S., Feild, T.S., Sano, Y., Sikkema, E.H., and Pittermann, J. 2007. Water transport in vesselless angiosperms: conducting efficiency and cavitation safety. International Journal of Plant Sciences 168: 1113-1126.

Hacke, U.G., Sperry, J.S., Pockman, W.T., Davis, S.D., and McCulloch, K.A. 2001a. Trends in wood density and structure are linked to prevention of xylem implosion by negative pressure. Oecologia 126: 457-461.

Hacke, U.G., Stiller, V., Sperry, J.S., Pittermann, J., and McCulloh, K.A. 2001b. Cavitation Fatigue. Embolism and refilling cycles can weaken the cavitation resistance of xylem. Plant Physiology 125: 779-786.

Hallett, R.A., Bailey, S.W., Horsley, S.B., and Long, R.P. 2006. Influence of nutrition and stress on sugar maple at a regional scale. Canadian Journal of Forest Research 36: 2235-2246.

Halman, J.M., Schaberg, P.G., Hawley, G.J., and Eagar, C. 2008. Calcium addition at the Hubbard Brook Experimental Forest increases sugar storage, antioxidant activity and cold tolerance in native red spruce (*Picea rubens*). Tree Physiology 28: 855-862.

Hedin, L., Granat, L., Likens, G., Buishand, T., Galloway, J., Butler, T., and Rodhe, H. 1994. Steep declines in atmospheric base cations in regions of Europe and North America. Nature 367: 351-354.

Heisey, R.M. 1995. Growth trends and nutritional status of sugar maple stands on the Appalachian plateau of Pennsylvania, U.S.A. Water, Air, and Soil Pollution 82: 675-693.

Hepler, P.K. 2005. Calcium: A central regulator of plant growth and development. Plant Cell 17: 2142-2155.

Herbette, S., and Cochard, H. 2010. Calcium is a major determinant of xylem vulnerability to cavitation. Plant Physiology 153: 1932.

Hollingsworth, R.G., and Hain, F.P. 1992. Balsam woolly adelgid (Homoptera: Adelgidae) and spruce-fir decline in the southern Appalachians: assessing pest relevance in a damaged ecosystem. Functional Ecology 74: 179-187.

Hoogesteger, J., and Karlsoon, P.S. 1992. Effects of defoliation on radial stem growth and photosynthesis in the mountain photosynthesis birch (*Betula pubescens* spp. *tortusa*). Functional Ecology 6: 317-323.

Horsley, S.B., Long, R.P., Bailey, S.W., Hallett, R.A., and Wargo, P.M. 2002. Health of eastern North American sugar maple forests and factors affecting decline. Northern Journal of Applied Forestry 19: 34-44.

Hubbard, R.M., Ryan, M.G., Stiller, V., and Sperry, J.S. 2001. Stomatal conductance and photosynthesis vary linearly with plant hydraulic conductance in ponderosa pine. Plant Cell and Environment 24: 113-121.

Huggett, B.A., Schaberg, P.G., Hawley, G.J., and Eagar, C. 2007. Long-term calcium addition increases growth release, wound closure, and health of sugar maple (*Acer saccharum)* trees at the Hubbard Brook Experimental Forest. Canadian Journal of Forest Research 37: 1692-1700.

Jacobsen, A.L., Ewers, F.W., Pratt, R.B., Paddock, W.A., III, and Davis, S.D. 2005. Do xylem fibers affect vessel cavitation resistance? Plant Physiology 139: 546-556.

Juice, S.M., Fahey, T.J., Siccama, T.G., Driscoll, C.T., Denny, E.G., Eagar, C., Cleavitt, N.L., Minocha, R., and Richardson, A.D. 2006. Response of sugar maple to calcium addition to northern hardwood forest. Ecology 87: 1267-1280.

Keating, R.C. 2003. Anatomy of the monocotyledons. Oxford University Press, Oxford.

Kirchner, J., and Lydersen, E. 1995. Base cation depletion and potential long-term acidification of Norwegian catchments. Environmental Science & Technology 29: 1953-1960.

Kirkby, E.A., and Pilbeam, D.J. 1984. Calcium as a plant nutrient. Plant, Cell & Environment 7: 397-405.

Kitin, P.B., Fujii, T., Abe, H., and Funada, R. 2004. Anatomy of the vessel network within and between tree rings of *Fraxinus lanuginosa* (Oleaceae). American Journal of Botany 91: 779-788.

Kitin, P.B., Sano, Y., and Funada, R. 2003. Three-dimensional imaging and analysis of differentiating secondary xylem by confocal microscopy. Iawa Journal 24: 211-222.

Koide, R.T., Robichaux, R.H., Morse, S.R., and Smith, C.M. 1989. Plant water status, hydraulic resistance and capacitance. *In* Plant physiological ecology. Springer. pp. 161-183.

Kolb, T.E., and McCormick, L.H. 1993. Etiology of sugar maple decline in four Pennsylvania stands. Canadian Journal of Forest Research 23: 2395-2402.

Lautner, S., Ehlting, B., Windeisen, E., Rennenberg, H., Matyssek, R., and Fromm, J. 2007. Calcium nutrition has a significant influence on wood formation in poplar. New Phytologist 173: 743-752.

Lautner, S., and Fromm, J. 2010. Calcium-dependent physiological processes in trees. Plant Biology 12: 268-274.

Lawrence, G.B., David, M.B., and Shortle, W.C. 1995. A new mechanism for calcium loss in forest-floor soils. Nature 378: 162-165.

Legge, R.L., Thompson, J.E., Baker, J.E., and Lieberman, M. 1982. The effect of caclium on the fluidity and phase properties of microsomal-membranes isolated from post-climacteric golden delicious apples. Plant and Cell Physiology 23: 161-169.

Lens, F., Sperry, J.S., Christman, M.A., Choat, B., Rabaey, D., and Jansen, S. 2010. Testing hypotheses that link wood anatomy to cavitation resistance and hydraulic conductivity in the genus *Acer*. New Phytologist 190: 709-723.

Likens, G.E., Driscoll, C., Buso, D., Siccama, T., Johnson, C., Lovett, G., Fahey, T., Reiners, W., and Ryan., D. 1998. The biogeochemistry of calcium at Hubbard Brook. Biogeochemistry 41: 89-173.

Likens, G.E., Driscoll, C.T., and Buso, D.C. 1996. Long-term effects of acid rain: response and recovery of a forest ecosystem. Science 272: 244-246.

Liu, X., Ellsworth, D.S., and Tyree, M.T. 1997. Leaf nutrition and photosynthetic performance of sugar maple (*Acer saccharum*) in stands with contrasting health conditions. Tree Physiology 17: 169-178.

Long, R.P., Horsley, S.B., Hallett, R.A., and Bailey, S.W. 2009. Sugar maple growth in relation to nutrition and stress in the northeastern United States. Ecological Applications 19: 1454-1466.

Long, R.P., Horsley, S.B., and Lilja, P.R. 1997. Impact of forest liming on growth and crown vigor of sugar maple and associated hardwoods. Canadian Journal of Forest Research 27: 1560-1573.

Mader, D.L., and Thompson, B.W. 1969. Foliar and soil nutrients in relation to sugar maple decline. Soil Science Society of America Journal 33: 794-800.

Mann, L.K., Johnson, D.W., West, D.C., Cole, D.W., Hornbeck, J.W., Martin, C.W., Riekerk, H., Smith, C.T., Swank, W.T., Tritton, L.M., and Van Lear, D.H. 1988. Effects of whole-tree and stem-only clearcutting on postharvest hydrologic losses, nutrient capital, and regrowth. Forest Science 34: 412-428.

Marschner, H. 1995. Mineral nutrition of higher plants. Academic Press, London and New York.

McClure, M.S. 1991. Density-dependent feedback and population cycles in *Adelges tsugae* (Homoptera: Adelgidae) on *Tsuga canadensis*. Environmental Entomology 20: 258-264.

McClure, M.S., Cheah, C., and Tigner, T.C. 1999. Is *Pseudoxymnus tsugae* the Solution to the Hemlock Woolly Adelgid Problem?: An Early Perspective. *In* Proceedings: Symposium on Sustainable Management of Hemlock Ecosystems in Eastern North America GTR-NE. p. 89.

McLaughlin, S.B., and Wimmer, R. 1999. Calcium physiology and terrestrial ecosystem processes. New Phytologist 142: 373-417.

Melcher, P.J., Holbrook, N.M., Burns, M.J., Zwieniecki, M.A., Cobb, A.R., Brodribb, T.J., Choat, B., and Sack, L. 2012. Measurements of stem xylem hydraulic conductivity in the laboratory and field. Methods in Ecology and Evolution 3: 685-694.

Melcher, P.J., Zwieniecki, M.A., and Holbrook, N.M. 2003. Vulnerability of xylem vessels to cavitation in sugar maple. Scaling from individual vessels to whole branches. Plant Physiology 131: 1775-1780.

Miflin, B.J., and Habash, D.Z. 2002. The role of glutamine synthetase and glutamate dehydrogenase in nitrogen assimilation and possibilities for improvement in the nitrogen utilization of crops. Journal of Experimental Botany 53: 979-987.

Miller-Pierce, M.R., Orwig, D.a., and Preisser, E. 2010. Effects of hemlock woolly adelgid and elongate hemlock scale on eastern hemlock growth and foliar chemistry. Environmental Entomology 39: 513-519.

Mitchell, R.G. 1967. Translocation of dye in grand and subalpine firs infested by the balsam woolly aphid. Pacific Northwest Forest and Range Experiment Station, US Department of Agriculture.

Montgomery, D.C. 2001. Design and analysis of experiments. 5th ed. John Wiley, New York.

Moore, J.D., Ouimet, R., and Duchesne, L. 2012. Soil and sugar maple response 15 years after dolomitic lime application. Forest Ecology and Management 281: 130-139.

Orwig, D.A., Barker Plotkin, A., Davidson, E., Lux, H., Savage, K., and Ellison, A. 2013. Foundation species loss affects vegetation structure more than ecosystem function in a northeastern USA forest. PeerJ 1: e41.

Orwig, D.A., and Foster, D. 1998. Forest Response to the Introduced Hemlock Woolly Adelgid in Southern New England , USA. Journal of the Torrey Botanical Society 125: 60-73.

Orwig, D.A., Foster, D., and Mausel, D. 2002. Landscape patterns of hemlock decline in New England due to the introduced hemlock woolly adelgid. Journal of Biogeography 29: 1475-1487.

Ouimet, R., Duchesne, L., Houle, D., and Arp, P.A. 2001. Critical loads and exceedances of acid deposition and associated forest growth in the northern hardwood and boreal coniferous forests in Québec, Canada. Water, Air, & Soil Pollution: Focus 1: 119-134.

Pearcy, R.W., Ehleringer, J.R., Mooney, H.A., and Rundel, P.W. 1989. Plant physiological ecology: field methods and instrumentation. Chapman and Hall, London ; New York.

Pelloux, J., Rustérucci, C., and Mellerowicz, E.J. 2007. New insights into pectin methylesterase structure and function. Trends in Plant Science 12: 267-277.

Peters, S.C., Blum, J.D., Driscoll, C.T., and Likens, G.E. 2004. Dissolution of wollastonite during the experimental manipulation of Hubbard Brook Watershed 1. Biogeochemistry 67: 309-329.

Pontius, J.A., Hallett, R.A., and Jenkins, J.C. 2006. Foliar chemistry linked to infestation and susceptibility to hemlock woolly adelgid (Homoptera: Adelgidae). Environmental Entomology 35: 112-120.

Puritch, G.S. 1971. Water permeability of the wood of grand fir (*Abies grandis* (Doug.) Lindl.) in relation to infestation by the balsam woolly aphid, *Adelges piceae* (Ratz.). Journal of Experimental Botany 22: 936-945.

Rengel, Z., and Zhang, W.H. 2003. Role of dynamics of intracellular calcium in aluminium-toxicity syndrome. New Phytologist 159: 295-314.

Rhodes, D., Verslues, P.E., and Sharp, R.E. 1999. Role of amino acids in abiotic stress resistance. *In* Plant amino acids. Biochemistry and biotechnology. Marcel Dekker, New York. pp. 319-356.

Rood, S.B., Patino, S., Coombs, K., and Tyree, M.T. 2000. Branch sacrifice: Cavitation-associated drought adaptation of riparian cottonwoods. Trees 14: 248-257.

Rossi, S., Simard, S., Deslauriers, A., and Morin, H. 2009. Wood formation in *Abies balsamea* seedlings subjected to artificial defoliation. Tree Physiology 29: 551-558.

Royo, A.A., and Knight, K.S. 2012. White ash (*Fraxinus americana*) decline and mortality: The role of site nutrition and stress history. Forest Ecology and Management 286: 8-15.

Sack, L., Bartlett, M., Creese, C., Guyot, G., Scoffoni, C., and contributors, P. 2011. Constructing and operating a hydraulics flow meter. Available from http://prometheuswiki.publish.csiro.au/tiki-citation.php?page=Constructing and operating a hydraulics flow meter [accessed March 10 2013].

Salleo, S., Nardini, A., Raimondo, F., Assunta, M., Gullo, L., and Pace, F. 2003. Effects of defoliation caused by the leaf miner *Cameraria ohridella* on wood production and efficiency in *Aesculus hippocastanum* growing in north-eastern Italy. Trees: 367-375.

Schaberg, P.G., DeHayes, D.H., and Hawley, G.J. 2001. Anthropogenic calcium depletion: A unique threat to forest ecosystem health? Ecosystem Health 7: 214-228.

Schaberg, P.G., Minocha, R., Long, S., Halman, J.M., Hawley, G.J., and Eagar, C. 2011. Calcium addition at the Hubbard Brook Experimental Forest increases the capacity for stress tolerance and carbon capture in red spruce (*Picea rubens*) trees during the cold season. Trees 25: 1053-1061.

Schaberg, P.G., Tilley, J.W., Hawley, G.J., DeHayes, D.H., and Bailey, S.W. 2006. Associations of calcium and aluminum with the growth and health of sugar maple trees in Vermont. Forest Ecology and Management 223: 159-169.

Schmohl, N., Pilling, J., Fisahn, J., and Horst, W.J. 2000. Pectin methylesterase modulates aluminium sensitivity in *Zea mays* and *Solanum tuberosum*. Physiologia Plantarum 109: 419-427.

Scholander, P.F., Hammel, H.T., Bradstreet, E.D., and Hemmingsen, E.A. 1965. Sap pressure in vascular plants: Negative hydrostatic pressure can be measured in plants. Science 148: 339-346.

Sheen, J. 1996. Ca^{2+}-dependent protein kinases and stress signal transduction in plants. Science 274: 1900-1902.

Shortle, W.C., and Smith, K.T. 1988. Aluminum-induced calcium deficiency syndrome in declining red spruce. Science 240: 1017-1018.

Soltis, N., Gómez, S., Gary, G., Preisser, E., and Orians, C. 2012. Mechanics of herbivory: Exotic insect increases branch brittleness of a native tree host. *In* ESA Annual Meeting Portland OR.

Souto, D., Luther, T., and Chianese., B. 1996. Past and current status of HWA in eastern and Carolina hemlock stands. *In* Proceedings of the first hemlock woolly adelgid review. USDA Forest Service, Morgantown, WV.

Sperry, J.S., Christman, M.A., Torres-Ruiz, J.M., Taneda, H., and Smith, D.D. 2012. Vulnerability curves by centrifugation: Is there an open vessel artefact, and are 'r' shaped curves necessarily invalid? Plant, Cell & Environment 35: 601-610.

Sperry, J.S., Donnelly, J.R., and Tyree, M.T. 1988. A method for measuring hydraulic conductivity and embolism in xylem. Plant, Cell & Environment 11: 35-40.

Sperry, J.S., Hacke, U., and Wheeler, J.K. 2005. Comparative analysis of end wall resistivity in xylem conduits. Plant, Cell & Environment 28: 456-465.

Sperry, J.S., Hacke, U.G., Feild, T.S., Sano, Y., and Sikkema, E.H. 2007. Hydraulic consequences of vessel evolution in angiosperms. International Journal of Plant Sciences 168: 1127-1139.

Sperry, J.S., Hacke, U.G., and Pittermann, J. 2006. Size and function in conifer tracheids and angiosperm vessels. American Journal of Botany 93: 1490-1500.

Sperry, J.S., and Ikeda, T. 1997. Xylem cavitation in roots and stems of Douglas-fir and white fir. Tree Physiology 17: 275-280.

Sperry, J.S., Nichols, K., Sullivan, J., and Eastlack, S. 1994. Xylem embolism in ring-porous, diffuse-porous, and coniferous trees of northern Utah and interior Alaska. Ecology 75: 1736-1752.

Sperry, J.S., and Saliendra, N. 1994. Intra- and inter-plant variation in xylem cavitation in *Betula occidentalis*. Plant, Cell & Environment 17: 1233-1241.

Sperry, J.S., and Tyree, M.T. 1988. Mechanism of water stress-induced xylem embolism. Plant Physiology 88: 581-587.

Stadler, B., Muller, T., Orwig, D., and Cobb, R. 2005. Hemlock woolly adelgid in New England forests: Canopy impacts transforming ecosystem processes and landscapes. Ecosystems 8: 233-247.

Stiller, V., and Sperry, J.S. 2002. Cavitation fatigue and its reversal in sunflower (*Helianthus annuus* L.). Journal of Experimental Botany 53: 1155-1161.

Stokes, M.A., and Smiley, T.L. 1996. An introduction to tree-ring dating. University of Arizona Press, Tucson.

Thomas, F., Bartels, C., and Gieger, T. 2006. Alterations in vessel size in twigs of *Quercus robur* and *Q. petraea* upon defoliation and consequences for water transport under drought. Iawa Journal 27: 395-407.

Tibbits, C.W., MacDougall, A.J., and Ring, S.G. 1998. Calcium binding and swelling behaviour of a high methoxyl pectin gel. Carbohydrate Research 310: 101-107.

Tomescu, A.M.F. 2007. On divides. Taxon 56: 289-291.

Tomlinson, G.H. 1993. A possible mechanism relating increased soil temperature to forest decline. Water, Air, and Soil Pollution 66: 365-380.

Tyree, M.T., Sinclair, B., Lu, P., and Granier, A. 1993. Whole Shoot Hydraulic Resistance in Quercus Species Measured with a New High-Pressure Flowmeter. Annales Des Sciences Forestieres 50: 417-423.

Vanderklein, D.W., and Reich, P.B. 1999. The effect of defoliation intensity and history on photosynthesis, growth and carbon reserves of two conifers with contrasting leaf lifespans and growth habits. New Phytologist 144: 121-132.

Wargo, P.M., Minocha, R., Wong, B.L., Long, R.P., Horsley, S.B., and Hall, T.J. 2002. Measuring changes in stress and vitality indicators in limed sugar maple on the Allegheny Plateau in north-central Pennsylvania. Canadian Journal of Forest Research 32: 629-641.

Wheeler, J.K., Huggett, B.A., Tofte, A.N., Rockwell, F.E., and Holbrook, N.M. 2013. Sampling methods can generate the appearance of rapid recovery from embolism. Plant, Cell & Environment *In revision*.

Wilmot, T.R., Ellsworth, D.S., and Tyree, M.T. 1995. Relationships among crown condition, growth, and stand nutrition in seven northern Vermont sugarbushes. Canadian journal of forest research 25: 386-397.

Wimmer, R., Strumia, G., and Holawe, F. 2000. Use of false rings in Austrian pine to reconstruct early growing season precipitation. Canadian Journal of Forest Research 1697: 1691-1697.

Young, R.F., Shields, K.S., and Berlyn, G.P. 1995. Hemlock woolly adelgid (Homoptera: Adelgidae): stylet bundle insertion and feeding sites. Annals of the Entomological Society of America 88: 827-835.

Zimmermann, M.H. 1971. Dicotyledonous wood structure (made apparent by sequential sections). *In* Encyclopaedia Cinematographica. *Edited by* G. Wolf. Institut für den wissenschaftlichen Film, Göttingen, Germany. p. .

Zimmermann, M.H. 1976. The study of vascular patterns in higher plants. *In* Transport and transfer processes in plants. *Edited by* I.F. Wardlaw, and J.B. Passioura. Academic Press, New York. pp. Pages 221–235.

Zimmermann, M.H. 1983. Xylem structure and the ascent of sap. Springer-Verlag, Berlin ; New York.

Zimmermann, M.H., and Jeje, A.A. 1981. Vessel-length distribution in stems of some American woody plants. Canadian Journal of Botany 59: 1882-1892.

Zimmermann, M.H., McCue, K.F., and Sperry, J.S. 1982. Anatomy of the palm *Rhapis excelsa*. VIII. Vessel network and vessel-length distribution in the stem. Journal of the Arnold Arboretum 63: 83–95.

Zwieniecki, M., Melcher, P., and Holbrook, N. 2001a. Hydraulic properties of individual xylem vessels of *Fraxinus americana*. Journal of Experimental Botany 52: 257-264.

Zwieniecki, M.A., Melcher, P.J., and Michele Holbrook, N. 2001b. Hydrogel control of xylem hydraulic resistance in plants. Science 291: 1059-1062.